CANADIAN THESES ON MICROFICHE

I.S.B.N.

THESES CANADIENNES SUR MICROFICHE

National Library of Canada
Collections Development Branch

Canadian Theses on
Microfiche Service

Ottawa, Canada
K1A 0N4

Bibliothèque nationale du Canada
Direction du développement des collections

Service des thèses canadiennes
sur microfiche

NOTICE

The quality of this microfiche is heavily dependent upon the quality of the original thesis submitted for microfilming. Every effort has been made to ensure the highest quality of reproduction possible.

If pages are missing, contact the university which granted the degree.

Some pages may have indistinct print especially if the original pages were typed with a poor typewriter ribbon or if the university sent us a poor photocopy.

Previously copyrighted materials (journal articles, published tests, etc.) are not filmed.

Reproduction in full or in part of this film is governed by the Canadian Copyright Act, R.S.C. 1970, c. C-30. Please read the authorization forms which accompany this thesis.

THIS DISSERTATION
HAS BEEN MICROFILMED
EXACTLY AS RECEIVED

AVIS

La qualité de cette microfiche dépend grandement de la qualité de la thèse soumise au microfilmage. Nous avons tout fait pour assurer une qualité supérieure de reproduction.

S'il manque des pages, veuillez communiquer avec l'université qui a conféré le grade.

La qualité d'impression de certaines pages peut laisser à désirer, surtout si les pages originales ont été dactylographiées à l'aide d'un ruban usé ou si l'université nous a fait parvenir une photocopie de mauvaise qualité.

Les documents qui font déjà l'objet d'un droit d'auteur (articles de revue, examens publiés, etc.) ne sont pas microfilmés.

La reproduction, même partielle, de ce microfilm est soumise à la Loi canadienne sur le droit d'auteur, SRC 1970, c. C-30. Veuillez prendre connaissance des formules d'autorisation qui accompagnent cette thèse.

LA THÈSE A ÉTÉ
MICROFILMÉE TELLE QUE
NOUS L'AVONS REÇUE

NL-339 (r. 82/08)

Canada

108

0-315-12422-9

National Library of Canada | Bibliothèque nationale du Canada

Canadian Theses Division | Division des thèses canadiennes

Ottawa, Canada K1A 0N4

60333

PERMISSION TO MICROFILM — AUTORISATION DE MICROFILMER

• Please print or type — Écrire en lettres moulées ou dactylographier

Full Name of Author — Nom complet de l'auteur

KEVIN LEONARD BASKIN

Date of Birth — Date de naissance	Country of Birth — Lieu de naissance
NOV. 26, 1956	CANADA

Permanent Address — Résidence fixe

34 GREENWOOD WAY
SHERWOOD PARK, ALBERTA
T8A 0J5

Title of Thesis — Titre de la thèse

BEHAVIOUR OF CONCRETE T-BEAMS WITH WELDED WIRE FABRIC WEB REINFORCEMENT

University — Université

UNIVERSITY OF ALBERTA

Degree for which thesis was presented — Grade pour lequel cette thèse fut présentée

MASTER OF SCIENCE

Year this degree conferred — Année d'obtention de ce grade	Name of Supervisor — Nom du directeur de thèse
1982	DR. J. G. MacGREGOR

Permission is hereby granted to the NATIONAL LIBRARY OF CANADA to microfilm this thesis and to lend or sell copies of the film.

The author reserves other publication rights, and neither the thesis nor extensive extracts from it may be printed or otherwise reproduced without the author's written permission.

L'autorisation est, par la présente, accordée à la BIBLIOTHÈQUE NATIONALE DU CANADA de microfilmer cette thèse et de prêter ou de vendre des exemplaires du film.

L'auteur se réserve les autres droits de publication; ni la thèse ni de longs extraits de celle-ci ne doivent être imprimés ou autrement reproduits sans l'autorisation écrite de l'auteur.

Date	Signature
AUGUST 10, 1982	Kevin Baskin

NL-91 (4/77)

THE UNIVERSITY OF ALBERTA

BEHAVIOR OF CONCRETE T-BEAMS WITH WELDED WIRE FABRIC WEB REINFORCEMENT

by

KEVIN L. BASKIN

(C)

A THESIS

SUBMITTED TO THE FACULTY OF GRADUATE STUDIES AND RESEARCH

IN PARTIAL FULFILLMENT OF THE REQUIREMENTS FOR THE DEGREE

OF MASTER OF SCIENCE

CIVIL ENGINEERING

EDMONTON, ALBERTA

FALL 1982

MICRO

THE UNIVERSITY OF ALBERTA

RELEASE FORM

NAME OF AUTHOR: KEVIN L. BASKIN

TITLE OF THESIS: BEHAVIOUR OF CONCRETE T-BEAMS WITH WELDED WIRE FABRIC WEB REINFORCEMENT

DEGREE FOR WHICH THESIS WAS PRESENTED: MASTER OF SCIENCE

YEAR THIS DEGREE GRANTED: FALL 1982

Permission is hereby given to THE UNIVERSITY OF ALBERTA LIBRARY to reproduce single copies of this thesis and to lend or sell such copies for private, scholarly or scientific research purposes only.

The author reserves other publication rights, and neither the thesis nor extensive extracts from it may be printed or otherwise reproduced without the author's written permission.

(SIGNED): Kevin Baskin

PERMANENT ADDRESS: 34 GREENWOOD WAY
SHERWOOD PARK
ALBERTA T8A 0J5

DATED JULY 28 1982

THE UNIVERSITY OF ALBERTA

FACULTY OF GRADUATE STUDIES AND RESEARCH

The undersigned certify that they have read, and recommend to the Faculty of Graduate Studies and Research, for acceptance, a thesis entitled Behaviour of Concrete T-Beams with Welded Wire Fabric Reinforcement, submitted by Kevin L. Baskin, in partial fulfillment of the requirements for the degree of Master of Science in Civil Engineering.

Supervisor

Date July 28, 1982

TO LEN AND JEAN

ABSTRACT

This thesis presents the results of tests conducted to investigate the behaviour of non-prestressed concrete T-beams reinforced with single leg welded wire fabric shear reinforcement. The size of the beams was chosen to approximate half of a full-sized double-tee beam. The layouts of the welded wire fabric reinforcement sheets were chosen in accordance with the proposals of the PCI Technical Activities Committee's Joint PCI/WRI Ad Hoc Committee on Welded Wire Fabric for Shear Reinforcement (1980).

Ten beams were tested. Eight beams were reinforced with different arrangements of welded wire fabric web reinforcement. Two beams with conventional reinforcement single leg stirrups were tested for comparison purposes. The beams were tested under static loading using a two point loading arrangement on a simple span so that the shear-span to depth ratio was approximately 3.0. The tension reinforcement ratio, ρ_w, was approximately 0.022 for all beams and the web reinforcement ratio, r, was between 1.04×10^{-3} and 1.52×10^{-3}. The instrumentation included measurements of load, deflection, stirrup strain, stirrup slip and crack width. The propagation of cracks was also monitored.

All beams tested had diagonal tension type failures. The test results indicated that the ACI and CSA Code equations for predicting beam shear strength were conservative for the welded wire fabric sheets used, provided that there was proper anchorage. The Code equations were less conservative as the web reinforcement ratio decreased. The best anchorage was provided with two horizontal cross-wires at the top and bottom of the reinforcement sheets as proposed by the PCI/WRI Ad Hoc Committee for the case of single leg welded wire fabric shear reinforcement sheets with smooth vertical wires. In the case of welded deformed wire fabric, anchorage with only one horizontal cross-wire top and bottom was also satisfactory, provided the bottom cross-wire was not above the lowest main reinforcement and the upper cross-wire was close to the top face of the beam. It should be noted that these anchorages were not effective in supporting the main reinforcement to prevent dowel splitting. This type of cracking along the main reinforcement was evident in every beam which had welded wire fabric web reinforcement.

Most of the vertical wires in the welded wire fabric sheets that were crossed by the failure crack in the region where they were well anchored, fractured when the beam failed. This was not the case in the beams with the conventional stirrup reinforcement.

ACKNOWLEDGEMENTS

This testing program was completed in the I.F. Morrison Structural Engineering Laboratory at the University of Alberta. The assistance given by Larry Burden and the other technicians during construction and testing is sincerely appreciated. The work done by Al Dunbar regarding the use of the NOVA computer is also gratefully acknowledged.

A special thanks is extended to Dr. J.G. MacGregor for his invaluable guidance and advice and for his easygoing manner that makes him so approachable.

The research project was financed by an operating grant from the National Scientific and Engineering Research Council.

TABLE OF CONTENTS

Chapter			PAGE
1	INTRODUCTION		1
2	LITERATURE REVIEW AND BACKGROUND INFORMATION		3
	2.1	Shear Strength of Concrete Beams	3
		2.1.1 General	3
		2.1.2 Design Procedures	3
		2.1.3 Equations for V_c	5
		2.1.4 Equations for V_s	7
	2.2	Welded Wire Fabric	10
		2.2.1 General	10
		2.2.2 Welded Wire Fabric for Shear Reinforcement	15
		2.2.3 Anchorage of Welded Wire Fabric Shear Reinforcement	18
3	BEAM SPECIMENS		25
	3.1	General	25
	3.2	Beam Dimensions	25
	3.3	Shear Reinforcement	31
		3.3.1 Single Leg WWF Mesh	31
		3.3.2 Conventional Reinforcement Stirrups	32
	3.4	Main Longitudinal Reinforcement	33
	3.5	Flange Reinforcement	35
	3.6	Beam Construction	35
4	MATERIAL PROPERTIES		41
	4.1	Reinforcement Properties	41
		4.1.1 WWF Mesh	41
		4.1.2 Conventional Reinforcement Stirrups	47
		4.1.3 Main Longitudinal Reinforcement	47
	4.2	Concrete Properties	49
5	TESTING PROGRAM		51
	5.1	General	51

5.2 Test Set-up 51

5.3 Instrumentation 51
5.3.1 Load Measurement 51
5.3.2 Beam Deflection 54
5.3.3 Stirrup Strain Gauges 54
5.3.4 Stirrup Slip Measurements 59
5.3.5 Crack Data 62

5.4 Test Procedure 63

6 BEAM TEST RESULTS 65

6.1 Behaviour of Typical Beam with WWF Web Reinforcement 65
6.1.1 Introduction 65
6.1.2 Crack Formation in Shear Span - TB 4 . 76
6.1.3 Inclined Cracking Load - TB 2 . . 79
6.1.4 Crack Formation in Pure Moment Region - TB 4 82
6.1.5 Mode of Failure - TB 4 82
6.1.6 Crack Widths - TB 4 85
6.1.7 Stirrup Strains - TB 2 86
6.1.8 Stirrup Slip and Anchorage Failure - TB 4 94
6.1.9 Deflection - TB 4 99

6.2 Comparison of Beam Strength 103

6.3 Comparison of Beam Behaviour 107
6.3.1 Introduction 107
6.3.2 Crack Formation 107
6.3.3 Crack Widths 116
6.3.4 Mode of Failure 127
6.3.5 Stirrup Strain 129
6.3.6 Stirrup Slip and Anchorage Behaviour . 134
6.3.7 Deflections 142

7 SUMMARY AND CONCLUSIONS 145

8 RECOMMENDATIONS FOR FURTHER STUDY 149

LIST OF REFERENCES 150

APPENDIX 153

LIST OF TABLES

		PAGE
2.1	ASTM and CSA Standards for WWF	12
3.1	Summary of Beam Web Reinforcement	26
4.1	Dimensions of Wire Stirrups	42
4.2	Average Wire Tension Test Results	44
4.3	Concrete Properties	50
6.1	Ratio of Test Strength Divided by Predicted Strength $\frac{V_{u,test}}{V_{u,calc}}$	104
6.2	Inclined Cracking Load	115
6.3	Crack Width Data	124
6.4	Suggested Maximum Crack Widths - ACI Committee 224 (1972)	126
6.5	Wire Stirrups Fractured at Failure	133
6.6	Final Slip Measurements in Failure Span - mm	135
6.7	Final Slip Measurements in Non-Failure Span - mm	135
6.8	Beam Deflection Prior to Failure	144
A.1	- Tension Test Results for W2.5 Wires	154
A.2	- Tension Test Results for W2.9 Wires	155
A.3	- Tension Test Results for D2.5 Wires	156
A.4	- Tension Test Results for D2.9 Wires	157
A.5	- Tension Test Results Supplied by Wire Manufacturer	158
A.6	- As-Built Beam Dimensions	159

LIST OF FIGURES

Figure		PAGE
2.1	Effect of Wire Size on Ultimate Strain	14
2.2	PCI/WRI Proposal for Single Leg WWF Shear Reinforcement Smooth Vertical Wires	19
2.3	PCI/WRI Proposal for Single Leg WWF Shear Reinforcement Deformed Vertical Wires	20
2.4	1983 ACI Code Proposal for Single Leg WWF Web Reinforcement	21
2.5	Anchorage of WWF - Leonhardt and Walther	23
3.1	Layout of WWF Mesh with 2 Horizontal Cross-Wire Top and Bottom (used in TB 1, TB 2, TB 3, TB 4, and TB 8)	27
3.2	Layout of WWF Mesh with Exterior Horizontal Cross-Wire Top and Bottom (used in TB 5 and TB 6)	28
3.3	Layout of WWF Mesh with Interior Horizontal Cross-wire Top and Bottom (used in TB 7)	29
3.4	Typical Cross-Sections of Beam in Testing Program with WWF Web Reinforcement (a) TB 1 to TB 4 (b) TB 8	30
3.5	Typical Cross-Section of Beam in Testing Program with Conventional 6 mm Diameter Stirrups	34
3.6	Beam Elevation Showing Reinforcement Layout with WWF Web Reinforcement	37
3.7	Beam Elevation Showing Reinforcement Layout with Conventional 6 mm Diameter Stirrups	38
3.8	Reinforcement in Forms Prior to Concrete Placement - TB 2	39
3.9	Reinforcement Cage for TB 7	40
3.10	Reinforcement Cage for TB 6	40

4.1 Typical Stress-Strain Curves for Wires 45

4.2 Stress-Strain Curve for 6 mm Diameter Stirrup Bars 48

5.1 Beam Loading Arrangement 52

5.2 Beam Test Set-up 53

5.3 Locations for Instrumentation for Beams with WWF Web Reinforcement 56

5.4 Locations for Instrumentation for Beams with Conventional 6 mm Diameter Stirrups . . . 57

5.5 Reinforcement Cage for TB 9 with Strain Gauges Installed 58

5.6 Strain Gauges on Stirrup in TB 9 (also note lug brazed on near the top of the stirrup) . . . 58

5.7 Dial Gauges for Measuring Stirrup Slip from Top of Beam 60

5.8 Dial Gauges for Measuring Stirrup Slip from Bottom of Beam 60

5.9 Mounting of Dial Gauge Apparatus for Measuring Stirrup Slip 61

5.10 Typical Load versus Time Graph for Beam Test (TB 10) 64

6.1 Cracking in East Shear Span of TB 4 at P = 30 kN . 66

6.2 Cracking in East Shear Span of TB 4 at P = 50 kN . 66

6.3 Cracking in East Shear Span of TB 4 at Ultimate Load (P_{ult} = 80 kN) 67

6.4 Cracking in East Shear Span of TB 4 After Testing 67

6.5 Cracking in West Shear Span of TB 4 at P = 30 kN . 68

6.6 Cracking in West Shear Span of TB 4 at P = 50 kN . 68

6.7 Cracking in West Shear Span of TB 4 at Ultimate Load (P_{ult} - 80 kN) 69

6.8 Cracking in West Shear Span of TB 4 After Testing 69

6.9 Cracking in Pure Moment Region of TB 4 After Testing 70

6.10 Cracking in West Shear Span of TB 2 at P = 30 kN . 71

6.11 Cracking in West Shear Span of TB 2 at P = 50 kN . 71

6.12 Cracking in West Shear Span of TB 2 at Ultimate Load (P_{ult} = 70 kN) 72

6.13 Cracking in West Shear Span of TB 2 After Testing 72

6.14 Cracking in East Shear Span of TB 2 at P = 30 kN . 73

6.15 Cracking in East Shear Span of TB 2 at P = 50 kN . 73

6.16 Cracking in East Shear Span of TB 2 at Ultimate Load (P_{ult} = 70 kN) 74

6.17 Cracking in East Shear Span of TB 2 After Testing 74

6.18 Cracking in Pure Moment Region of TB 2 After Testing 75

6.19 Failure Crack Above Exterior Anchorage Wire at Top of TB 2 84

6.20 Point Load versus Stirrup Strain for East Shear Span of TB 2 88

6.21 Point Load versus Stirrup Strain for West Shear Span of TB 2 89

6.22 Graphs of Load versus Strain for Strain Gauges 5 and 6 from TB 2 Showing the Difference in Strain Due to Bond 92

6.23 Graphs of Load versus Strain for Strain Gauges 15 and 16 from TB 2 Showing the Difference in Strain Due to Bond 93

6.24 Graph of Load versus Stirrup Slip as Measured from the Top Gauges of TB 4 in the East Shear Span . 95

6.25 Graph of Load versus Stirrup Slip as Measured from the Bottom Gauges of TB 4 in the West Shear Span . 96

6.26 Graph of Load versus Stirrup Slip as Measured from the Top Gauges of TB 4 in the West Shear Span . 97

6.27 Damage to Anchorage at Bottom of Failure Crack in TB 4 100

6.28 Load versus Midspan Deflection for TB 4 . . . 101

6.29 Locations of Failure Cracks in TB 1 to TB 8 . . 110

6.30 Locations of Failure Cracks in TB 9 and TB 10 . 111

6.31 Typical Shrinkage Cracks at Bottom of Web-to-Flange Taper 113

6.32 Graphs of $\frac{P}{P_{ult}}$ versus Average Crack Width for TB 3, TB 4, TB 5, TB 7 and TB 8 117

6.33 Graphs of $\frac{P}{P_{ult}}$ versus Average Crack Width for TB 1, TB 2 and TB 6 118

6.34 Graphs of $\frac{P}{P_{ult}}$ versus Average Crack Width for TB 9 and TB 10 119

6.35 Graphs of $\frac{P}{P_{ult}}$ versus Maximum Crack Width for TB 3, TB 4, TB 5, TB 7 and TB 8 120

6.36 Graphs of $\frac{P}{P_{ult}}$ versus Maximum Crack Width for TB 1, TB 2 and TB 6 121

6.37 Graphs of $\frac{P}{P_{ult}}$ versus Maximum Crack Width for TB 9 and TB 10 122

6.38 Graph of Load versus Strain for Strain Gauges 5 and 6 from TB 8 Showing Unbonding Between Concrete and Stirrup Wire 131

6.39 Crack Forming Above 9.5 mm Bar at Top of Failure Crack in TB 10 138

6.40 Illustration Showing How the Anchorage Wires at the Top of the Beams were Damaged at the Beam Failure Load 139

6.41 Damage to Anchorage at Bottom of Failure Crack in TB 5 141

6.42 Damage to Anchorage at Bottom of Failure Crack in TB 8 141

A.1 East Shear Span of TB 1 after Failure . . . 160
A.2 West Shear Span of TB 1 after Failure . . . 160
A.3 East Shear Span of TB 3 after Failure . . . 161
A.4 West Shear Span of TB 3 after Failure . . . 161
A.5 East Shear Span of TB 5 after Failure . . . 162
A.6 West Shear Span of TB 5 after Failure . . . 162
A.7 East Shear Span of TB 6 after Failure . . . 163
A.8 West Shear Span of TB 6 after Failure . . . 163
A.9 East Shear Span of TB 7 after Failure . . . 164
A.10 West Shear Span of TB 7 after Failure . . . 164
A.11 East Shear Span of TB 8 after Failure . . . 165
A.12 West Shear Span of TB 8 after Failure . . . 165
A.13 East Shear Span of TB 9 after Failure . . . 166
A.14 West Shear Span of TB 9 after Failure . . . 166
A.15 East Shear Span of TB 10 after Failure . . . 167
A.16 West Shear Span of TB 10 after Failure . . . 167
A.17 Pure Moment Region of TB 1 after Failure . . 168
A.18 Pure Moment Region of TB 3 after Failure . . 168
A.19 Pure Moment Region of TB 5 after Failure . . 169
A.20 Pure Moment Region of TB 6 after Failure . . 169
A.21 Pure Moment Region of TB 7 after Failure . . 170
A.22 Pure Moment Region of TB 8 after Failure . . 170
A.23 Pure Moment Region of TB 9 after Failure . . 171
A.24 Pure Moment Region of TB 10 after Failure . . 171

LIST OF SYMBOLS

a = shear span distance

A_s = area of tension reinforcement

A_v = area of shear reinforcement within a distance s

b = width of compression face of member (flange width of the T-beams tested)

b_w = web width of T-beams

c = horizontal projection of an inclined crack between the top of the main reinforcement and the bottom of the web-to-flange taper

d = effective depth of beam; distance from the extreme compression fiber to the centroid of the tension reinforcement

d' = depth from compressed surface to anchorage of shear reinforcement in tensile zone

E = Young's Modulus (Modulus of Elasticity)

f'_c = compressive strength of concrete

f_{su} = stress in reinforcement at ultimate

f_{vy} = yield strength of shear reinforcement

f_y = yield strength of reinforcement

$f_{y,ACI}$ = stress in wire shear reinforcement measured at a strain of 0.0035 (i.e. yield strength for reinforcement with f_y greater than 60 ksi as specified by the ACI Code)

$f_{y,ASTM}$ = stress in wire shear reinforcement measured at a strain of 0.005 (i.e. yield strength for wire reinforcement as specified in ASTM Standards)

h = overall depth of member

I_e = effective moment of inertia for computation of deflection

LF = load factor (1.4 for dead load and 1.7 for live load)

M = moment at section considered

M_n = nominal moment strength

P = point load applied in beam tests

P_{ult} = point load applied at beam failure

r = web reinforcement ratio $(= \frac{A_v}{b_w s \sin\alpha})$

s = shear reinforcement spacing in direction of longitudinal reinforcement

t = thickness of compression flange in T-beams

v_b = basic shear stress; shear stress carried by the concrete in non-prestressed beams

v_c = shear stress carried by the concrete

$v_{c,ACI}$ = shear stress carried by the concrete as given in the ACI Code $(= 1.9\sqrt{f'_c} + 2500\, \rho_w \frac{Vd}{M})$

v_u = shear stress at ultimate

$v_{u,test}$ = shear stress at the beam failure load for the tests conducted in this program

V = shear at section being considered

V_c = shear force carried by the concrete

$V_{c,ACI}$ = shear force carried by the concrete as given in the ACI Code

V_{cr} = shear force producing shear cracking

V_n = nominal shear strength

V_s = shear force carried by shear reinforcement

V_u = shear force at ultimate load

$V_{u,test}$ = shear force at the beam failure load for the tests conducted in this program

α = angle between shear reinforcement and the longitudinal axis of the member

ε_u = ultimate strain in reinforcement as determined from a direct tension test

θ_{avg} = average inclination of an inclined crack measured from the horizontal

ρ = longitudinal reinforcement ratio $(= \frac{A_s}{bd})$

ρ_w = longitudinal reinforcement ratio based on web width $(= \frac{A_s}{b_w d})$

ϕ = strength reduction factor (= 0.85 for shear)

ϕ_L = diameter of longitudinal wire in welded wire mesh

ϕ_s = diameter of stirrup

CHAPTER 1

INTRODUCTION

The PCI Technical Activities Committee Joint PCI/WRI Ad Hoc Committee on Welded Wire Fabric for Shear Reinforcement (1980) has indicated that the use of welded wire fabric shear reinforcement in webs of double-tee beams has increased significantly. This Committee has proposed wire sizes and methods of anchorage for sheets of single leg welded wire fabric for shear reinforcement for these types of beams. The purpose of this program was to investigate the behaviour, under shear loading, of non-prestressed concrete T-beams with welded wire fabric web reinforcement selected in accordance with these proposals. The ductility of the beams and the behaviour of the anchorage of the web reinforcement were of particular interest.

In this program, eight beams with welded wire fabric web reinforcement and two beams with conventional single leg reinforcement stirrups were tested. All of the beams had the same dimensions, the same amount of main reinforcement, and the same loading arrangement. The main variables were the type and size of the vertical wires in the welded wire fabric sheets and the arrangement of the anchorage for these sheets. The beam dimensions were chosen to approximate half of a full-sized double-tee beam.

A brief review of some procedures for calculating beam shear capacity is presented in Chapter 2. This chapter also presents some background information about welded wire fabric as well as results of some previous investigations regarding its use as shear reinforcement. A detailed description of the beam specimens and the material properties is given in Chapters 3 and 4, respectively. Chapter 5 explains the testing arrangement as well as the instrumentation used.

In Chapter 6, the results of the tests are presented. This chapter has been broken into three sections. The first section describes in detail the behaviour, up to and including failure, of a typical beam with welded wire fabric web reinforcement. The next section compares the ultimate strengths determined from the various tests with the predicted strengths obtained from various procedures (as described in Chapter 2). The final section of this chapter points out differences and similarities in the behaviour of the various beams tested.

Chapter 7 presents a summary of the results along with conclusions and Chapter 8 suggests areas where further investigation should be made.

CHAPTER 2

LITERATURE REVIEW AND BACKGROUND INFORMATION

2.1 Shear Strength of Concrete Beams

2.1.1 General

A tremendous amount of work has been done on evaluating and predicting the shear strength of reinforced concrete beams. However, due to the extremely complex nature of shear failure and the large variety of types of concrete beams, no one universal method of design has been developed. There are many different proposed procedures to determine the shear strength depending on such properties as amount of longitudinal or web reinforcement, type of cross-section, concrete strength and a/d ratio. In order to limit discussion, only a brief review will be presented of existing code procedures as well as previous testing and analysis relating to shear strength of beams similar to those tested in this project. An extensive review of factors affecting the shear strength of beams was published by ACI-ASCE Committee 426 (1973).

2.1.2 Design Procedures

The method used in the ACI Building Code, ACI 318-77 (1977) for calculating beam shear strength is an adaptation of the semi-empirical method proposed by ACI-ASCE Committee 326 (1962). The nominal shear strength, V_n, is calculated as follows:

$$V_n = V_c + V_s \qquad (2.1)$$

V_c is described as the nominal shear strength provided by the concrete. In the ACI Code it is empirically assumed that this is equal to the inclined cracking shear and would be the failure load for a beam with no web reinforcement. V_s is the nominal shear strength provided by the web reinforcement assuming that the horizontal projection of the failure crack is equal to the effective depth of the beam, d. For a concrete beam with shear reinforcement perpendicular to the axis of the member, these quantities are calculated as shown:

$$V_c = (1.9\sqrt{f'_c} + 2500\,\rho_w \frac{Vd}{M})\, b_w d \leq 3.5\sqrt{f'_c}\, b_w d \qquad (2.2)$$

$$V_s = \frac{Avfyd}{s} \leq 8\sqrt{f'_c}\, b_w d \qquad (2.3)$$

where: f'_c = concrete compressive strength (psi)

b_w = beam web width (in.)

d = beam effective depth; distance from extreme compression fiber to centroid of longitudinal tension reinforcement (in.)

f_y = yield strength of tension reinforcement (psi)

s = spacing of shear reinforcement in direction parallel to longitudinal reinforcement (in.)

V, M = shear and moment due to load at section being considered

A_v = area of shear reinforcement within a distance s (sq. in.)

$\rho_w = \frac{A_s}{b_w d}$

A_s = area of tension reinforcement (sq. in.)

The equation for V_c is generally simplified to:

$$V_c = 2\sqrt{f'_c}\, b_w d \text{ (psi)} \qquad (2.4)$$

The CSA Code procedure in CAN3-A23.8-M77 is very similar to the ACI Code procedure.

Although this approach provides conservative estimates of shear strength for a wide range of beams, it has been shown to be unconservative for beams with low values of ρ_w (Rajagopalan and Ferguson, 1968). Also, this method does not correctly predict the effects resulting from variations in such properties as concrete strength, a/d ratios and amount of longitudinal and web reinforcement (Haddadin et al, 1971). Some of the research done on the magnitude of V_c and V_s is reported in the next sections.

2.1.3 Equations for V_c

Several investigators have proposed alternative equations for calculating V_c. Zsutty (1968) showed that the ACI equation gave poor predictions of test results for beams with no web reinforcement and low values of $\frac{V_c}{bd\sqrt{f'_c}}$ and $\frac{\rho V_c d}{M\sqrt{f'_c}}$

He carried out a combined dimensional and regression analysis and proposed the following equation for the calculation of shear at inclined cracking, which the ACI Code assumes is the shear V_c:

$$V_c = \left(59 \sqrt[3]{f'_c \rho \frac{d}{a}}\right) b_w d \text{ (psi)} \qquad (2.5)$$

where: a = shear span distance (in.)

b = width of compression face of member (in.)

$= \frac{A_s}{bd}$

M = moment at section being considered

Starting from a failure theory for concrete, Placas and Regan (1971) derived yet another equation for the shear force producing shear cracking, V_{cr}:

$$V_{cr} = 8\left[f'_c \frac{100\ A_s}{b_w d}\right]^{1/3} b_w d \text{ (psi)} \qquad (2.6)$$

This equation gives similar results to that derived by Zsutty for beams with a/d ratios of approximately 4.5.

Rajagopalan and Ferguson (1968) proposed an equation for V_c based on a study of beams with no web reinforcement and low values of the longitudinal reinforcement ratio, ρ.

$$V_c = (0.8 + 100\ \rho) \sqrt{f'_c}\ b_w d \leq 2.0\sqrt{f'_c}\ b_w d \text{ (psi)} \qquad (2.7)$$

It was shown that for beams with ρ less than about 1.2 percent, the shear strength was significantly decreased and that the ACI equation did not predict this.

ACI-ASCE Committee 426 (1977) proposed a design equation similar to that developed by Rajagopalan and Ferguson.

$$\sqrt{f'_c} \leq v_b = (0.8 + 120\,\rho_w)\sqrt{f'_c} \leq 2.3\sqrt{f'_c} \text{ (psi)} \quad (2.8)$$

The quantity v_b is defined as the basic shear stress and in the case of non-prestressed beams it is taken to be the shear stress carried by the concrete.

Batchelor and Kwun (1981) have suggested an alternative equation for v_b:

$$\sqrt{f'_c} \leq v_b = (0.6 + 110\,\rho_w)\sqrt{f'_c} \leq 2.25\sqrt{f'_c} \text{ (psi)} \quad (2.9)$$

Equations 2.5 to 2.9 are empirically derived and attempt to allow for the effects of ρ and f'_c on V_c. All give similar results.

2.1.4 Equations for V_s

In addition to the work done to determine the shear stress carried by the concrete, extensive research has been carried out to examine the effectiveness of web reinforcement in reinforced concrete beams. Haddadin, Hong and Mattock

(1971) tested a series of T-beams with varying amounts of web reinforcement and derived the following equations:

$$v_u - v_c = 1.75\, rf_{vy} \quad \text{when } rf_{vy} < 0.112\, f'_c\sqrt{\frac{d}{a}} \qquad (2.10)$$

$$v_u - v_c = 0.5\, rf_{vy} + 0.14\, f'_c\sqrt{\frac{d}{a}} \quad \text{when } rf_{vy} > 0.112\, f'_c \sqrt{\frac{d}{a}} \qquad (2.11)$$

where:

$$v_c = 1.9\sqrt{f'_c} + 2500\, \rho_w \frac{V_d}{M} \leq 3.5\sqrt{f'_c} \qquad (2.2a)$$

v_c = shear stress carried by concrete, also nominal shear stress at diagonal tension cracking (psi).

v_u = nominal ultimate shear stress

$r = \dfrac{A_v}{b_w s \sin \alpha}$

α = angle between inclined stirrups and longitudinal axis of member

It was shown that these equations gave a better representation of test data than the ACI equation for the effectiveness of web reinforcement. It should be emphasized that the value of V_c used in the analysis was calculated using the ACI equation. Based on this, these tests showed that for small amounts of web reinforcement the effectiveness of the reinforcement is about 1.75 times as great as predicted by the ACI approach. This is indicated by Equation 2.10. One

possible explanation would be that the crack has a horizontal projection of 1.75d rather than d as assumed in the ACI equation or that the web reinforcement extended the time over which aggregate interlock and dowel action were effective. Haddadin et al also showed that the ACI equations do not accurately reflect the trends in behaviour as parameters such as a/d and concrete strength are varied.

Attiogbe, Palaskas and Darwin (1980) tested concrete T-beams with small amounts of web reinforcement and longitudinal reinforcement and concluded that the web reinforcement is 1.5 times as effective as that predicted by the modified truss analogy with a 45 degree crack. Their beams used strand as longitudinal reinforcement to get the necessary flexural strength with small amounts of longitudinal steel. In evaluating the effectiveness of the web reinforcement, these investigators used $v_u - v_c$ where both of these quantities were determined from various test measurements and not from any of the previously stated equations. These results are in line with those of Haddadin, Hong and Mattock. Thus, small amounts of web reinforcement were found to be more effective than predicted by Equation 2.3.

Placas and Regan (1971) derived equations for predicting the shear failure load, shear compression failure load, and web

crushing load for beams with web reinforcement. For T-beams failing in shear the applicable equation was:

$$V_u = [2(d'-t)\, b_w\, rf_{vy}] + [25(f'_c)^{1/3}\, t(b_w + 6)] \text{ (psi)} \quad (2.12)$$

where:

t = thickness of compression flange

d' = depth from compressed surface to anchorage of shear reinforcement in tensile zone

The first term represents V_s and the second term V_c. In the derivation of V_c, it is assumed that a width of flange extending 3 inches on either side of the web was effective in transmitting V_c.

2.2 Welded Wire Fabric

2.2.1 General

The use of welded wire fabric (WWF) began in the early part of this century. At that time, it was used primarily as reinforcement in concrete pavements. This type of reinforcement improved the performance of the pavements by preventing deterioration after cracking and by providing more effective crack control. These properties, together with the relative ease of placement of the fabric, contributed to extensive growth in its use. Today, welded wire fabric is used as reinforcement for concrete pipe, slabs, walls, footings, and beams as well as concrete pavements.

The manufacture of welded wire fabric is covered by the Specifications listed in Table 2.1. The ASTM and CSA Standards for WWF set out required properties and practices which must be met by the manufacturers. These specifications limit material chemistry and require minimum tensile strengths. Although there is no requirement for minimum elongation at failure, an attempt is made to define a minimum ductility by stating a minimum reduction in area and bend test requirements.

The ACI 318-77 Building Code has several sections related to the use of WWF in reinforced concrete. Generally speaking, welded wire fabric can be substituted directly for bar reinforcement provided certain anchorage details are provided. A Manual of Standard Practice for Welded Wire Fabric (1979) has been published by the Wire Reinforcement Institute (WRI) based on these specifications. The existing design rules, however, do not clarify all matters relating to properties and uses of WWF.

A possible area for confusion results from the difference in determination of the yield strength required by the ASTM and CSA material specifications compared to that used in design under the ACI or CSA Building Code requirements for reinforced concrete. The ASTM or CSA Standards for WWF

TABLE 2.1

ASTM AND CSA STANDARDS FOR WWF

ASTM Standard	CSA Standard	Title
ASTM A 82	CSA G30.3	Cold-drawn Steel Wire for Concrete Reinforcement
ASTM A 185	CSA G30.5	Welded Steel Wire Fabric for Concrete Reinforcement
ASTM A 496	CSA G30.14	Deformed Steel Wire for Concrete Reinforcement
ASTM A 497	CSA G30.15	Welded Deformed Steel Wire Fabric for Concrete Reinforcement

specify yield strength as the strength measured at a strain of 0.005 whereas the ACI and CSA Codes for concrete design specify that the yield strength shall be taken as 400 MPa (60 ksi) or the value corresponding to a strain of 0.0035, if the latter value is available.

The value of ultimate strain for wires obtained from tension tests has been shown to be substantially lower than that of conventional bars for the tests conducted by Wiss, Janney, Elstner and Associates (1969). Mirza and MacGregor (1981) have plotted the WJE data as a function of bar area as shown in Figure 2.1. Although the wires had yield strengths of approximately 515 to 585 MPa (75 to 85 ksi), the reduced ultimate elongation could be of concern for reinforced concrete members where, at ultimate load, the wire would be subjected to tensions similar to those resulting from direct tension tests. The reduced ultimate strain could result in a less ductile member. A large reduction in ductility would be undesirable, as the design of reinforced concrete members is based on achieving ductile failures to allow advance warning of failure and to allow moment redistribution in structures designed to resist earthquake loadings. This concern was analytically investigated by Mirza and MacGregor (1981) who indicated that while slabs reinforced with welded wire fabric develop the anticipated ultimate flexural

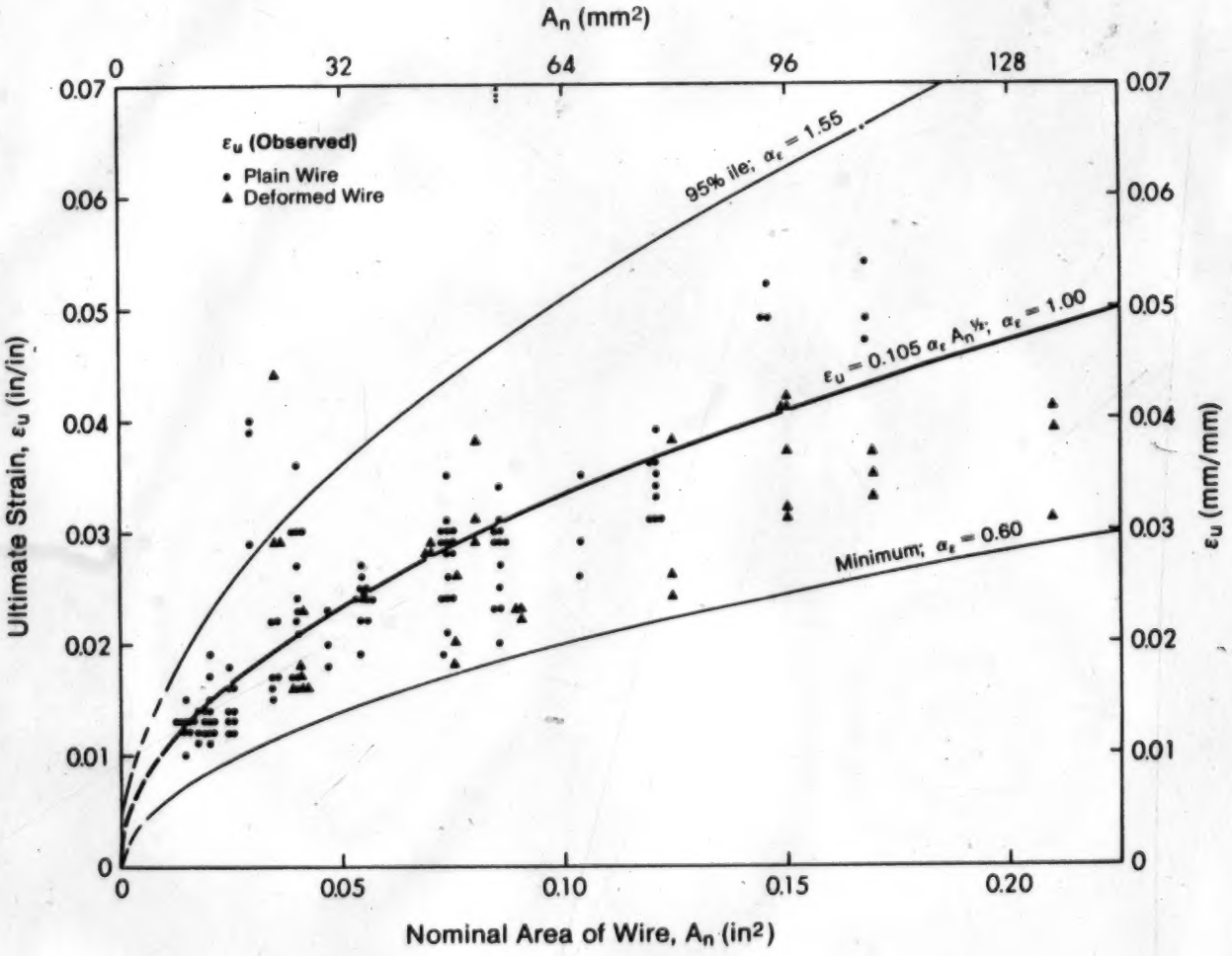

FIGURE 2.1 - Effect of Wire Size on Ultimate Strain

strength, they may not develop ductility comparable to identical slabs reinforced with conventional rebars. Some of the assumptions and conclusions made by Mirza and MacGregor have been questioned by the WRI in a discussion written by Mr. A.B. Dove of Stelco (1982). Mr. Dove felt that design rules for welded wire fabric should not be based upon values of ultimate elongation. He also suggested that some of the low values for ultimate elongation result from wire failures in the grips of the testing machine. Further work will be necessary to clarify this question.

2.2.2 Welded Wire Fabric for Shear Reinforcement

The number of tests conducted to investigate the use of welded wire fabric as shear reinforcement has been limited. Leonhardt and Walther (1965) tested T-beams with shear reinforcement consisting of mesh made of slightly deformed wires. The vertical bars in the meshes were between 5.0 mm and 10.0 mm in diameter and the spacing of these wires was between 50 mm and 200 mm. The diameter of the horizontal (or longitudinal) bars were between 4.0 mm and 8.0 mm and the spacings were either 225 mm or 250 mm. The mats were bent in a U-shape and enclosed the longitudinal reinforcement. The results indicated that mats with 50 mm to 100 mm spacing of the stirrups were best with respect to crack widths and web compressive stresses. During testing, slip of the upper anchorage of the stirrups was noticed. This

resulted in slightly lower ultimate loads than for equivalent beams with web reinforcement made from deformed, twisted bars. Tests to determine the behaviour of different types of anchorage were then conducted. The results are shown in the following section.

Taylor and El-Hammasi (1980) carried out a testing program to investigate the web cracking behaviour of T-beams with welded wire fabric shear reinforcement. They concluded that welded wire fabric appeared to be suitable as shear reinforcement in these beams and that the use of WWF was effective for crack control. This is in agreement with the results of the tests done by Leonhardt and Walther. Unfortunately, no ultimate load data is reported for these tests.

Even though there has been only a small amount of research, WWF shear reinforcement is commonly used by precast and prestressed concrete manufacturers. The use of WWF as shear reinforcement is permitted by the ACI 318-77 Code. The definition of stirrups in Chapter 2 of the code includes welded wire fabric (smooth or deformed) as one form of stirrup. Section 11.5.1.1 states that WWF with wires perpendicular to the axis of the member may be used for shear reinforcement. The ACI code method of determining the shear strength provided by WWF shear reinforcement in beams is straightforward and is the same as for conventional stirrup

reinforcement. Code Section 12.14.2.4 describes the anchorage required for smooth WWF stirrups. No similar clause was given for deformed wire stirrups.

Limitations in the existing ACI code were pointed out by the Joint Prestressed Concrete Institute-Wire Reinforcement Institute Ad Hoc Committee on Welded Wire Fabric for Shear Reinforcement (1980). One important area requiring clarification was the development or anchorage of WWF shear reinforcement. This will be discussed in the following section. The Committee also indicated that the wire spacing requirements presented in Sections 3.5.3.6 and 3.5.3.7 for normal WWF mats should not apply in the case of WWF shear reinforcement.

The Ad Hoc Committee, in addition to examining code restrictions for WWF shear reinforcement, also explored the possibility of developing standard sizes of this type of reinforcement. As a result, a rationale was presented for the acceptance of straight sheets of wire fabric as well as possible "standards" for this type of reinforcement. The proposed standards were for straight sheets of WWF anchored in both the tension and compression sides of the beam as follows:

1. For smooth WWF, two longitudinal wires with a minimum spacing of 2 inches (51 mm), with the

inner wire not less than the greater of d/4 or 2 inches (51 mm) from the mid-depth of the member.

2. For deformed WWF, one longitudinal wire not more than d/4 from the extreme faces, plus a development length above and below mid-depth in accordance with Section 12.8.2 of ACI 318-77.

These proposals are summarized in Figures 2.2 and 2.3. The recommended vertical wire sizes for the WWF sheets are W2.9 or D2.9 and W2.5 or D2.5 which are the most common in current practice. The most common spacing between vertical wires is 6 inches (152 mm) for W2.5 and D2.5 and either 6 inches (152 mm) or 7.5 inches (190 mm) for W2.9 and D2.9. The use of W1.4 cross wires (i.e. horizontal wires) in the meshes was recommended. These cross wires were only provided where needed for anchorage.

The 1983 ACI Code will recognize the use of these meshes but will require anchorage as shown in Figure 2.4. Also in the 1983 code the spacing provisions in Sections 3.5.3.6 and 3.5.3.7 of the existing code will not apply to welded wire fabric used as stirrups.

2.2.3 Anchorage of Welded Wire Fabric Shear Reinforcement

In order to develop the full strength of web reinforcement, proper anchorage is very important. However, until

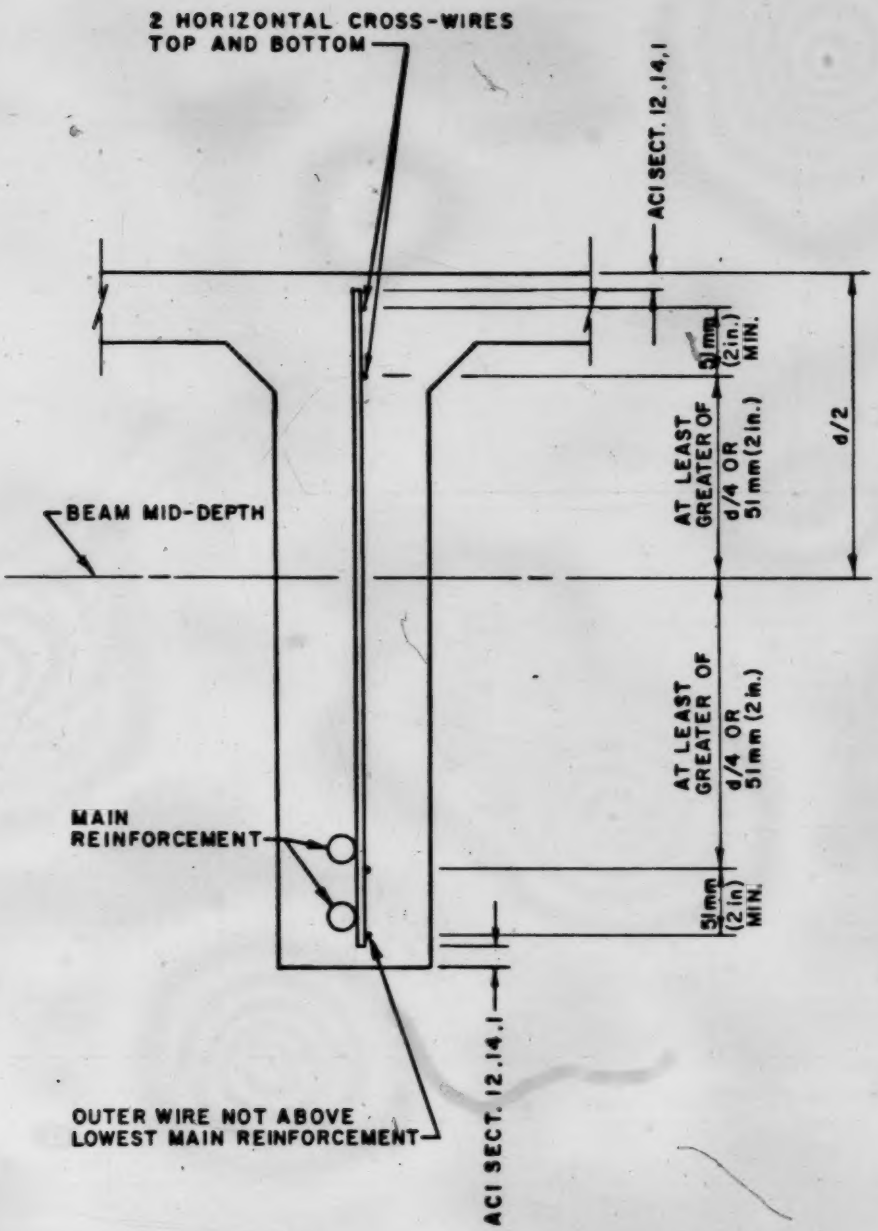

FIGURE 2.2 - PCI/WRI Proposal for Single Leg WWF Shear Reinforcement - Smooth Vertical Wires

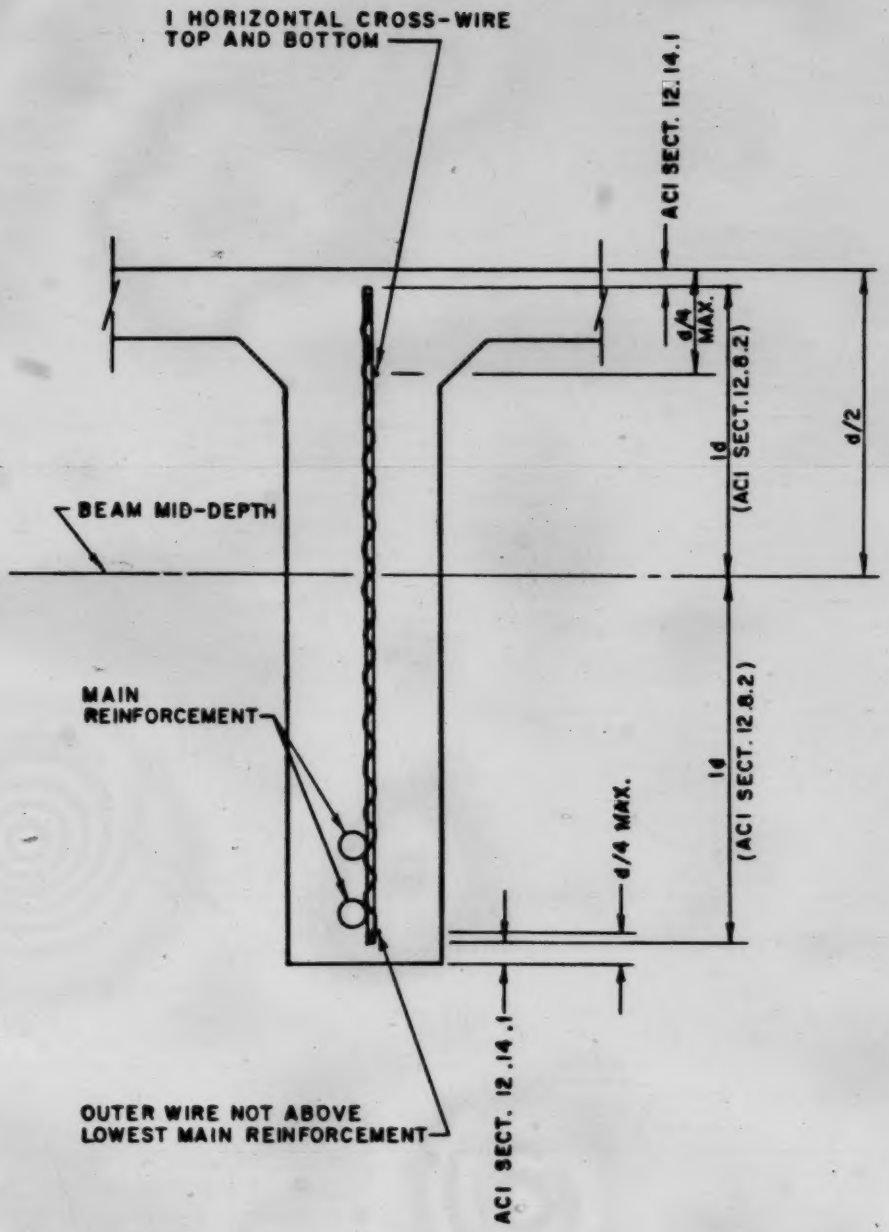

FIGURE 2.3 - PCI/WRI Proposal for Single Leg WWF Shear Reinforcement - Deformed Vertical Wires

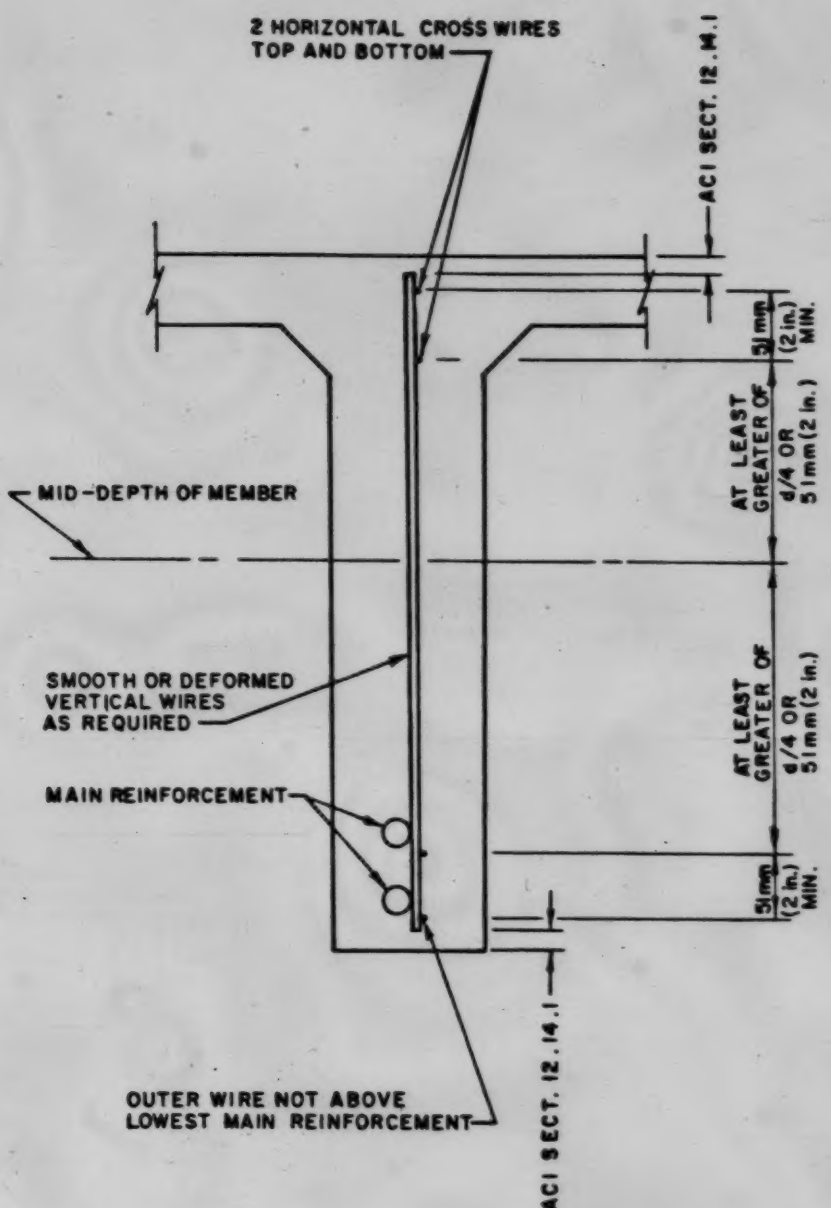
2 HORIZONTAL CROSS WIRES TOP AND BOTTOM
ACI SECT. 12.M.1
51mm (2 in.) MIN.
AT LEAST GREATER OF d/4 OR 51mm (2 in.)
MID-DEPTH OF MEMBER
SMOOTH OR DEFORMED VERTICAL WIRES AS REQUIRED
MAIN REINFORCEMENT
AT LEAST GREATER OF d/4 OR 51mm (2 in.)
51mm (2 in.) MIN.
OUTER WIRE NOT ABOVE LOWEST MAIN REINFORCEMENT
ACI SECT. 12.14.1

FIGURE 2.4 - 1983 ACI Code Proposal for Single Leg WWF Web Reinforcement

recently, there has been little data regarding the anchorage of WWF shear reinforcement.

In 1965, Leonhardt and Walther recommended types of compression zone anchorages for WWF meshes after testing different anchorages using slightly deformed 6 mm (0.24 inch) diameter stirrups. These recommendations are shown in Figure 2.5. No information was provided regarding anchorage in the tension zone since it was assumed that the stirrups would be U-shaped and would enclose the longitudinal bars.

The only section in the ACI 318-77 Code related directly to the development of WWF web reinforcement is in Section 12.14.2.4 which specifies methods of anchorage of smooth welded wire fabric forming simple U-stirrups. This anchorage only applies in the compression zone. There are no specific rules for tension zone anchorage or for other cases involving the use of welded smooth wire fabric or for cases involving the use of welded deformed wire fabric. The requirements for development of WWF in tension in Sections 12.8 and 12.9 of the ACI Code offer some guidelines and the specifications for anchorage of conventional reinforcing bar and deformed wire stirrups can be applied in some cases.

In 1980, proposals for anchoring single sheets of both welded deformed and welded smooth wire fabric in the tension

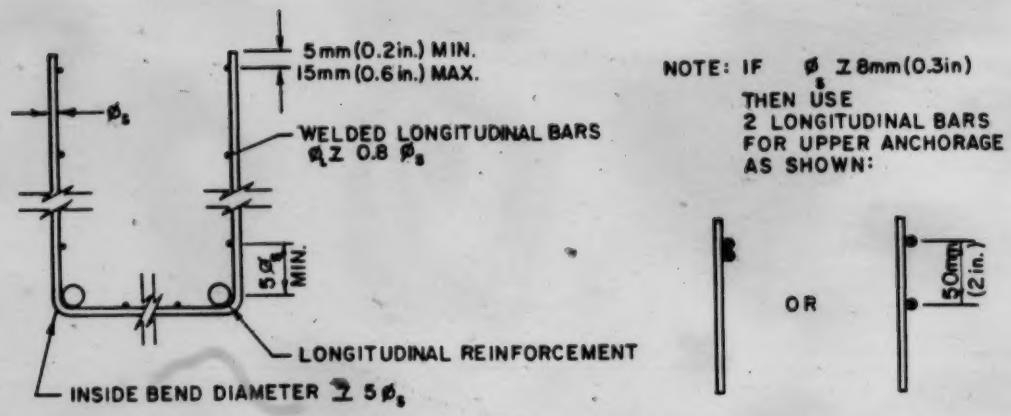

(a) ANCHORAGE WITH WELDED LONGITUDINAL BARS

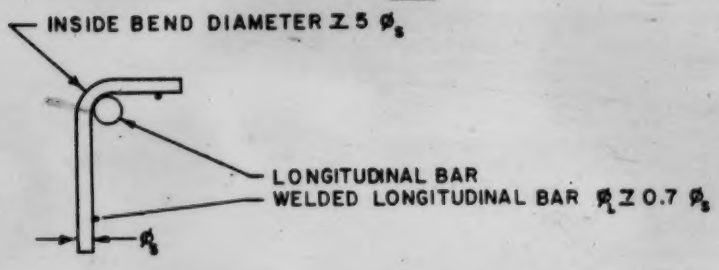

(b) ANCHORAGE WITH 90° HOOKS BENT INWARDS

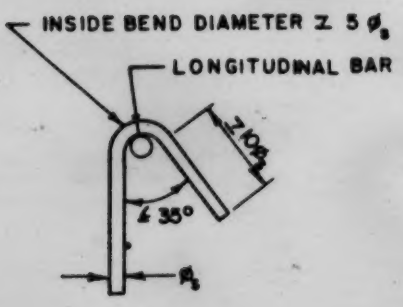

(c) ANCHORAGE WITH HOOKS BENT OUTWARD OR INWARD

FIGURE 2.5 - Anchorage of WWF - Leonhardt and Walther

and compression zones were made by the PCI/WRI Ad Hoc Committee, as described in the previous section. As a result, the use of shear reinforcement made from single sheets of WWF will be specifically permitted in the 1983 ACI Code. However, the method of anchorage has been modified from the Ad Hoc Committee proposals to require two cross wires, top and bottom, as shown in Figure 2.4.

These recent proposals help to clarify the problem of anchorage, but testing is required to investigate the behaviour of beams with this type of web reinforcement. This thesis presents the results of tests of T-beams with shear reinforcement based on the PCI/WRI proposals.

CHAPTER 3

BEAM SPECIMENS

3.1 General

The experimental specimens were designed to evaluate the behaviour of welded wire fabric web reinforcement in reinforced concrete T-beams and to compare this behaviour with that of identical beams having conventional deformed bar stirrups. Particular attention was given to the anchorage of the WWF web reinforcement and to the ductility of the beams. The beam dimensions were chosen to approximate half of a full sized double-tee section. Ten beams were tested in this program. WWF shear reinforcement was used in eight beams and conventional stirrups were used in the remaining two. A summary of the web reinforcement for each beam is given in Table 3.1. TB 1 to TB 8 had WWF web reinforcement while TB 9 and TB 10 had conventional stirrups. The layouts for the WWF meshes are shown in Figures 3.1 to 3.3

3.2 Beam Dimensions

The design dimensions for the T-beams tested included a total depth of 508 mm (20 inches), a flange width of 508 mm (20 inches), a flange depth of 51 mm (2 inches), and a web width of 102 mm (4 inches). The effective depth, d, was 445 mm (17.5 inches). The cross-section is shown in Figure 3.4.

TABLE 3.1

SUMMARY OF BEAM WEB REINFORCEMENT

Beam Number	Stirrup Size	Type of Stirrup Anchorage
TB 1	W2.5 (smooth)	2 horizontal wires top and bottom
TB 2	D2.5 (deformed)	2 horizontal wires top and bottom
TB 3	W2.9 (smooth)	2 horizontal wires top and bottom
TB 4	D2.9 (deformed)	2 horizontal wires top and bottom
TB 5	D2.9 (deformed)	exterior horizontal wire top and bottom
TB 6	D2.5 (deformed)	exterior horizontal wire top and bottom
TB 7	D2.9 (deformed)	interior horizontal wire top and bottom
TB 8*	W2.9 (smooth)	2 horizontal wires top and bottom
TB 9	6 mm (deformed)	180° hook around longitudinal bars
TB 10	6 mm (deformed)	180° hook around longitudinal bars

*Only this beam did not have the WWF web reinforcement centered in the web (see Figure 3.4)

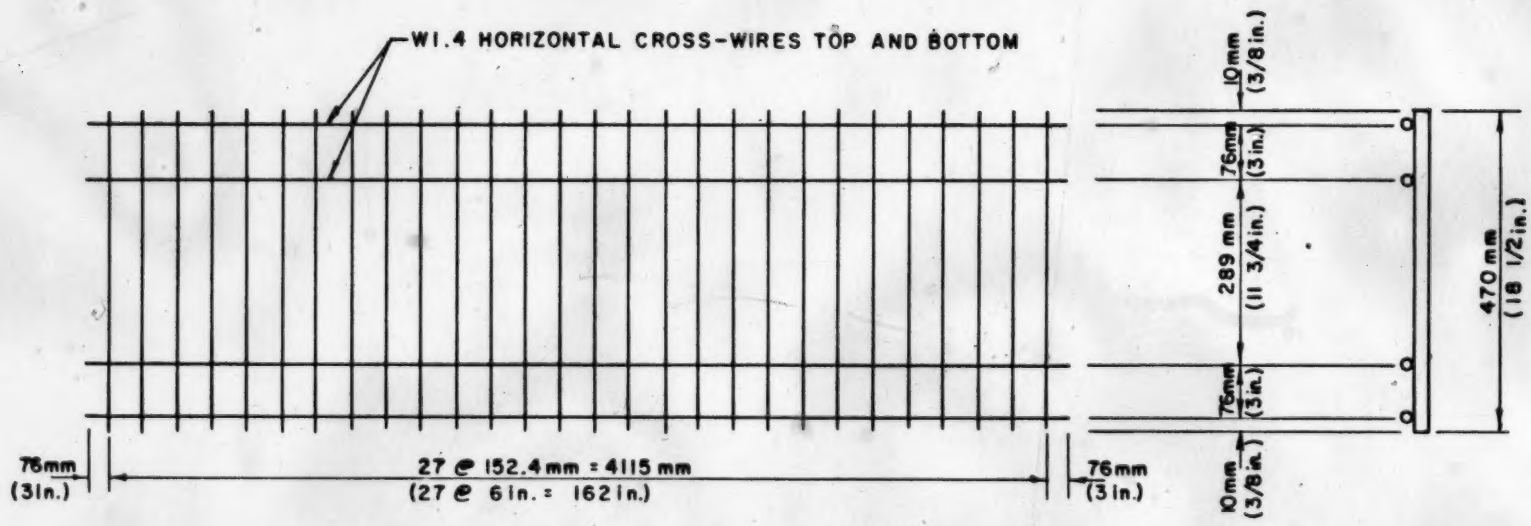

FIGURE 3.1 - Layout of WWF Mesh with 2 Horizontal Cross-Wires Top and Bottom (used in TB 1, TB 2, TB 3, TB 4 and TB 8) (Not to Scale)

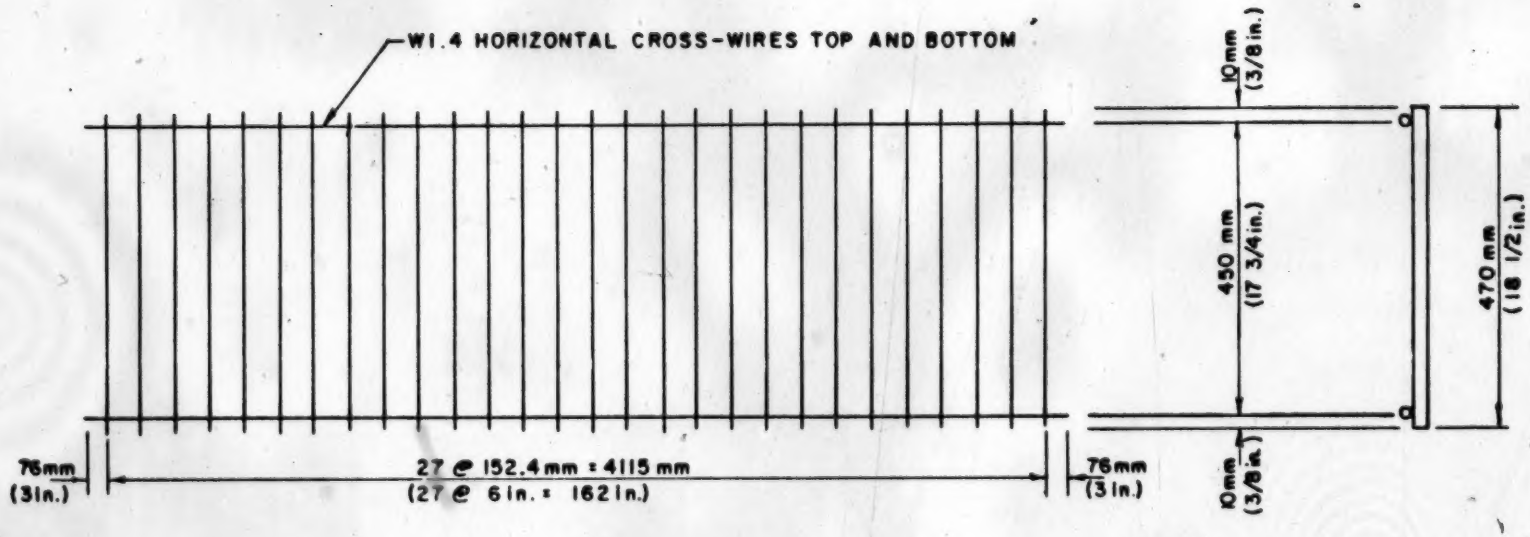
W1.4 HORIZONTAL CROSS-WIRES TOP AND BOTTOM
10mm (3/8 in.)
450 mm (17 3/4 in.)
470 mm (18 1/2 in.)
10mm (3/8 in.)
76mm (3 in.)
27 @ 152.4 mm = 4115 mm
(27 @ 6 in. = 162 in.)
76mm (3 in.)

FIGURE 3.2 - Layout of WWF Mesh with Exterior Horizontal Cross-Wire Top and Bottom (used in TB 5 and TB 6) (Not to Scale)

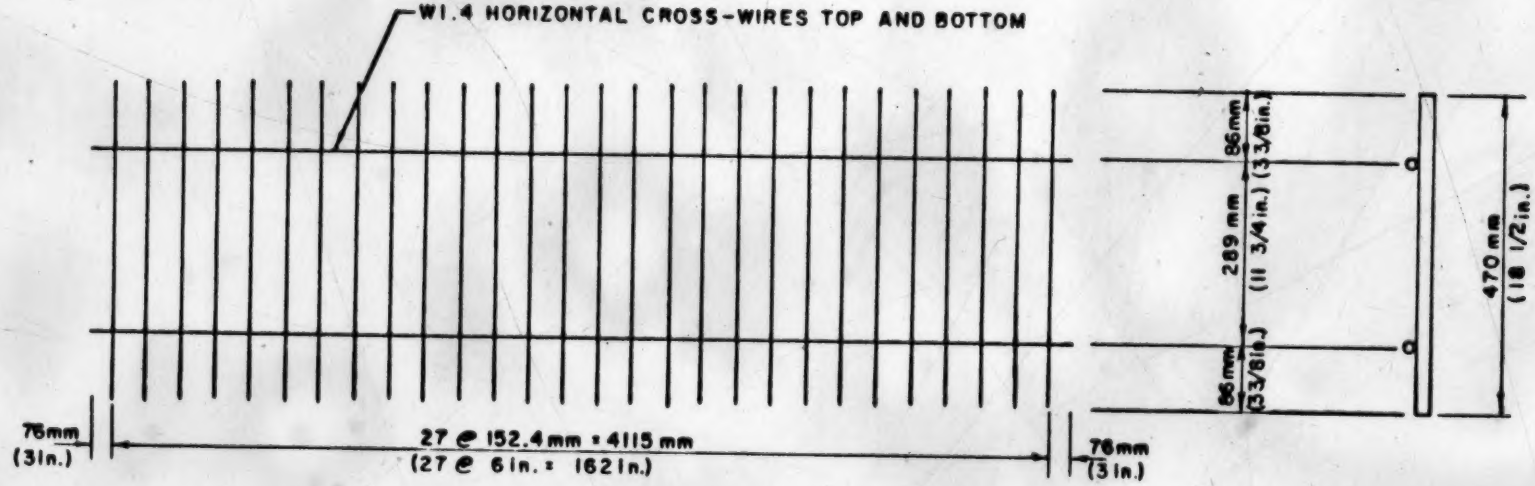

FIGURE 3.3 - Layout of WWF Mesh with Interior Horizontal Cross-Wire Top and Bottom (used in TB 7) (Not to Scale)

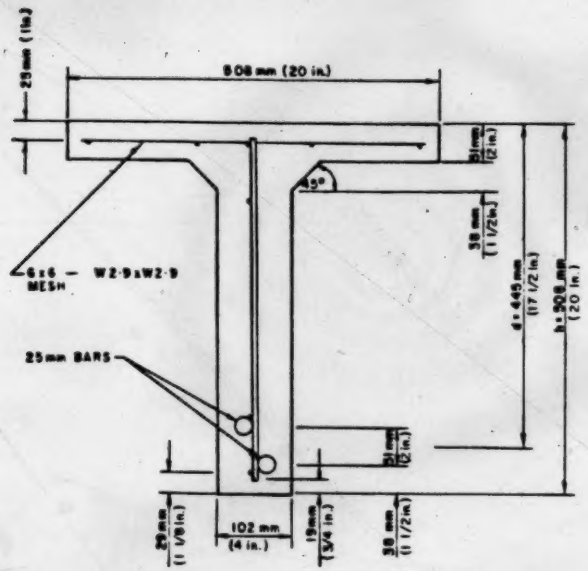

(a) TB 1 to TB 4

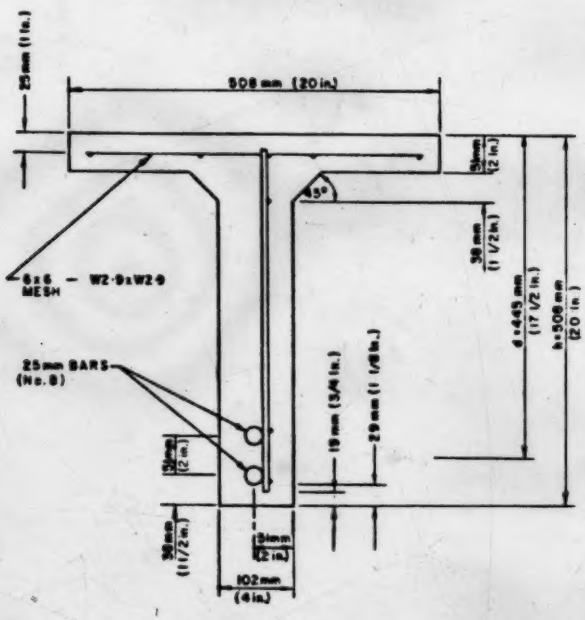

(b) TB 8

FIGURE 3.4 - Typical Cross-Sections of Beam in Testing Program with WWF Web Reinforcement

The overall beam length was 4560 mm (179.5 inches). Two concentrated loads were applied so that the a/d ratio was approximately 3.0, where a was the distance from support to load and d was the effective depth.

The actual beam dimensions varied slightly from the design values. The actual dimensions are summarized in the Appendix.

3.3 Shear Reinforcement

3.3.1 Single Leg WWF Mesh

The WWF web reinforcement was selected to conform to the recommendations presented by the Joint PCI/WRI Ad Hoc Committee (PCI/WRI, 1980). The meshes used consisted of W2.5, D2.5, W2.9 or D2.9 vertical wires at 152 mm (6 inch) spacings because these represent wire sizes and spacings commonly used by double-tee manufacturers. Both welded smooth and deformed wire meshes were used so that the behaviour of each of these could be investigated.

The anchorage of the WWF was also made according to the proposals of the Ad Hoc Committee as shown in Figures 2.2 and 2.3. Two horizontal W1.4 wires were used at the top and at the bottom for anchorage of the smooth wire meshes. The deformed wire meshes were anchored with either one or two W1.4 horizontal wires top and bottom.

The WWF meshes were made by a local member company of the WRI. The wires were manufactured from hot rolled rods which were cold-drawn to the specified diameters. The deformations for the deformed wires were crimped into the wires using gears as the wire was being cold-drawn. The welds in the meshes were done by an automatic welding machine.

The WWF was centered in the web of the beam except for TB 8 where the mesh was offset from the web centerline by about 12 mm (0.5 in.). Typical cross-sections showing the location of the WWF are in Figure 3.4. There was approximately 20 mm (0.75 inches) of cover between the ends of the vertical wires and the surface of the beams.

3.3.2 Conventional Reinforcement Stirrups

The conventional rebar stirrup arrangement was selected to give approximately the same design value for V_s as for the WWF arrangements. The stirrups had a single leg with 180 degrees hooks at each end and were made of deformed 6 mm (0.24 inch) diameter reinforcing bars manufactured in Sweden. The deformations were in the form of raised ribs which were perpendicular to the longitudinal axis of the bars. At the top of the beam, the hook was placed around a 9.5 mm (No. 3) longitudinal bar to improve the anchorage.

The clear cover from the upper surface of the flange to the top of the hooks was about 20 mm (0.75 inches). The bottom hooks fit around the main longitudinal reinforcement. The stirrup spacing was 220 mm (8.67 inches) center to center. The orientation of the stirrups was alternated so that all of the stirrup legs would not be on the same side of the web. Figure 3.5 shows a typical cross-section with this type of stirrup.

3.4 Main Longitudinal Reinforcement

Two 25 mm (No. 8) bars were used for the main reinforcement. To ensure that a shear failure occurred, the beams were designed so that the flexural strength was approximately 1.5 times as large as the shear strength. The main steel was anchored using 90 degree bends in the overhanging section of the beam. The reinforcement ratio, ρ_w, was about 0.022.

The center of gravity of the 25 mm bars was at the vertical centerline of the web for all of the beams. One bar was placed on each side of the web reinforcement in the beams that had the WWF located at the web centerline (beams TB 1 to TB 7). For the other beams, the two bars were placed at the centerline, one above the other. This is illustrated in Figures 3.4 and 3.5.

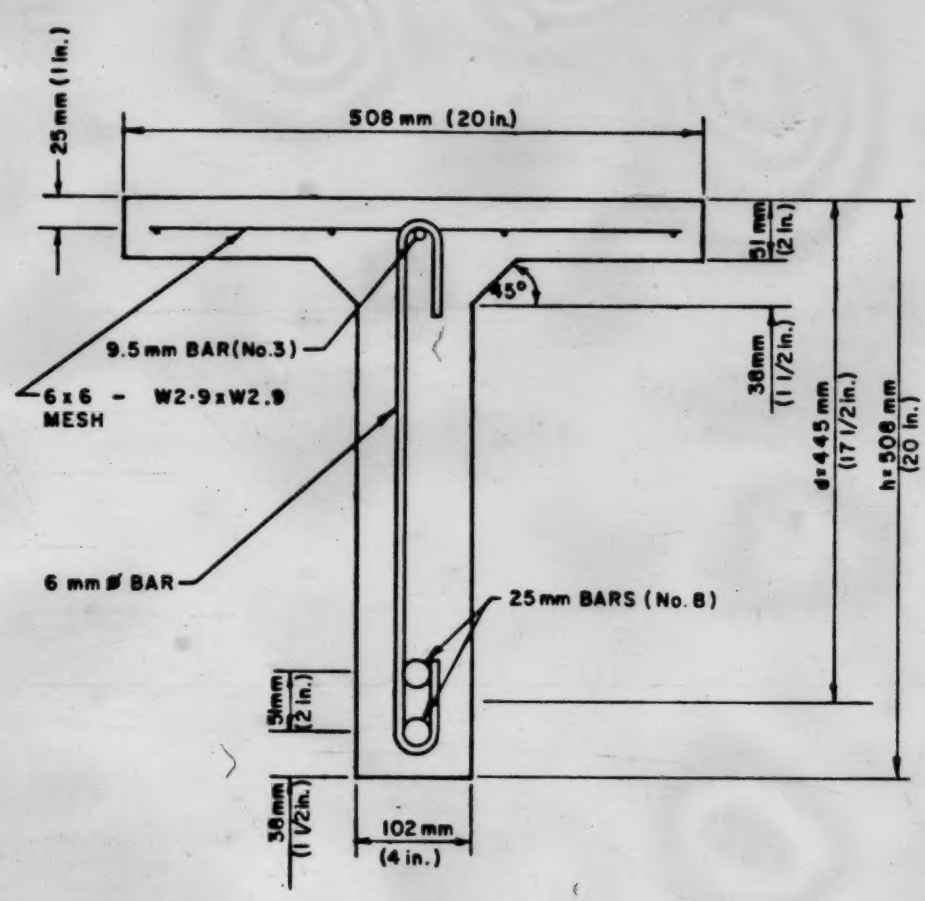
25 mm (1 in.)
508 mm (20 in.)
51 mm (2 in.)
45°
9.5 mm BAR (No.3)
6 x 6 - W2·9 x W2.9 MESH
38mm (1 1/2 in.)
d = 445 mm (17 1/2 in.)
h = 508 mm (20 in.)
6 mm ø BAR
25 mm BARS (No. 8)
38mm (1 1/2 in.)
38mm (1 1/2 in.)
102 mm (4 in.)

FIGURE 3.5 - Typical Cross-Section of Beam in Testing Program with Conventional 6 mm Diamter Stirrups

3.5 Flange Reinforcement

Flange reinforcement consisting of 6 x 6 - W2.9 x W2.9 mesh was placed within the center 3050 mm (120 inches) of each beam at mid-depth of the flange. This reinforcement was intended to ensure that longitudinal cracks in the flange would not separate the flange of the beam from the web at failure.

3.6 Beam Construction

The beams were constructed in the laboratory at the University of Alberta. The reinforcing cages were put together using tie-wire. Cement and plastic chairs were used to position the cages in the forms. The forms were constructed of steel and wood with a painted interior surface for protection and to give a smooth finish to the concrete. Two beams were cast at one time. The concrete was vibrated using a hand held vibrator. Four batches of concrete were required for each casting and three or four concrete test cylinders were made from each batch.

The beams were covered with wet burlap and enclosed in plastic for approximately one week after they were made. They were then allowed to cure uncovered in the laboratory until the time of testing. The test cylinders were cured in the same manner so as to get a better representation of the actual properties of the concrete in the beams.

Figures 3.6 and 3.7 show the reinforcement layouts for two typical beams. Figure 3.6 shows the typical layout for TB 1 to TB 8 with WWF web reinforcement. The only change in this layout would be in the location and number of horizontal anchorage wires. Figure 3.7 shows the layout used for TB 9 and TB 10.

Some photographs of construction are shown in Figures 3.8 to 3.10. Figure 3.8 shows the reinforcement in place in the forms just prior to concrete placement. Figures 3.9 and 3.10 show the reinforcing cages for TB 7 and TB 6 as well as the tying of the WWF to the main longitudinal reinforcement.

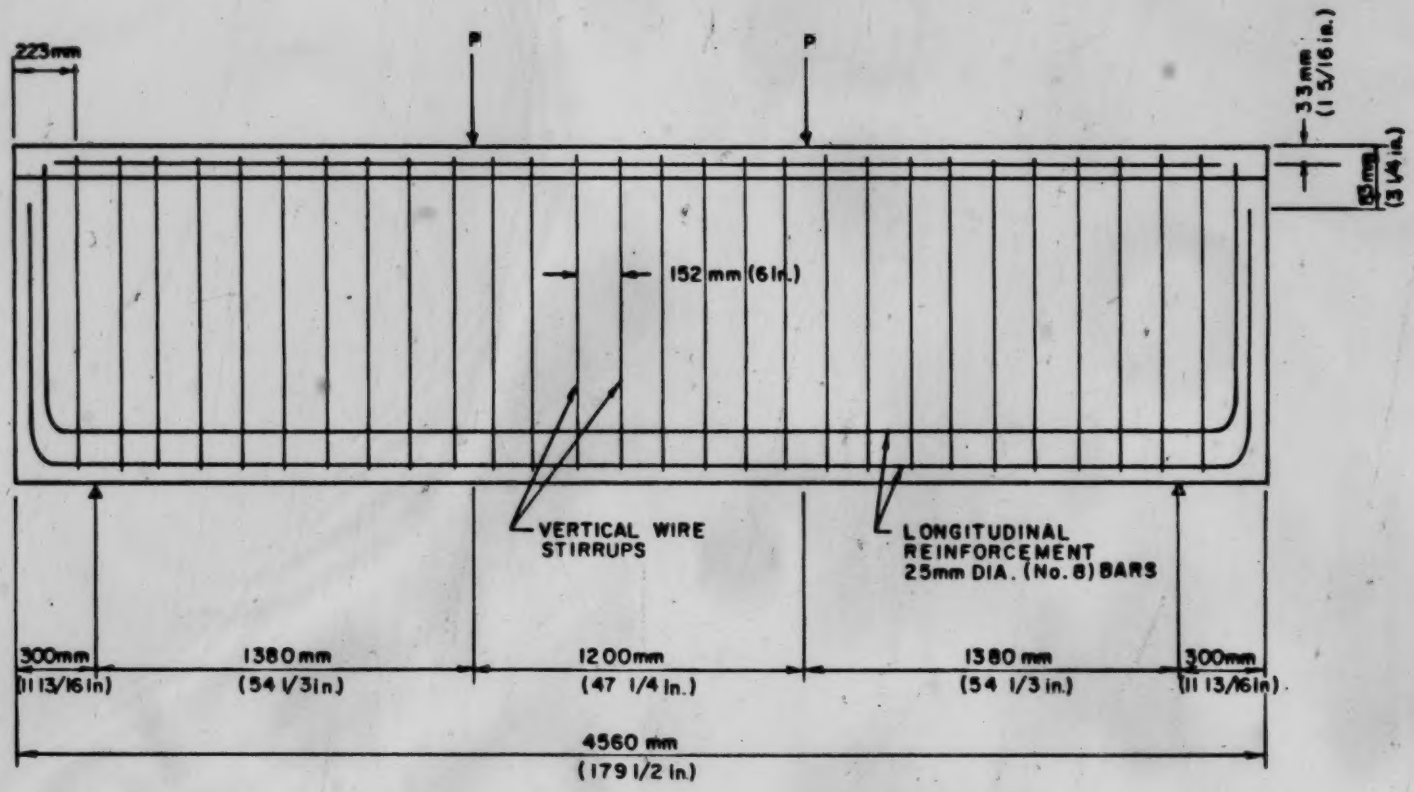

FIGURE 3.6 - Beam Elevation Showing Reinforcement Layout with WWF Web Reinforcement (Not to Scale)

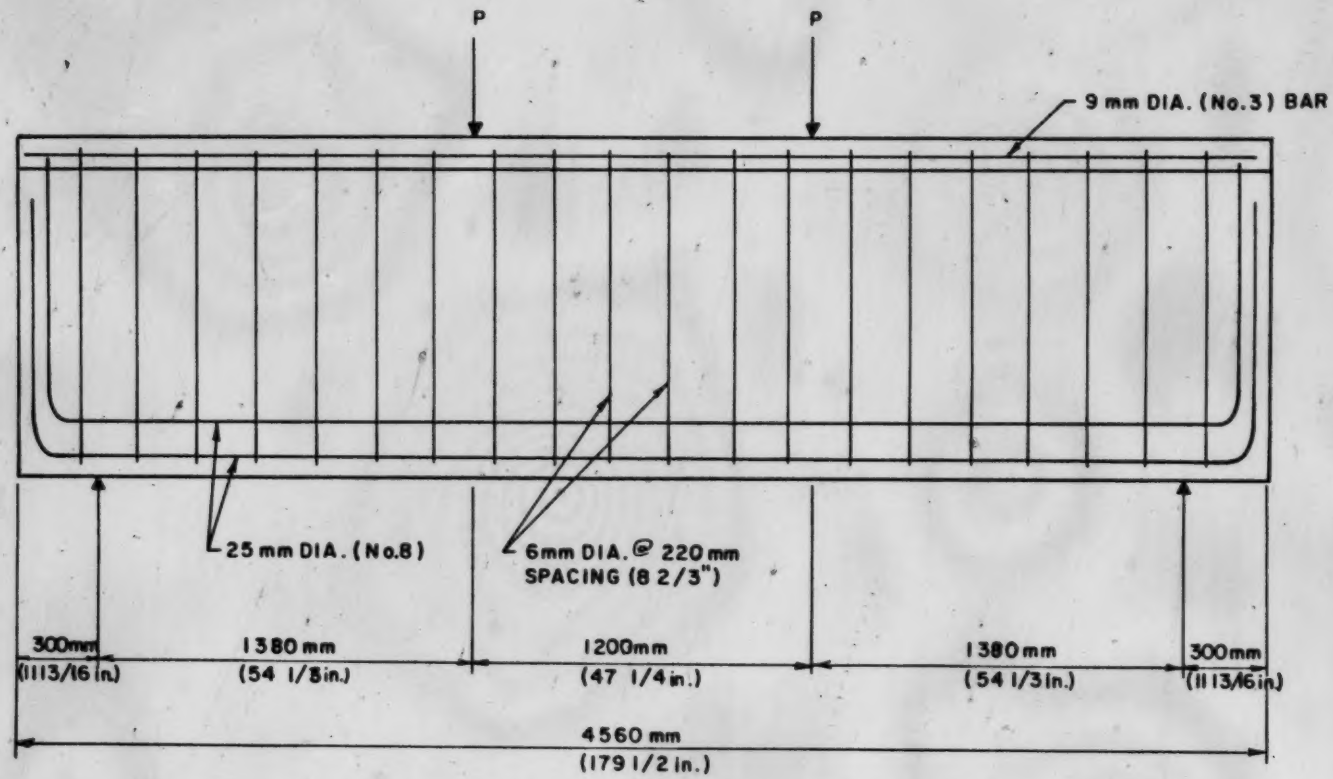

FIGURE 3.7 - Beam Elevation Showing Reinforcement Layout with Conventional 6 mm Diameter Stirrups (Not to Scale)

FIGURE 3.8 - Reinforcement in forms prior to concrete placement - TB 2

FIGURE 3.9 - Reinforcement cage for TB 7

FIGURE 3.10 - Reinforcement cage for TB 6

CHAPTER 4

MATERIAL PROPERTIES

4.1 Reinforcement Properties

4.1.1 WWF Mesh

The vertical wire sizes used in the WWF meshes were W2.5, D2.5, W2.9 and D2.9. The longitudinal wire size for all meshes was W1.4. The specified and measured dimensions of the wires are summarized in Table 4.1. The measured area was determined from the weight of the wire specimen using the unit density of steel of 7850 kg/m^3. The deformation dimensions were measured according to the applicable ASTM standards.

As shown in Table 4.1, there was considerable variation in some of the wire dimensions for the deformed wires. However, the average values for deformation spacing and height for the D2.9 wires met the specification requirements and the average measured area for this wire size was very close to the nominal area. The average height of deformation and the deformation spacing were larger for the D2.5 wires than for the D2.9 wires. The deformation spacing for the D2.5 wire was slightly larger than the ASTM and CSA specifications but the deformation height met the requirements of these specifications. Also, the average measured area was lower than the nominal area for this wire size.

TABLE 4.1

DIMENSIONS OF WIRE STIRRUPS

Wire Size	Cross-Sectional Area		Nominal Diameter		Height of Deformations			Deformation Spacing	
	Nominal sq. mm	Measured[1] sq. mm	Specified mm	Measured[1] mm	Specified[2] Minimum mm	Measured Range mm	Measured Average mm	Specified[2] mm	Measured mm
W2.5	16.1	15.8	4.52	4.49	-	-	-	-	-
D2.5	16.1	14.9	4.52	4.37	0.181	0.191 to 0.368	0.309	4.62 to 7.24	8.9
W2.9	18.7	18.3	4.88	4.83	-	-	-	-	-
D2.9	18.7	18.3 to 19.5	4.88	4.83 to 4.99	0.195	0.089 to 0.381	0.209	4.62 to 7.24	6.5
W1.4	9.03	-	3.40	-	-	-	-	-	-

(1) Determined from weight of specimens

(2) From ASTM A496 - Standard specification for deformed steel wire for concrete reinforcement

The stress-strain curves and ultimate elongation were determined from tension tests done using the vertical wires from the meshes. The initial portion of the curve up to a strain of 0.005 was obtained using an extensometer with a 51 mm (2 inch) gauge length and a load-strain plotter. A 203 mm (8 inch) gauge length using center punched gauge marks was used to obtain strain readings for the remainder of the curve as well as ultimate strain. The standard 254 mm (10 inch) gauge length was not used because of the short length of the test specimens.

The tension test results are summarized in Table 4.2. The results from individual tests are shown in the Appendix along with test data supplied by the manufacturer. It should be noted that all stress calculations are based on nominal area. Typical stress-strain curves obtained from tension tests are shown in Figure 4.1. These show the range in the results.

Tests were done with and without welded cross-wires located between the gauge marks. In the former case, the welded cross-wire was located within the gauge length, approximately 15 mm (0.6 inches) from one end of it. The initial portion of the stress-strain curve and the ultimate load were not affected when failure occurred at welded cross-wires in the specimen. Also, in the case of deformed wire,

TABLE 4.2

AVERAGE WIRE TENSION TEST RESULTS

Wire Size	$f_{y,ACI}$[1] MPa	$f_{y,ASTM}$[2] MPa	f_{su} MPa	ε_u %	E From Test MPa
W2.5	625	673	693	1.4[3] 3.1[4]	203×10^3
D2.5	494	522	536	1.1	180×10^3
W2.9	563	597	640	2.8	205×10^3
D2.9	545	577	604	1.6	199×10^3

(1) Stress measured at $\varepsilon = 0.0035$

(2) Stress measured at $\varepsilon = 0.005$

(3) ε_u for failure at cross-wire

(4) ε_u for failure away from cross-wire

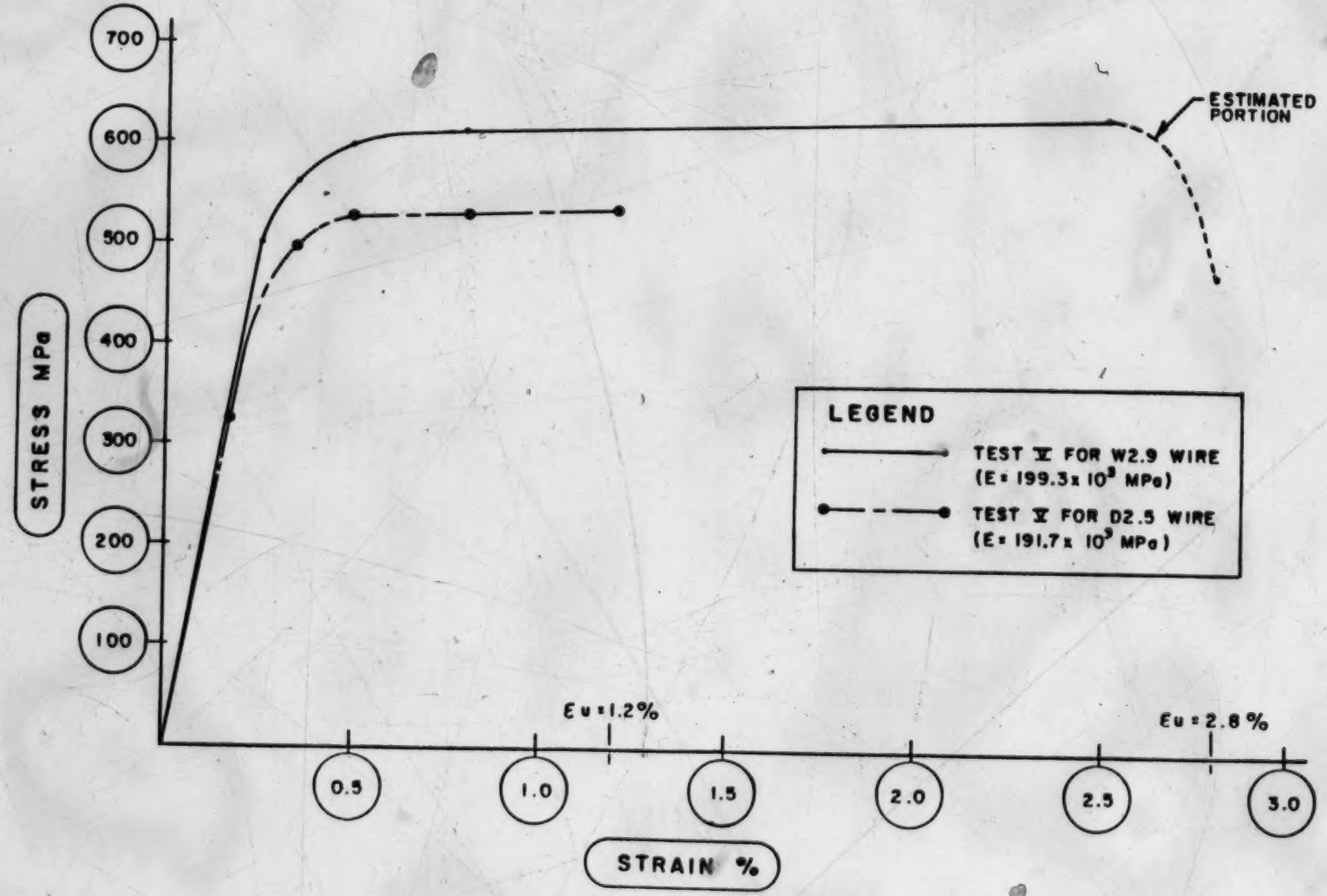

FIGURE 4.1 - Typical Stress-Strain Curves for Wires

the value of ultimate strain was unchanged whether failure occurred at or away from the cross-wires. The ultimate strain of the W2.5 wire was higher when failure occurred away from the cross-wires than when failure occurred at the cross-wires. In the case of the W2.9 wire, no failures occurred at the cross-wires within the gauge length.

Several test specimens failed either in the grips or outside of the gauge marks. Such tests were not considered when determining the ultimate strain, but the results for the initial portion of the stress-strain curve and for the ultimate load were considered to be valid.

The smooth wire had higher ultimate loads and ultimate strains than the deformed wire. This was partly due to the reduced cross-sectional area of the deformed wires at the deformation indents. The deformed wire specimens that did not fail at the cross wires failed at these deformation indents.

Reduction in area measurements as specified in ASTM A82 (CSA G30.3) were made using the smooth wire specimens. As mentioned by Mr. Dove (1982) in his discussion of the Mirza and MacGregor paper (1981), the reduction in area is a measure of the ductility in the wire. The reduction in area was between 55 and 60 percent for the smooth wire. This was

almost twice the specified ASTM and CSA requirement. On the other hand, the measured strains at failure ranged from 1.1 percent in the case of the D2.5 wire to 2.8 percent in the case of the W2.9 wire indicating relatively little ductility. There is no requirement in the ASTM and CSA Standards for reduction of area for deformed bars. No weld shear tests or bend tests were performed.

4.1.2 Conventional Reinforcement Stirrups

The stress-strain curve for the 6 mm (0.24 inch) diameter stirrup shown in Figure 4.2 was determined using the same test procedure as for the WWF wires. The cross-sectional area determined by weighing a sample of the bar was 34.0 square mm (0.0527 square inches). Using this value for the area, the yield strength, f_y, was 477 MPa (69.2 ksi) and the ultimate strength, f_{su}, was 659 MPa (95.6 ksi). The ultimate strain, ε_u, was approximately 15 percent.

4.1.3 Main Longitudinal Reinforcement

The 25 mm (No. 8) bars used for the main reinforcement had a yield strength, f_y, of 348 MPa (50.5 ksi) and an ultimate strength, f_{su}, of 574 MPa (83.3 ksi). All calculations are based on the nominal area of 500 square mm (0.78 square inches). The ultimate strain, ε_u, was aproximately 15 percent.

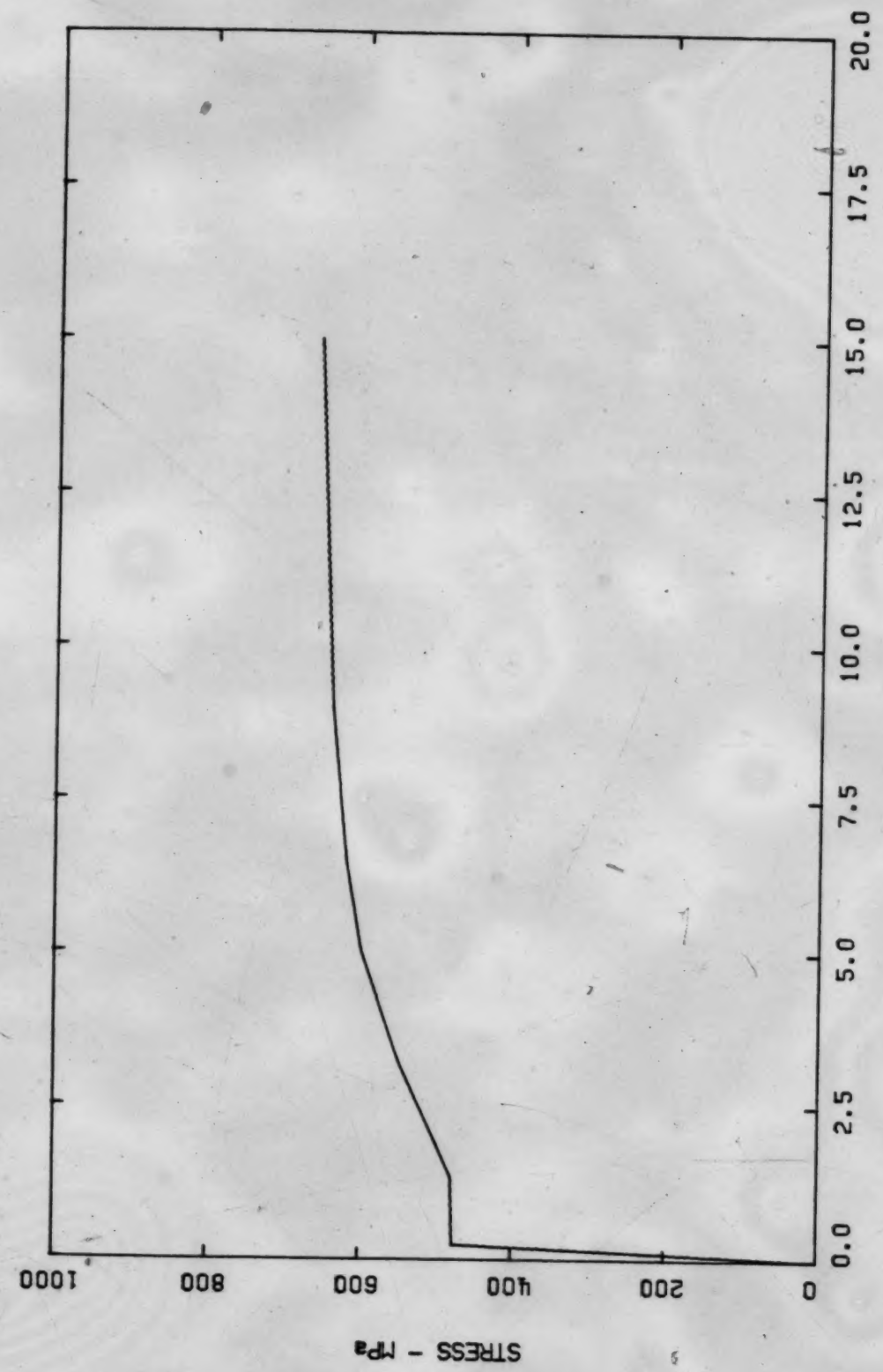

FIGURE 4.2 - Stress-Strain Curve for 6 mm Diameter Stirrup Bars

4.2 Concrete Properties

Two mix designs were used in the program. The mix design used in TB 1 and TB 3 had a compressive strength of approximately 20 MPa (2900 psi) at the time of testing and the remaining beams used a mix design with a compressive strength of approximately 30 MPa (4350 psi). In both cases, the concrete was made with normal Portland cement and a maximum aggregate size of 10 mm (3/8 inch). No additives were used. The average slump was approximately 100 mm (4 inches).

The compressive strength, f'_c, Young's Modulus, E, and the tensile splitting strengths for the concrete used in each beam are shown in Table 4.3. The concrete cylinders used for testing were 152 mm (6 inches) in diameter and 305 mm (12 inches) in length. They were prepared and tested in accordance with the applicable ASTM and CSA Standards.

TABLE 4.3

CONCRETE PROPERTIES

Beam No.	Average Compressive Strength f'_c MPa	Young's Modulus from Test E MPa	Tensile Splitting Strength MPa	Beam Age at Test
TB 1	19.1	15900 17400	2.61 2.16	70
TB 2	28.9	19700 18600 19600 19500	2.47 2.50 2.44	51
TB 3	19.4	14400 18200	2.38	77
TB 4	29.3	20800 21700	3.16 2.75	61
TB 5	28.6	18100 21300	2.64 2.61	56
TB 6	30.7	20800 21300 18700 20400	2.91 2.91 2.92	59
TB 7	29.5	18800 18800 20300 21300	2.66 2.64 2.90	57
TB 8	29.5	See TB 7	See TB 7	54
TB 9	28.9	See TB 2	See TB 2	47
TB 10	30.7	See TB 6	See TB 6	62

CHAPTER 5

TESTING PROGRAM

5.1 General

The beams were tested using a two-point loading arrangement on a simple span to give a region of constant shear (excluding self weight) at each end and a region of zero shear in the center. The data taken during testing included load measurements, deflections at midspan and load points, slip of the web reinforcement, crack widths, and stirrup strain. The propagation of the cracks during loading was also marked. This data was considered to be the most important for the analysis of beam behaviour, beam ductility and anchorage of web reinforcement.

5.2 Test Set-up

The testing was done using a 6.2 MN (1.4 million pound) MTS testing machine which applied load from above the beam. The test set-up is shown in Figure 5.1. The actual shear spans varied slightly from the values shown in the figure. The actual a/d values are given in the Appendix. Figure 5.2 shows a photograph of the test set-up.

5.3 Instrumentation

5.3.1 Load Measurement

The load was recorded directly from the MTS machine. The beam point loads were one-half of this. During the testing

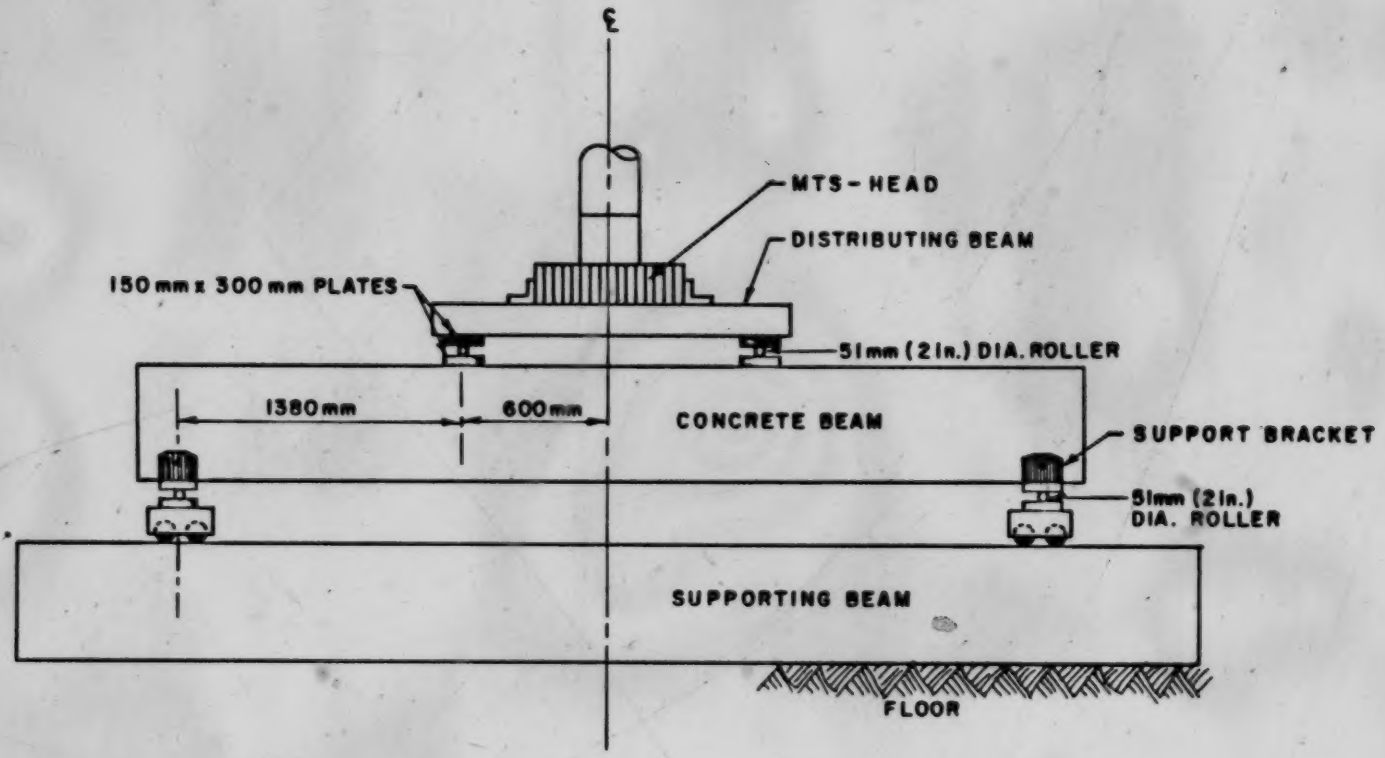

FIGURE 5.1 - Beam Loading Arrangement

FIGURE 5.2 - Beam test set-up

of TB 1, TB 3, TB 4 and TB 5, the load was recorded from the digital display on the machine but for the remaining tests the load was recorded directly by the NOVA computer. The machine could be read to the nearest 0.1 kN. At this load level, the machine was accurate to within $\pm$ 0.2 kN.

5.3.2 Beam Deflection

Deflection was measured at the midspan of the beam and at both load points using linear variable differential transformers (LVDT) with a range of $\pm$ 75 mm (3 inches). For TB 1, TB 3, TB 4 and TB 5, the LVDT voltage was recorded using a digital voltmeter, but for the remaining tests the readings were recorded by the computer.

Load-deflection graphs were plotted using the MTS plotter for the tests of TB 2, TB 6, TB 7, TB 8 and TB10. In these plots, the load was the MTS load and the deflection was the deflection of the MTS loading head. These graphs were made for comparison with the LVDT data and to monitor the deflection at failure.

5.3.3 Stirrup Strain Gauges

Foil type electrical resistance strain gauges were used to measure stirrup strain. The gauge lengths were 1.5 mm (0.06 inches) and the gauge factors were 2.02 $\pm$ 1.0 percent at 24^{o}C (75^{o}F). One gauge was installed at each location

where the strain was measured. The gauges were waterproofed and wrapped in tape for protection. The lengths of the wrapped portions averaged about 35 mm (1.5 in.). In order to get a smooth surface to mount the gauges on the deformed wire in the WWF, some of the deformations had to be ground down. This was done very carefully so as not to significantly reduce the cross-sectional area of the wire at the base of the deformation.

The locations where the gauges were mounted are shown in Figure 5.3 for the beams with WWF and in Figure 5.4 for the beams with conventional stirrups. TB 1, TB 2, TB 6, TB 8 and TB 9 had all 16 gauges while the other beams only had gauges 5, 8, 10 and 11. Not all of the gauges worked properly as some were damaged during construction.

Figures 5.5 and 5.6 show photographs of some strain gauges installed on the stirrups in TB 9.

The strains were recorded using a digital voltmeter for the tests of TB 1, TB 3 and TB 5. A Budd Strain Indicator was used to determine the strains for the test of TB 4. The strains were automatically recorded by computer for the other tests.

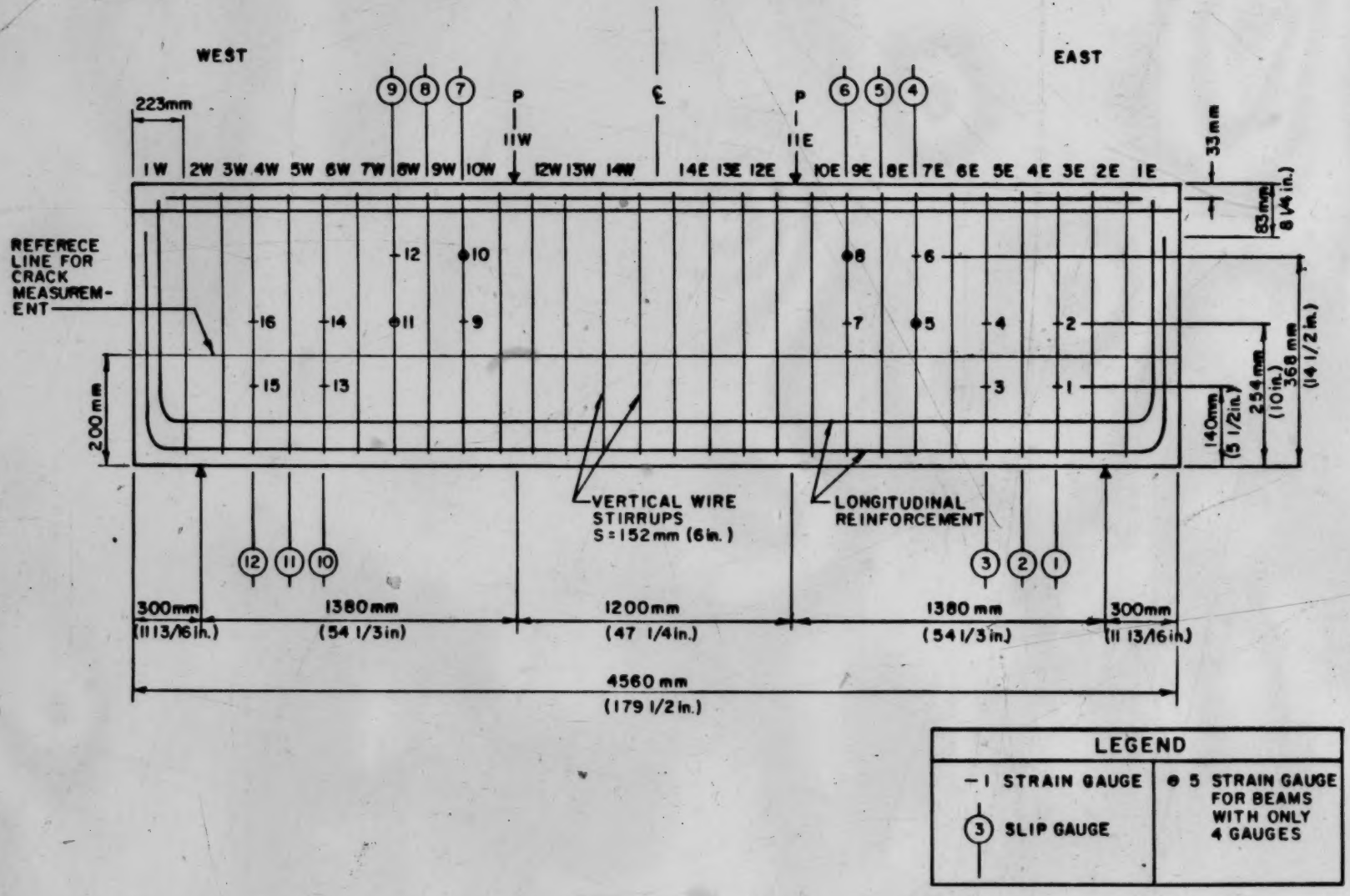
WEST
EAST
223mm
P
P
℄
1W 2W 3W 4W 5W 6W 7W 8W 9W 10W 11W 12W 13W 14W 14E 13E 12E 11E 10E 9E 8E 7E 6E 5E 4E 3E 2E 1E
33mm
83mm (3 1/4 in.)
REFERECE LINE FOR CRACK MEASUREMENT
200 mm
140mm (5 1/2in.)
254 mm (10in.)
368 mm (14 1/2 in.)
VERTICAL WIRE STIRRUPS S=152mm (6in.)
LONGITUDINAL REINFORCEMENT
300mm (11 13/16 in.)
1380mm (54 1/3in)
1200mm (47 1/4in.)
1380 mm (54 1/3 in.)
300mm (11 13/16 in.)
4560 mm (179 1/2 in.)
LEGEND
1 STRAIN GAUGE
3 SLIP GAUGE
5 STRAIN GAUGE FOR BEAMS WITH ONLY 4 GAUGES

FIGURE 5.3 - Locations for Instrumentation for Beams with WWF Web Reinforcement (Not to Scale)

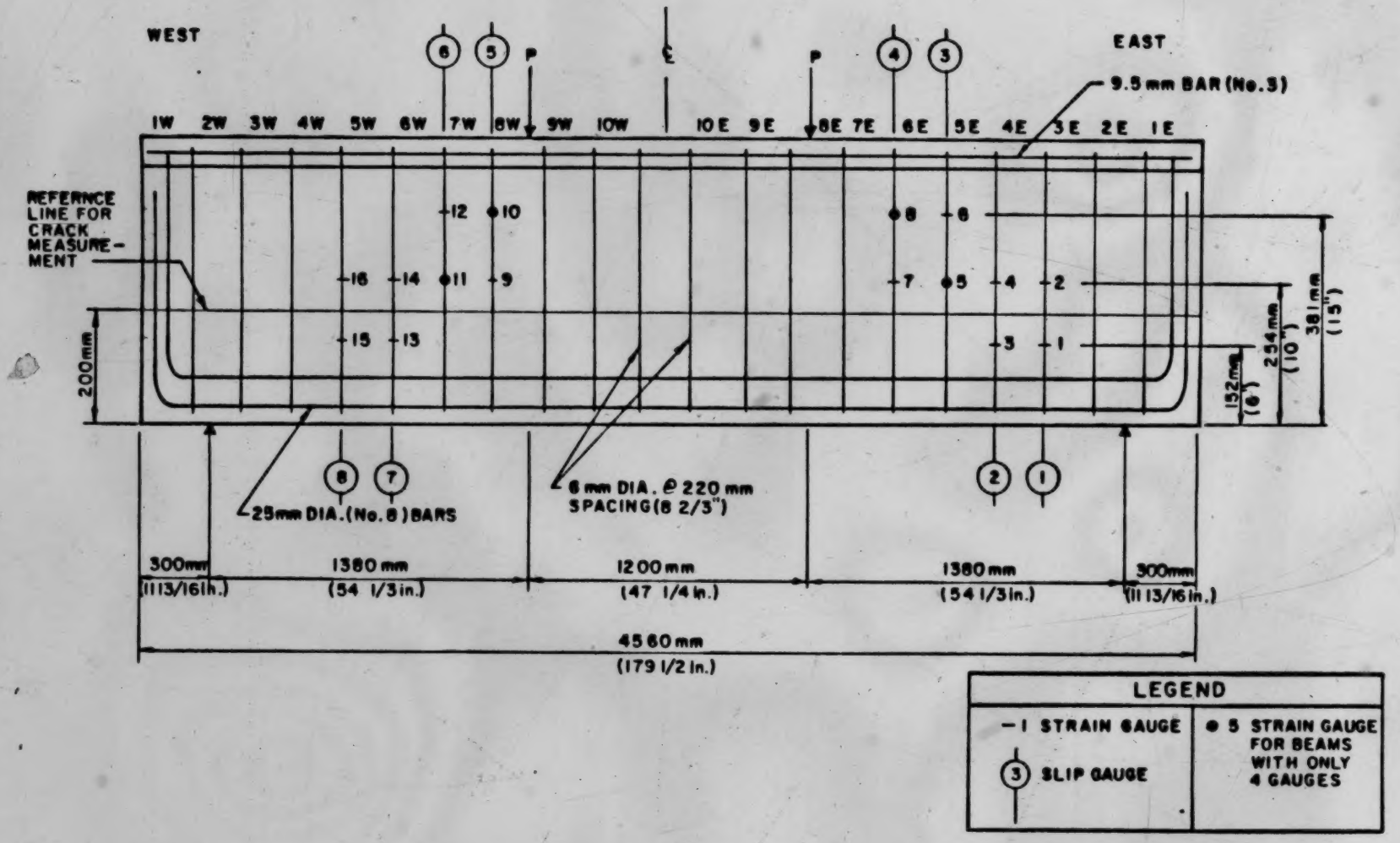
WEST
EAST
9.5 mm BAR (No.3)
1W 2W 3W 4W 5W 6W 7W 8W 9W 10W 10E 9E 8E 7E 6E 5E 4E 3E 2E 1E
REFERNCE LINE FOR CRACK MEASURE-MENT
200mm
25mm DIA.(No.8)BARS
6 mm DIA. @ 220 mm SPACING(8 2/3")
132mm (6")
234mm (10")
381mm (15")
300mm (11 13/16in.)
1380 mm (54 1/3in.)
1200 mm (47 1/4 in.)
1380 mm (54 1/3in.)
300mm (11 13/16in.)
4560 mm (179 1/2 in.)
LEGEND
1 STRAIN GAUGE
3 SLIP GAUGE
5 STRAIN GAUGE FOR BEAMS WITH ONLY 4 GAUGES

FIGURE 5.4 - Locations for Instrumentation for Beams with Conventional 6 mm Diameter Stirrups (Not to Scale)

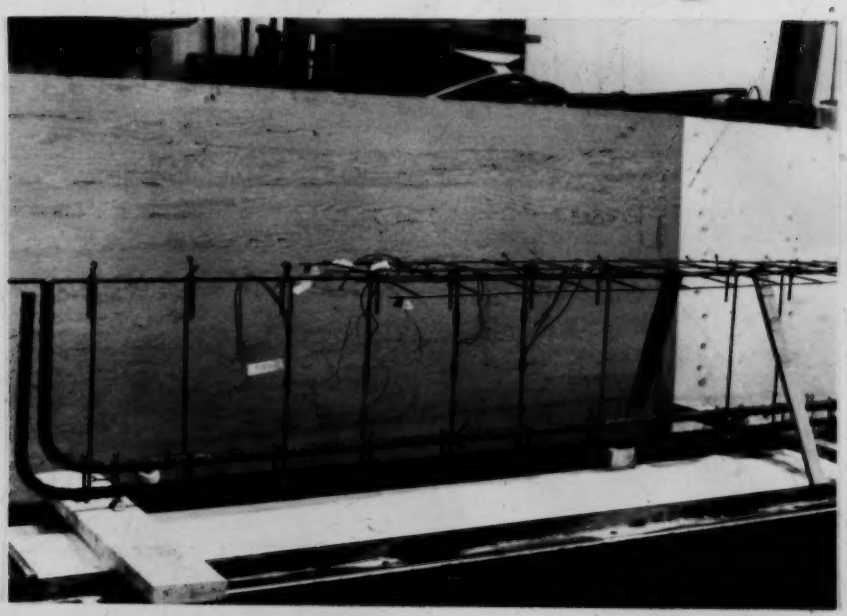

FIGURE 5.5 - Reinforcement cage for TB 9 with strain gauges installed

FIGURE 5.6 - Strain gauges on stirrup in TB 9 (also note lug brazed on near the top of the stirrup)

5.3.4 Stirrup Slip Measurements

Dial gauges with an accuracy of 0.0025 mm (0.0001 inches) were used to measure stirrup slip. The base of the dial gauge apparatus was attached to the concrete beam and the stem of the gauge was placed so that it rested on the top of a stirrup wire. The slip was measured as the change in the dial reading. Photographs of the slip gauges are shown in Figures 5.7 and 5.8. Figure 5.9 shows a diagram of this arrangement. During construction, rubber hose was placed around the ends of the stirrups that were to be monitored for slip. This hose was removed before testing, leaving a space for the stem of the dial gauge. Lugs were brazed onto the 6 mm diameter stirrups near the point of tangency of the 180 degree hooks to provide a suitable location for measuring their slip. This is shown in Figure 5.9. Lugs were also brazed onto the ends of the wire stirrups in cases where it would not otherwise have been possible to get a measurement. The locations and numbering for the slip measurements are shown in Figures 5.3 and 5.4. Slip was not measured at locations 1, 2 and 3 in TB 2, TB 4 and TB 5 in order to determine whether the absence of the slip measuring holes in the bottom of the beam had any effect on the crack formation. It appeared that these holes had no effect. It should also be noted that during testing several of the dial gauges used to measure the slip from the bottom of the beam

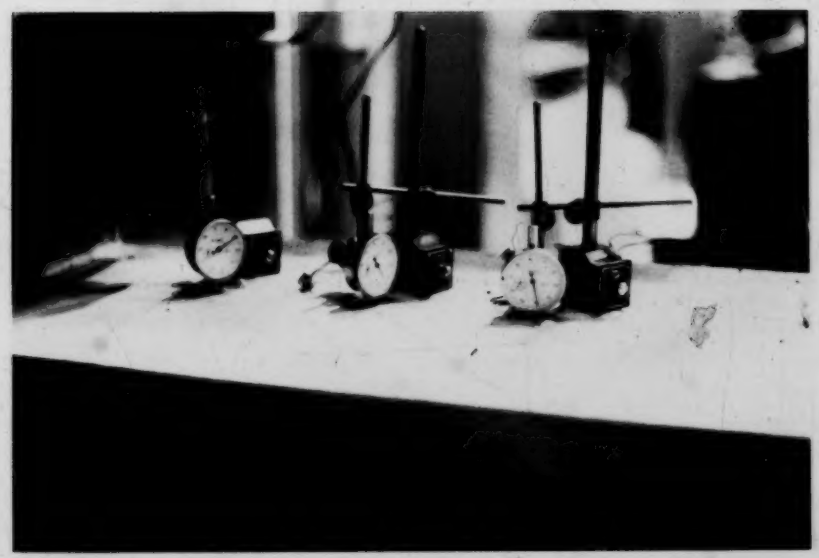

FIGURE 5.7 - Dial gauges for measuring stirrup slip from top of beam

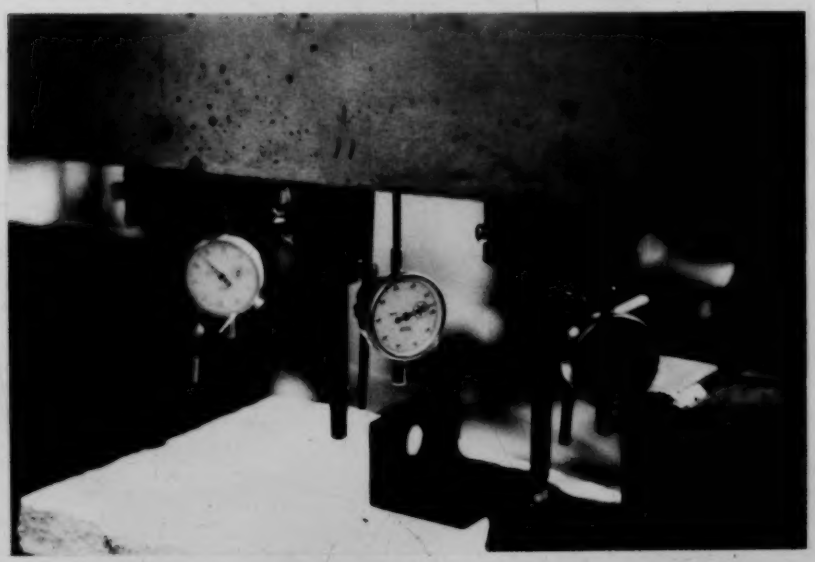

FIGURE 5.8 - Dial gauges for measuring stirrup slip from bottom of beam

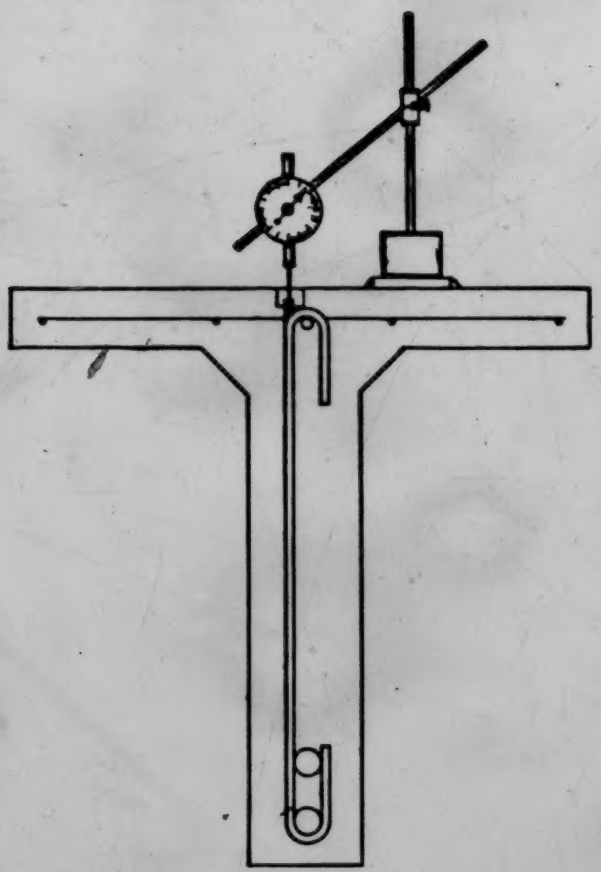

FIGURE 5.9 - Mounting of Dial Gauge Apparatus for Measuring Stirrup Slip

fell off, so that readings could not be taken right up to failure.

5.3.5 Crack Data

The crack widths and crack growth were monitored during testing. Crack inclination was measured after failure.

The crack widths were determined by comparing the width of the crack to lines of known width marked on photographic paper. In order to identify the cracks, the beam was split up into numbered segments marked by the location of each stirrup as shown in Figures 5.3 and 5.4. The crack number was determined by the location within the segment where it crossed a reference line drawn along the beam at 200 mm (7.9 inches) above the base. Thus, crack 6.1E crossed the reference line at 6.1 stirrup spaces from the east end of the beam. The crack widths were measured perpendicular to the direction of the cracks at the level of the reference line.

The growth of the cracks was recorded by marking the end of the crack after each load step. Photographs were also taken of each shear span at various stages of testing and after failure to show the progression of the crack formation.

5.4 Test Procedure

The data was taken and the cracks were marked at the end of each load increment. The load was kept constant while the readings were made. Each of the two point loads was increased in increments of either 10 kN (2.25 kips) or 5 kN (1.12 kips) until close to failure, when smaller increments of 2.5 kN (0.6 kips) or 1.0 kN (0.2 kips) were used. The tests lasted between two and four hours. The point loads were increased at an average rate of 30 kN/hour (6.7 kips/hour). A typical load vs time plot is shown in Figure 5.10.

It should be noted that TB 3 was initially loaded up to 45 kN (10 kips) in the first load step. The load was removed and the test was re-started but inclined cracks had already formed.

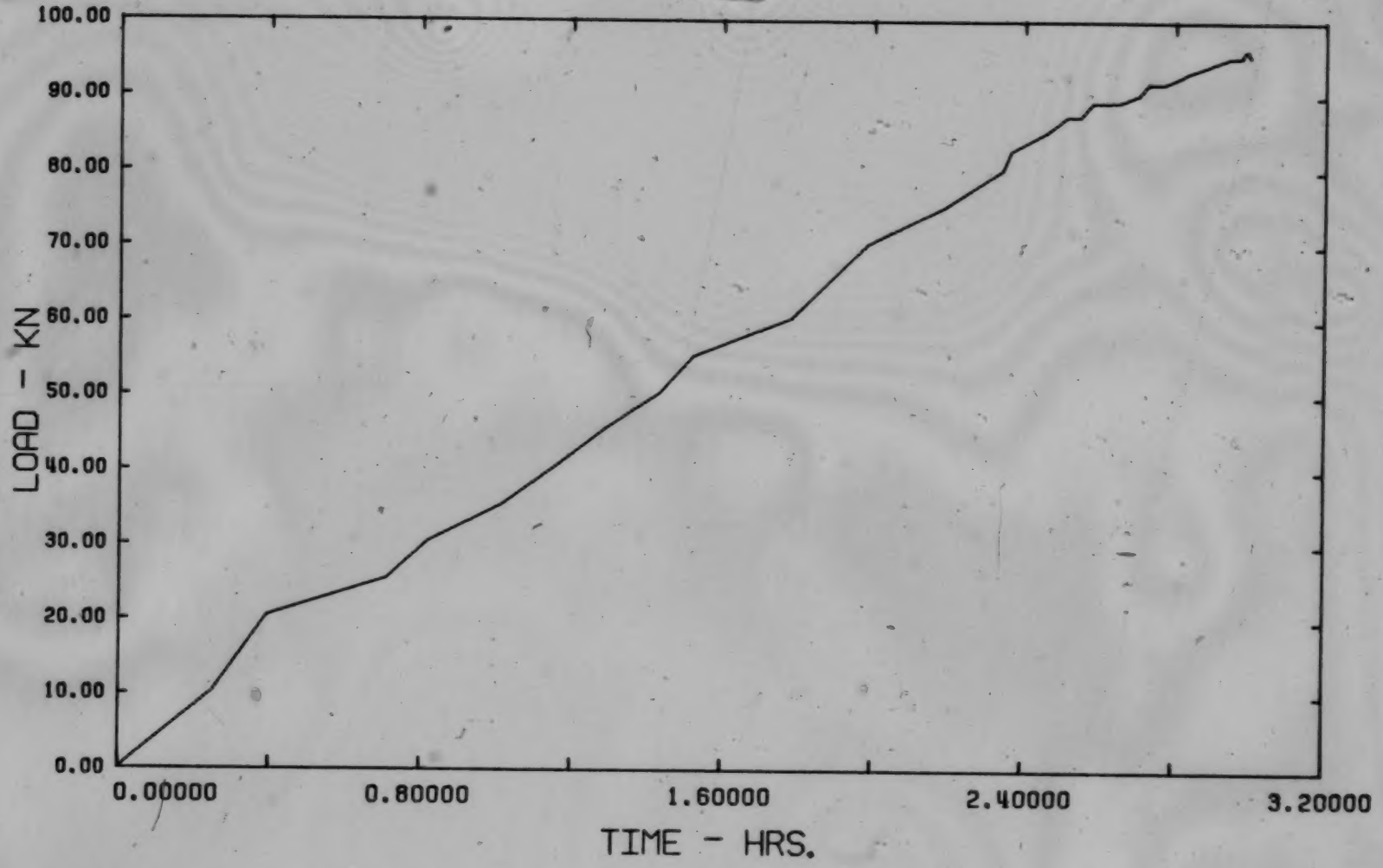

FIGURE 5.10 - Typical Load versus Time Graph for Beam Test (TB 10)

CHAPTER 6

BEAM TEST RESULTS

6.1 Behaviour of Typical Beam with WWF Web Reinforcement

6.1.1 Introduction

The purpose of this section is to describe in detail the typical behaviour of the test beams with WWF web reinforcement using the results of two particular beam tests. Beams TB 2 and TB 4 were considered to be the most representative of the typical behaviour and one or the other is used for the descriptions in each of the following sections. A comparison of the results from all the beam tests is made in Section 6.3.

Photographs of TB 2 and TB 4 during loading and after failure are shown in Figures 6.1 to 6.18. Beam TB 2 failed at 70 kN (15.7 kips) and TB 4 failed at a load of 80 kN (18.0 kips). The WWF web reinforcement in TB 2 had D2.5 vertical wires at 152 mm (6 inch) spacing while TB 4 had D2.9 vertical wires with the same spacing. In both cases, the WWF mats had two horizontal cross-wires top and bottom. It should be noted that TB 4 failed immediately after all measurements were taken at the 80 kN load level while TB 2 failed as measurements were being taken at the 70 kN load level.

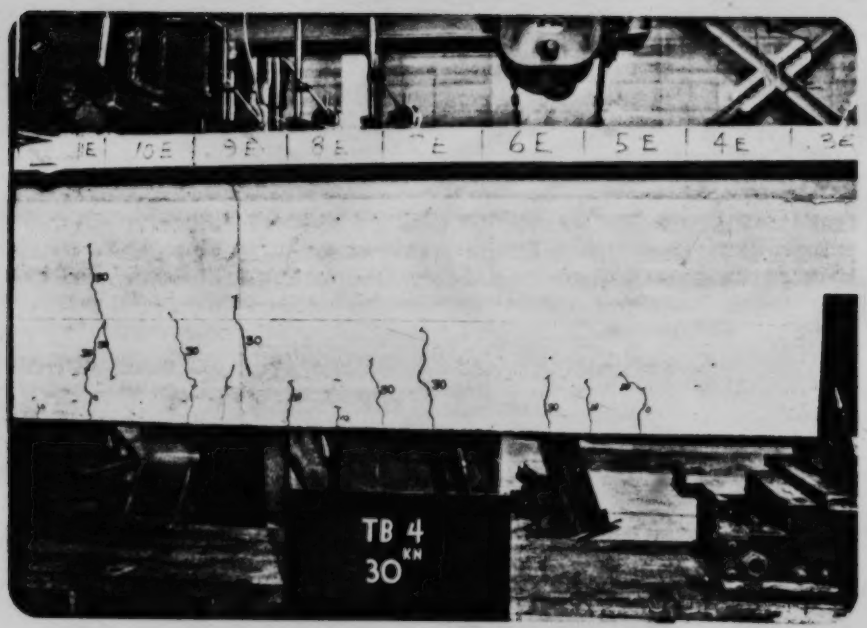

FIGURE 6.1 - Cracking in east shear span of TB 4 at P = 30 kN

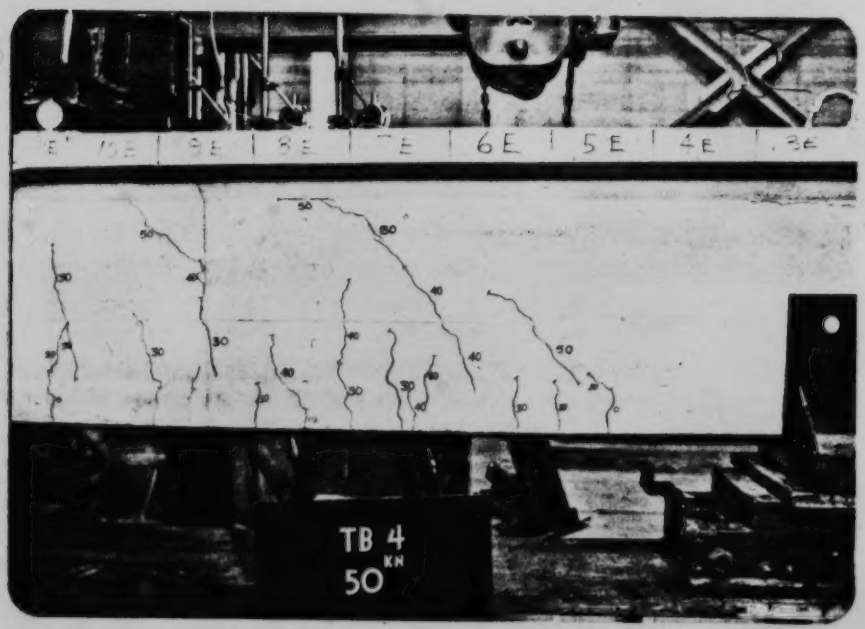

FIGURE 6.2 - Cracking in east shear span of TB 4 at P = 50 kN

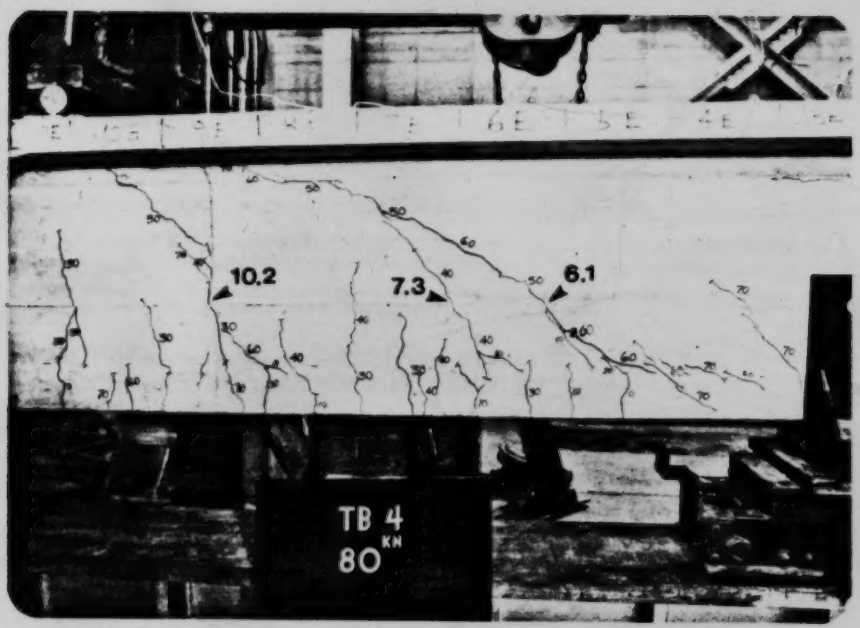

FIGURE 6.3 - Cracking in east shear span of TB 4 at ultimate load (P_{ult} = 80 kN) with crack numbers shown

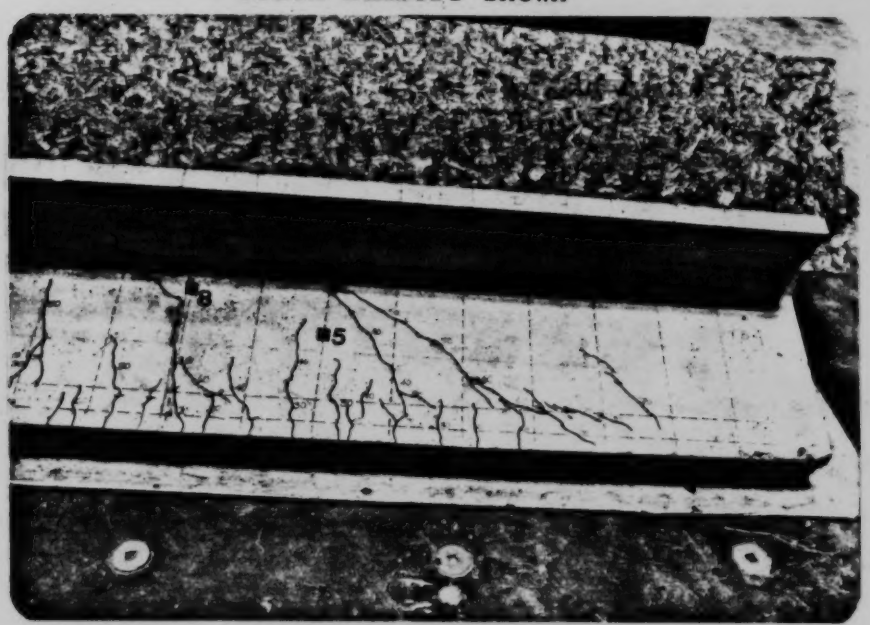

FIGURE 6.4 - Cracking in east shear span of TB 4 after testing with strain gauge locations shown

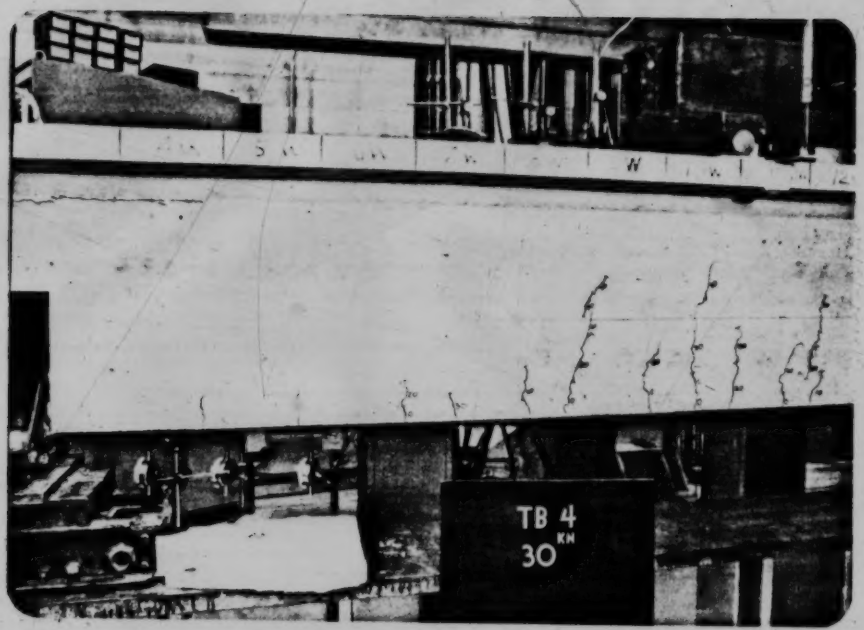

FIGURE 6.5 - Cracking in west shear span of TB 4 at P = 30 kN

FIGURE 6.6 - Cracking in west shear span of TB 4 at P = 50 kN

FIGURE 6.7 - Cracking in west shear span of TB 4 at ultimate load (P_{ult} = 80 kN) with crack numbers shown

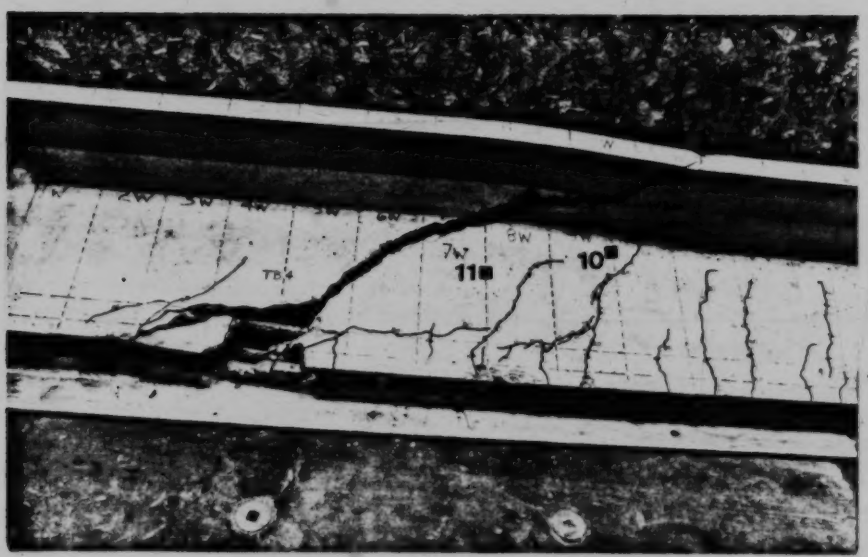

FIGURE 6.8 - Cracking in west shear span of TB 4 after testing with strain gauge locations shown

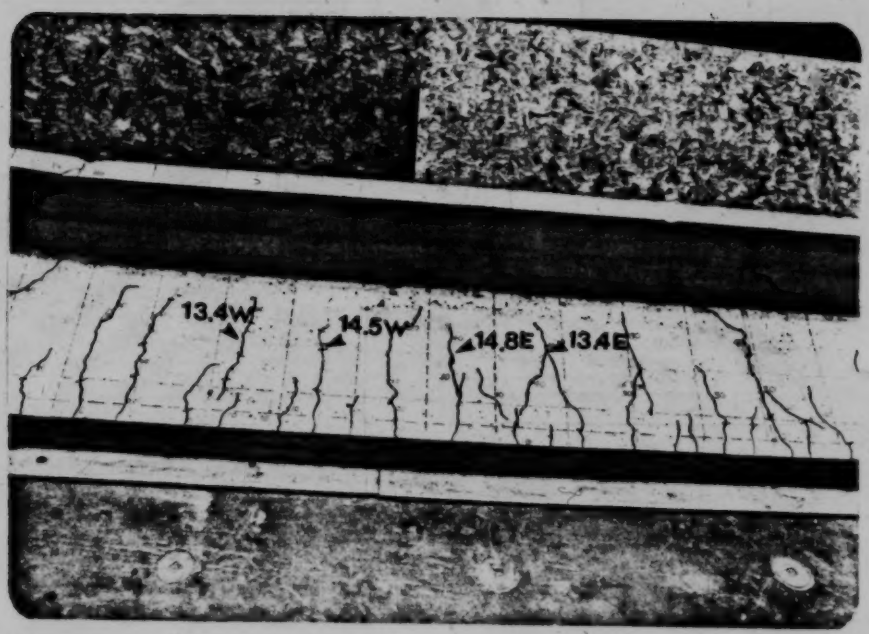

FIGURE 6.9 - Cracking in pure moment region of TB 4 after testing with crack numbers shown

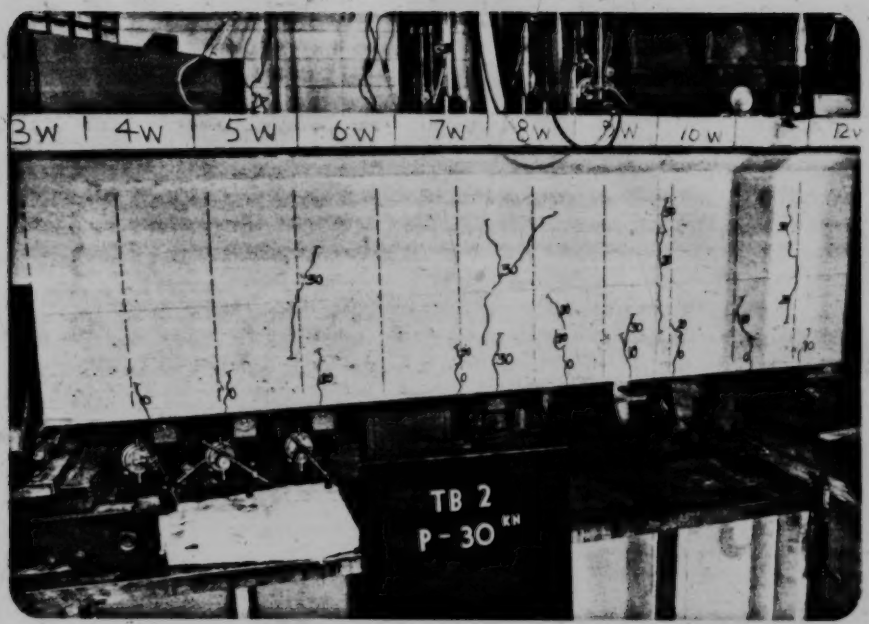

FIGURE 6.10 - Cracking in west shear span of TB 2 at P = 30 kN

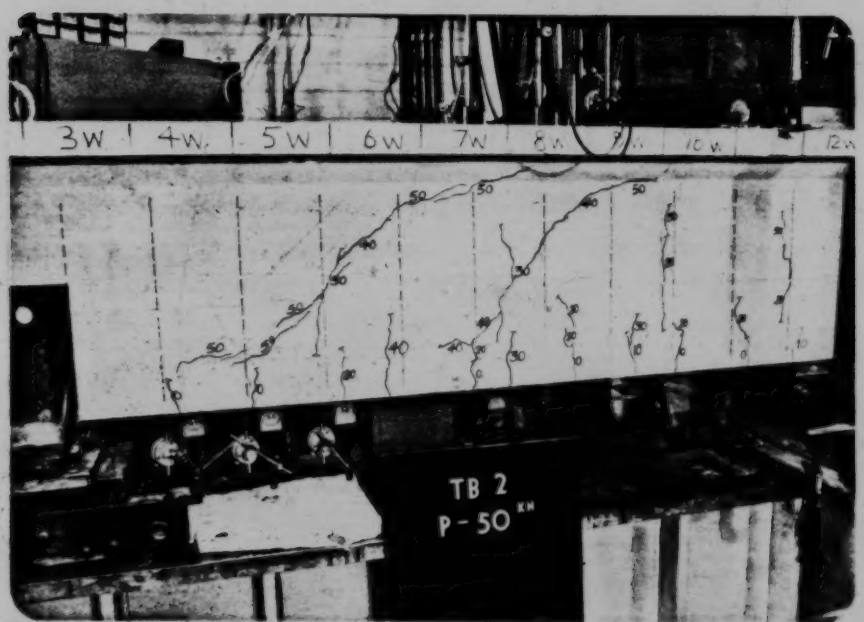

FIGURE 6.11 - Cracking in west shear span of TB 2 at P = 50 kN

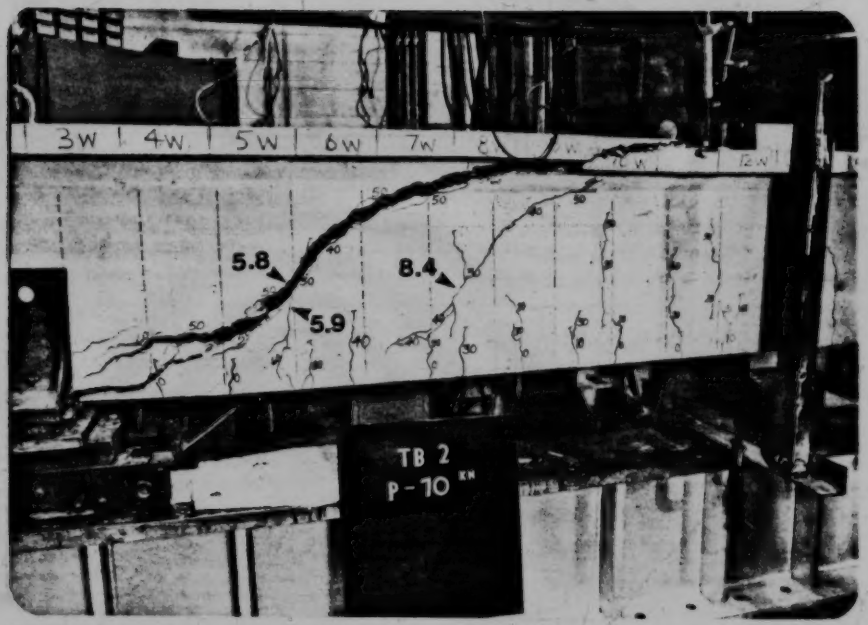

FIGURE 6.12 - Cracking in west shear span of TB 2 at ultimate load (P_{ult} = 70 kN) with crack numbers shown

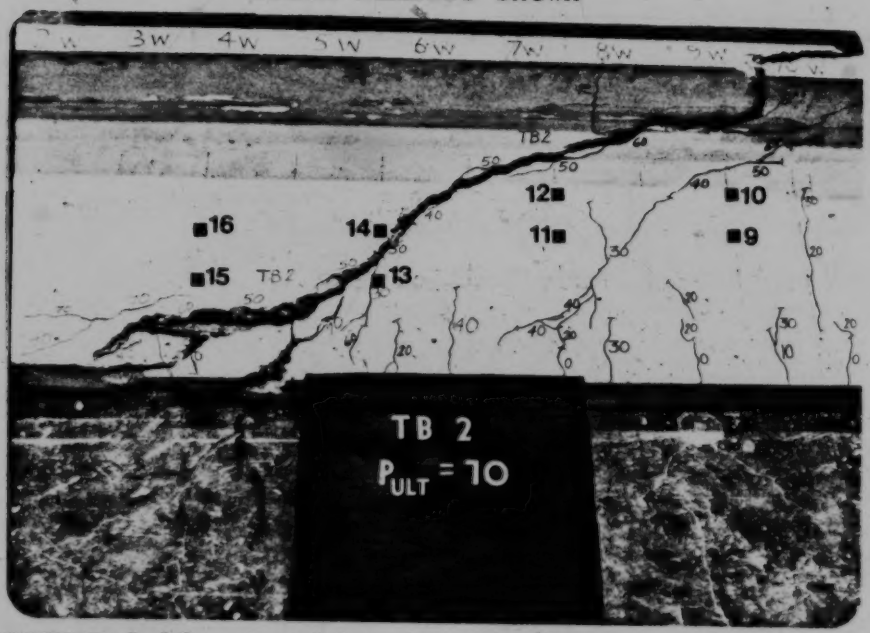

FIGURE 6.13 - Cracking in west shear span of TB 2 after testing with strain gauge locations shown

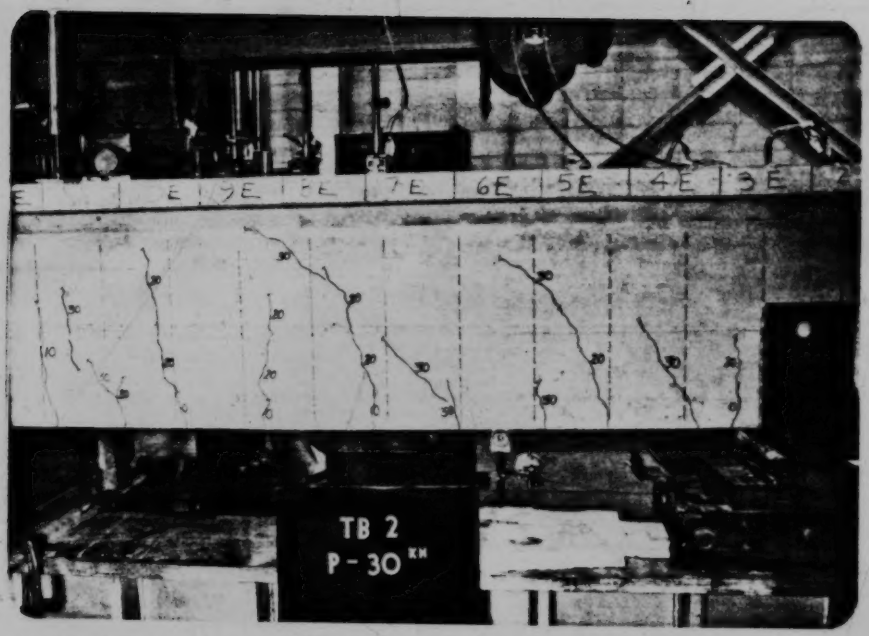

FIGURE 6.14 - Cracking in east shear span of TB 2 at P = 30 kN

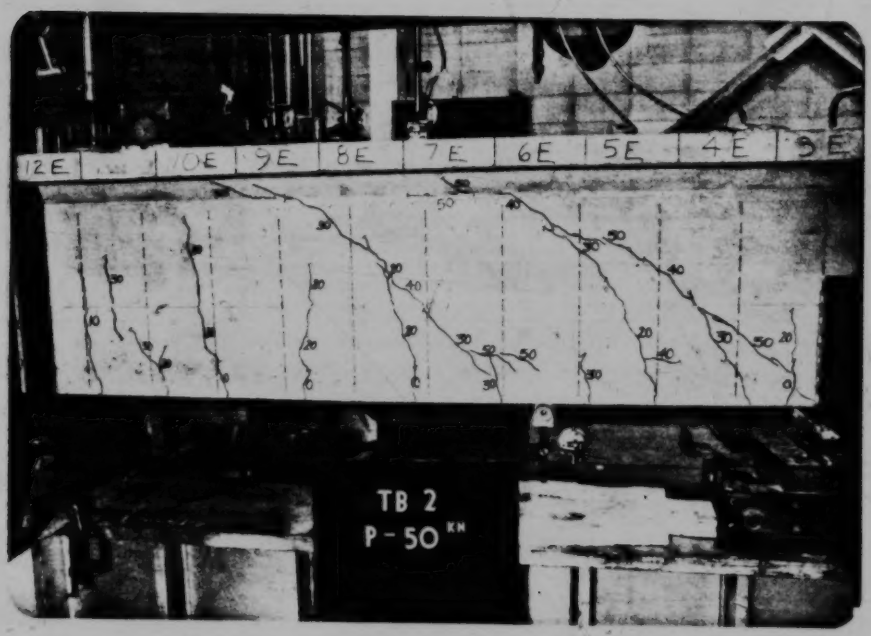

FIGURE 6.15 - Cracking in east shear span of TB 2 at P = 50 kN

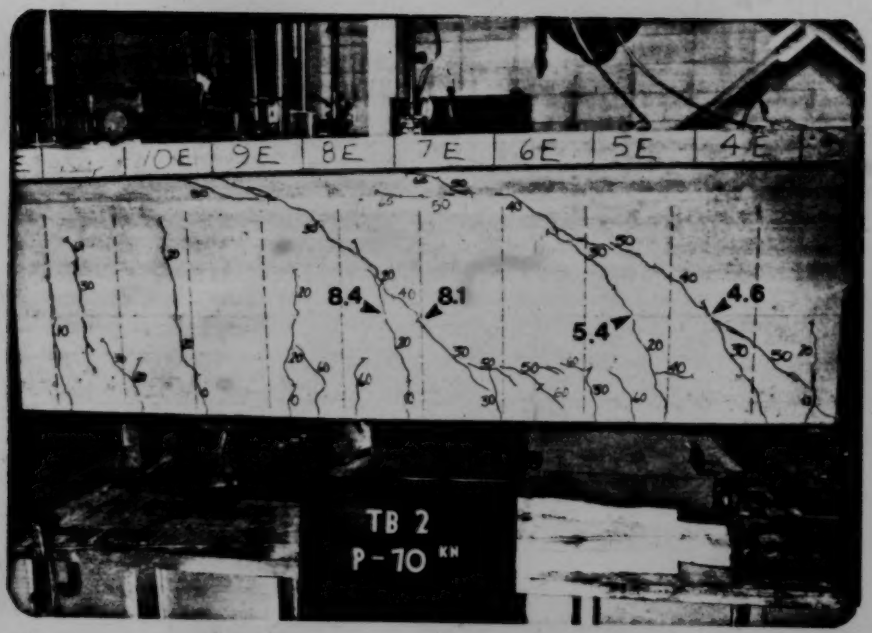

FIGURE 6.16 - Cracking in east shear span of TB 2 at ultimate load (P_{ult} = 70 kN) with crack numbers shown

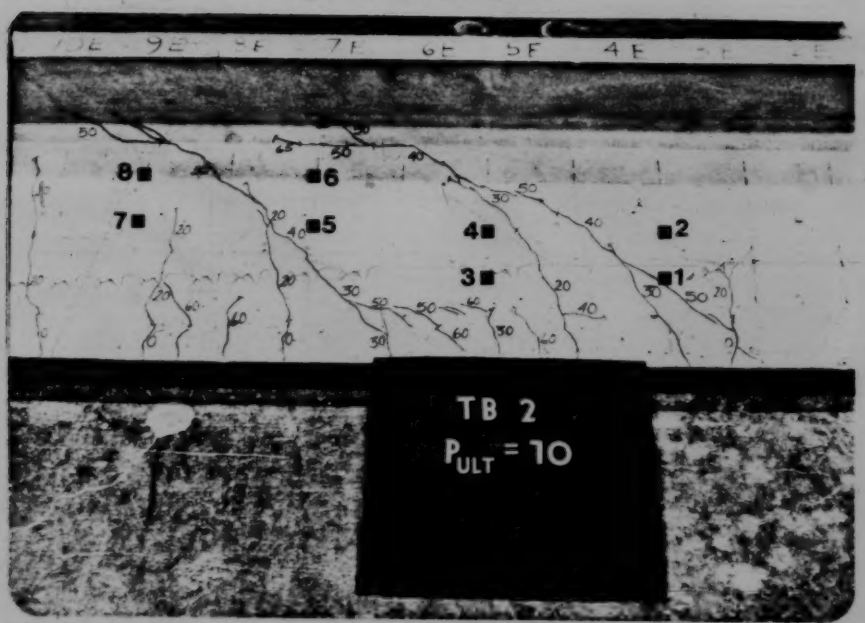

FIGURE 6.17 - Cracking in east shear span of TB 2 after testing with strain gauge locations shown

FIGURE 6.18 - Cracking in pure moment region of TB 2 after testing with crack numbers shown

6.1.2 Crack Formation in Shear Spans - TB 4

At failure there were 11 cracks in the two shear spans of TB 4 that crossed the reference line drawn at 200 mm (8 inches) above the bottom of the beam. Six of these were in the east shear span (Figure 6.3) and five were in the west shear span (Figure 6.7). The west shear span was the failure span. Three of the cracks in the east shear span and two in the west span developed into inclined cracks that extended upwards beyond the centroidal axis of the uncracked section. The numbers assigned to these inclined cracks are shown in Figures 6.3 and 6.7. They were numbered according to where they crossed the reference line as explained in Section 5.3.5.

The first cracks to form in each shear span were short vertical flexural cracks which started from the bottom of the beam and extended up to approximately the top of the main reinforcement. As the load was increased, a few of these cracks extended beyond the reference line. In general, however, the flexural cracks did not extend beyond the level of the top of the main reinforcement. The presence of the holes in the bottom of the beams used to measure the stirrup slip did not appear to have any effect on the locations where the flexural cracks formed.

As the load increased from 30 to 40 kN (6.7 to 9.0 kips) some inclined cracks were formed in the web and as the load increased further, more inclined cracks began to form. Most cracks, such as 6.1E, 7.3E, 10.2E and 5.8W formed in the region between the top of the main reinforcement and the centroidal axis of the uncracked section and then propagated up to the web-to-flange transition as the load increased. Other inclined cracks such as 8.3W and 9.6W also formed in this manner but they formed as extensions to existing flexural cracks. All of these inclined cracks were considered to be "flexure-shear" cracks.

The cracks that formed closer to the load point were steeper than those farther away and all cracks tended to be steeper below the centroidal axis. Also, in most cases, the initial inclined cracks were relatively steep and subsequent cracks were flatter. In the east shear span, crack 7.3E propagated up to the web-to-flange transition at a load of 50 kN (11.2 kips). This crack crossed the reference line at an angle of approximately 60 degrees with the horizontal. As the load increased up to 60 kN (13.5 kips), a flatter inclined crack, 6.1E, formed on the support side of 7.3E and joined the upper portion of it. The flatter crack had an inclination of about 50 degrees with the horizontal at the level of the reference line. The average inclination of 7.3E and 6.1E were 43 and 29 degrees, respectively.

The average inclination of the cracks was determined as follows:

$$\alpha_{avg} = \tan^{-1} \left(\frac{318}{C}\right)$$

where:

α_{avg} = average inclination measured from the horizontal

C = horizontal projection of the crack between the top of the main reinforcement and the bottom of the web-to-flange taper (mm)

318 = the vertical distance in mm between the top of the main reinforcement and the bottom of the web-to-flange taper

This method was used because the stirrups crossed by this portion of the cracks were most effective. Also, there were large variations in the actual inclination along the cracks so the average inclination was better for comparison.

The average inclination of the cracks in TB 4 ranged from 29 to 56 degrees. The average inclination of the failure crack, 5.8W, was 35 degrees so it had a horizontal projection of 456 mm. This was equal to 1.02 d.

The inclined cracks crossed the reference line in the range from location 5.8 to location 10.2 (see Section 5.3.5).

There did not seem to be any pattern as to where they formed but there was at least one inclined crack in each half of each shear span.

Secondary cracks formed along the main reinforcement at the lower ends of the inclined cracks in the same load range that the inclined cracks were propagating up to the flange.

As the load approached ultimate, the flatter inclined cracks widened and more secondary cracks formed. Finally, at the failure load, crack 5.8W propagated up through the flange to the load point. It simultaneously propagated along the main reinforcement and then down to the bottom of the beam near the support as shown in Figure 6.7.

6.1.3 Inclined Cracking Load - TB 2

In this testing program, an exact value of the inclined cracking load was not obtained. However, the load range corresponding to the testing load increment in which inclined cracking occurred was determined both from the crack pattern and from the strain gauge readings on the web reinforcement.

Two estimated load ranges for inclined cracking were obtained from the crack patterns of the beams. In Method 1 this was determined from the load range in which a crack

crossed the centroidal axis of the uncracked beam, 322 mm (12.7 inches) above the bottom of the beam, at an angle of 45 degrees or less at that location. With this method, it was possible for the lower portion of the crack to be relatively steep even though it had the proper angle at the height of the centroidal axis. The estimate for Method 2 was obtained from the load range in which a crack with an average inclination of approximately 45 degrees or less first extended from the main reinforcement to the web-to-flange transition. The average inclination was determined as described in the previous section. The inclined cracking load for a beam with no web reinforcement is considered to be the failure load. One of the load ranges determined from these two methods would probably have been the failure load range if the beams tested did not have web reinforcement.

Using the stirrup strain, the inclined cracking load was determined from the load range in which a significant increase in strain first occurred. Before inclined cracking, the stirrups would not be required to carry load, so, once the stirrup strains started to increase it was assumed that inclined cracking had taken place.

In the east shear span of TB 2 (Figure 6.14), the load range for inclined cracking using Method 1 was determined to be 20 to 30 kN (4.5 to 6.7 kips). This was the load range in

which cracks 8.4E and 5.4E crossed the centroidal axis making angles of 29 and 38 degrees, respectively, with the horizontal at that location. Using Method 2, the inclined cracking load range was estimated to be 30 to 40 kN (6.7 to 9.0 kips) which was the range in which crack 8.1E formed with an average inclination of 42 degrees. From the stirrup strains, the inclined cracking load range was between 20 and 30 kN (4.5 to 6.7 kips) as determined by strain gauge 5 on stirrup 7E which was crossed by crack number 8.1E. This location is shown in Figures 6.16 and 6.17.

In the west shear span of TB 2, the inclined cracking load range using Method 1 was estimated as 20 to 30 kN (4.5 to 6.7 kips). This was determined from crack 8.4W which crossed the centroidal axis at an angle of 36 degrees. The load range using Method 2 was 30 to 40 kN (6.7 to 9.0 kips) and was determined from crack 8.4W which had an average inclination of 43 degrees. From the stirrup strains, the estimated inclined cracking load range was 20 to 30 kN (4.5 to 6.7 kips) from strain gauge 13 on stirrup 5W. This stirrup was crossed by crack 5.9W (see Figures 6.12 and 6.13).

All of these estimates were below the value of V_c = 44.4 kN (10 kips) calculated using the ACI and CSA Code equations. A summary of the estimated inclined cracking load ranges for

all the beams and comparisons to the ACI and CSA value for V_c are given in Section 6.3.

6.1.4 Crack Formation in Pure Moment Region - TB 4

As expected, the cracks in the constant moment region were generally vertical flexural cracks which started at the bottom of the beam and propagated upwards during testing. The longest cracks extended approximately up to the level of the neutral axis. Several cracks formed above the main reinforcement without starting at the bottom of the beam. Crack 14.5W started in this manner but it eventually extended to the bottom of the beam. Crack 13.4W, however, did not extend to the bottom. In this case, the main reinforcement probably acted to confine the crack and prevent it from opening.

6.1.5 Mode of Failure - TB 4

The failure of TB 4 was a diagonal tension type failure. As the beam was loaded, inclined flexure-shear cracks formed in each span. The flatter of these cracks widened as the load was increased. At failure, one of the wider cracks propagated up to the top of the flange at the load point and down to the bottom of the beam at the support. The failure crack widened, the beam began to deflect rapidly and the applied load dropped off immediately. As the failure crack widened, the segment farthest from the support dropped down relative

to the segment closest to the support. This caused the flange to kink in the region near the load point. Transverse cracks formed across the top of the flange at the load point and also in the region between sections 7W and 8W as shown in Figure 6.7. A longitudinal crack along the center of the top of the flange also formed between these two transverse cracks. There was no evidence of concrete crushing after failure. In this beam, the failure crack was 5.8W in the west shear span. Failure occurred immediately after the measurements were completed at the 80 kN (18 kip) load level.

The upper end of the failure crack propagated along the web-to-flange transition before entering the flange near the loading point. This horizontal portion of the crack crossed above the horizontal cross-wires used to anchor the stirrups in this region. Therefore, as the segment of the beam farthest from the support dropped in relation to the other segment, these stirrups were no longer anchored in the flange and could not carry any load across the crack. A photograph of how this portion of the failure crack formed above the anchorage is shown in Figure 6.19 for TB 2.

The failure crack in TB 4 crossed four stirrups in the region between the top of the main reinforcement and the web-to-flange transition. Stirrups 5W and 6W were crossed

FIGURE 6.19 - Failure crack above exterior anchorage wire at top of TB 2

in the middle region of the beam. Both of these stirrups were well anchored above and below the failure crack and as the failure crack widened, they yielded and fractured. Stirrup 4W was crossed near the top of the main reinforcement and stirrup 7W was crossed near the web-to-flange transition. These stirrups did not fracture because their anchorages were damaged and they were not able to develop enough load.

The lower portion of the failure crack propagated along the top of the main reinforcement for about 250 mm (10 inches) along the secondary cracks that had formed. It then extended to the bottom of the beam near the support. The stirrups in this region did not develop enough load to fracture. This was probably due to the reduced effectiveness of the anchorages resulting from the large amount of cracking near the anchorage or due to damage caused to the anchorage at failure. This will be discussed more fully in Sections 6.1.8 and 6.3.6.

6.1.6 Crack Widths - TB 4

There was no well defined relationship between inclined crack width and load. The flatter inclined crack, however, widened considerably more than the others.

In the west shear span of TB 4, crack 5.8W was 1.78 mm (0.070 inches) wide at the load step prior to failure. Crack 9.6W was steeper than 5.8W and at this same load step it had a width of 0.28 mm (0.011 inches). Crack 5.8W widened considerably with each load step while 9.6W widened more slowly. The other cracks that crossed the reference line in this shear span did not widen during loading.

In the east shear span, the widths of cracks 10.2E, 7.3E and 6.1E at the load step prior to failure were 0.25 mm (0.010 inches), 0.18 mm (0.007 inches) and 0.61 mm (0.024 inches), respectively. Crack 6.1E was the flattest inclined crack. Crack 7.3E widened only until crack 6.1E joined up with it.

As the load approached ultimate, it was clear from the crack widths that either crack 5.8W or crack 6.1E would be the failure crack. Crack 5.8W became considerably wider as the load increased and it ultimately caused the failure.

6.1.7 Stirrup Strains - TB 2

The stirrup strain was negligible until the stirrup was crossed by a visible inclined crack. The strain then increased significantly and continued to increase as the beam was loaded. In some cases, the strain did not begin to increase until the load step after that during which the stirrup was crossed by a crack. As mentioned previously,

the load range in which the strain began to increase significantly was used as an estimate of the inclined cracking load.

In TB 2, 16 strain gauges were installed but only 11 gave reliable readings. Four of these were in the east shear span (gauges 2, 5, 6 and 7) and seven in the west span (gauges 9, 10, 12, 13, 14, 15 and 16). Two gauges were mounted on each stirrup that was monitored. These gauges were located as shown in Figures 6.13 and 6.17. Figures 6.20 and 6.21 plot stirrup strain versus load using the strain gauges that gave the highest readings for each stirrup monitored. Strain gauges 14 in the west span and 5 in the east span recorded the largest strains. These gauges were installed on well anchored stirrups that were crossed by the widest inclined cracks in the region between the top of the main reinforcement and the web-to-flange transition. Because these stirrups were well anchored on each side of the cracks, they were able to develop larger loads, as was borne out by the measured strains. The gauges that gave lower readings were located on stirrups that were either crossed by narrow inclined cracks (gauge 10 in Figure 6.13) or they were crossed by the wider inclined cracks in the regions near the web-to-flange transition (gauge 7 in Figure 6.17) or near the main reinforcement (gauge 15 in Figure 6.13).

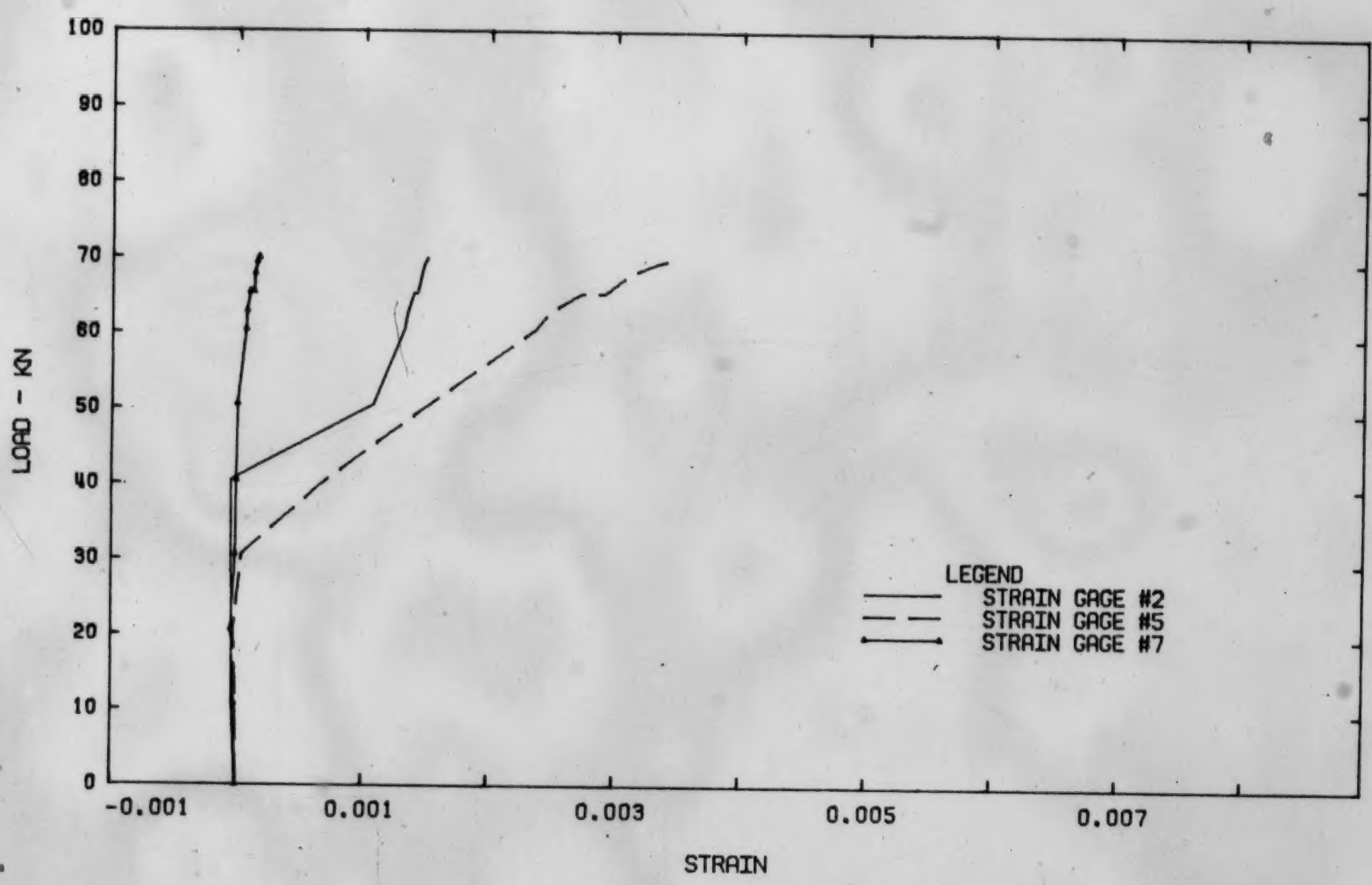

FIGURE 6.20 - Point Load Versus Stirrup Strain for East Shear Span of TB 2

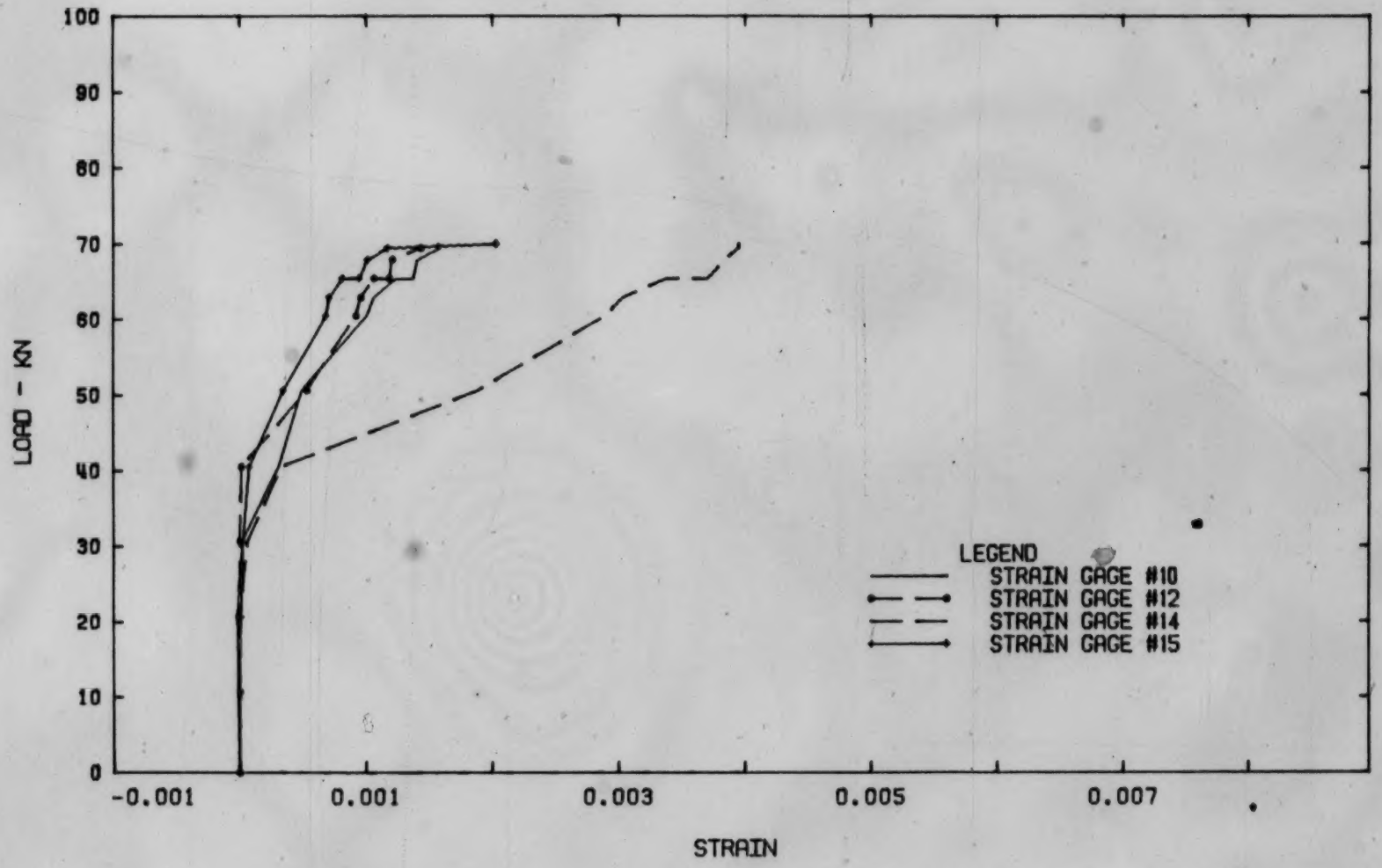

FIGURE 6.21 - Point Load Versus Stirrup Strain for West Shear Span of TB 2

If the yield strain of the vertical wires is taken as 0.0035 as given in the ACI and CSA Codes, then the only gauge that measured a strain larger than yield prior to failure of the beam was gauge 14. Strain gauge 5 gave a reading that was very close to yield.

Stirrups 4W, 5W, 6W and 7W, fractured when the beam failed. Stirrup 5W started to yield at the load step prior to failure as indicated by the reading from strain gauge 14. It was not possible to determine whether stirrups 4W and 6W were yielding prior to failure because they were not instrumented. In the case of stirrup 7W, strain gauge 12 did not show a reading near yield at the load step prior to failure. However, this gauge was located approximately 40 mm (1.5 inches) below the interior anchorage wire at the top of the beam whereas the stirrup fractured approximately 25 mm (1 inch) above this anchorage wire. It is probable that this stirrup had a higher strain near where it fractured than it had at the location of strain gauge 12. This suggests that the cross-wire was an effective anchorage for the stirrup wire.

The efficiency of the bond between the concrete and the deformed wire stirrups can be estimated from the difference in the readings from two gauges installed on the same stirrup in cases where a crack crossed either above or below

both gauges and not between them. This occurred for gauges 5 and 6 and gauges 15 and 16 in TB 2. The difference between the strain readings for these gauges as shown in Figures 6.22 and 6.23, represents a change in wire stress due to bond or friction. In each case, the strain gauge with the largest reading was closest to the crack.

Gauge 5 was located approximately 70 mm (2.7 inches) from the crack and gauge 6 was approximately 180 mm (7.1 inches) away. The basic development length of D2.5 wire given by ACI Code Section 12.2.2 is 137 mm (5.4 inches) if the 200 mm (8 inch) minimum value is neglected. The bond length between these two gauges was between 50 mm (2 inches) and 75 mm (3 inches). This was less than the 110 mm (4.3 inch) spacing between them because of the protection that was wrapped around the gauges. If the stirrup was well bonded over this length, then the difference in stress between the gauges should have been about 180 MPa (26 ksi) at a load of 40 kN (9 kips). However, the difference in strain corresponds to a difference in stress of only 35 MPa (5.1 ksi) or approximately 20 percent of that expected from the ACI Code procedure. This suggests that the bond was relatively poor in this case.

A similar situation existed in the case of strain gauges 15 and 16. Gauge 15 was 50 mm (2 inches) from the crack while

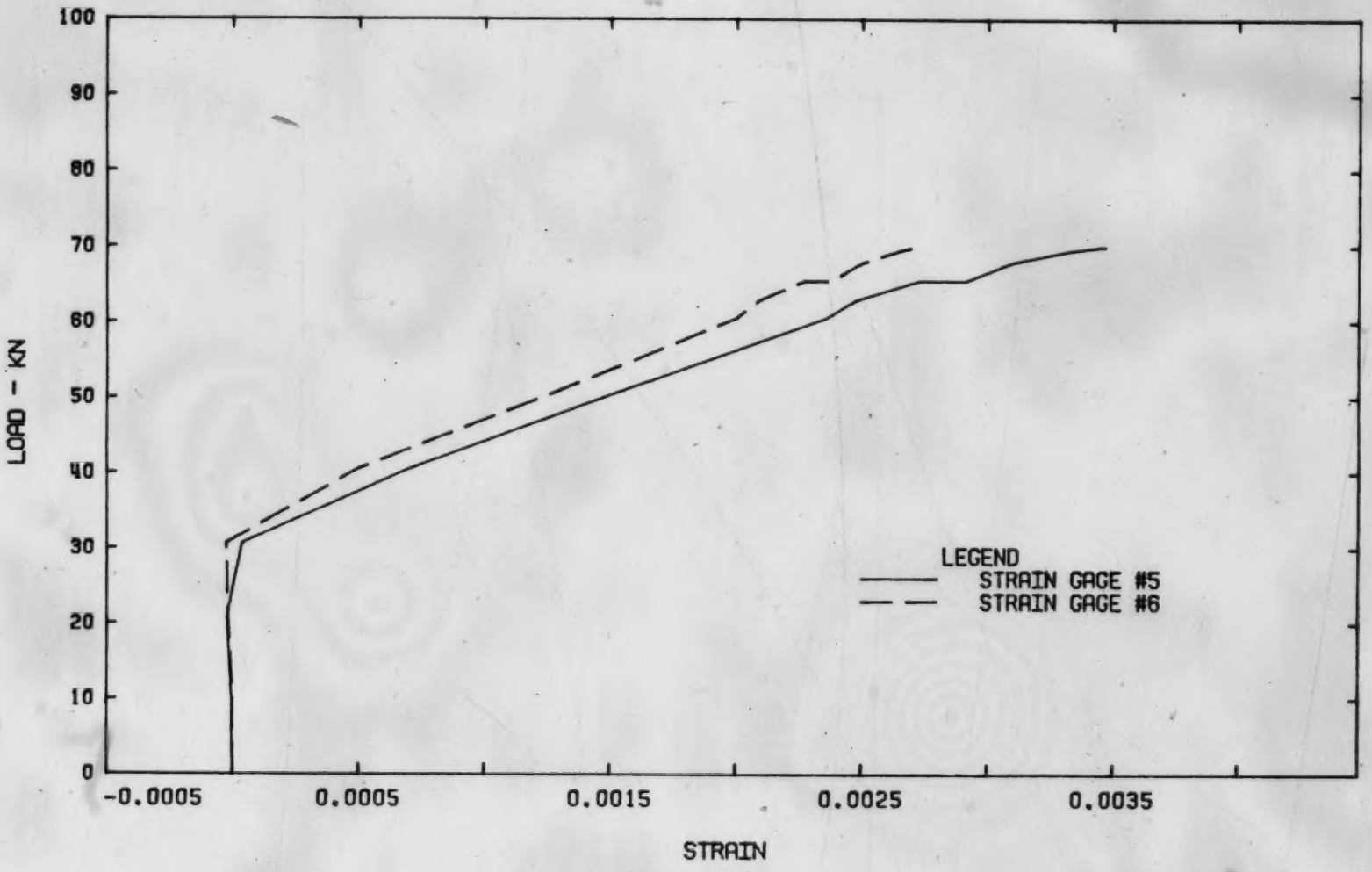

FIGURE 6.22 - Graphs of Load Versus Strain for Strain Gauges 5 and 6 from TB 2 Showing the Difference in Strain Due to Bond

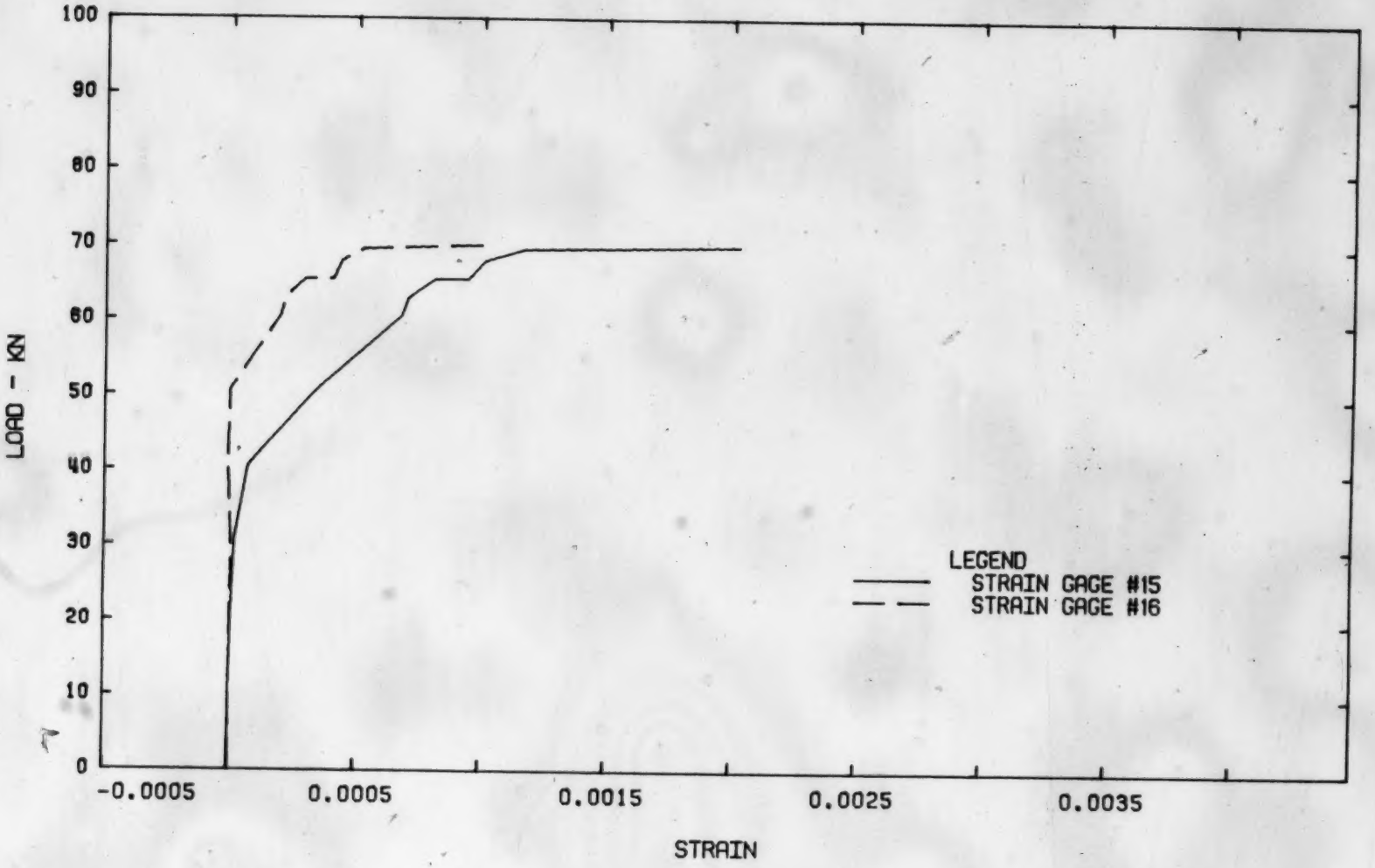

FIGURE 6.23 - Graphs of Load Versus Strain for Strain Gauges 15 and 16 from TB 2 Showing the Difference in Strain Due to Bond

gauge 16 was 110 mm (4.3 inches) farther away. The difference in strain at a load of 60 kN (13.5 kips) corresponded to a stress reduction of 100 MPa (14.4 ksi) which was much less than the expected value.

6.1.8 Stirrup Slip and Anchorage Failure - TB 4

The graphs of load versus stirrup slip were very similar in shape to the graphs of load versus stirrup strain. The measurements were negligible until inclined cracks formed across the stirrups. The readings then began to increase and continued to do so as the beam was loaded.

Slip gauges 4 to 12 were installed on TB 4 and measurements were taken at each load step up to and including the failure. The load versus stirrup slip graphs appear in Figures 6.24 to 6.26. The reading at the failure load was taken while the beam was still stable before the failure crack began to open. No readings could be taken after failure either because the slip that occurred was too great or because the gauges became unseated. Slip gauge 12 fell off at the load step prior to failure of the beam.

The largest slip measurements occurred at the stirrups which were crossed by the inclined cracks either in the region of the top or bottom cross-wire anchorage. The readings in the failure span were generally larger than the readings in the

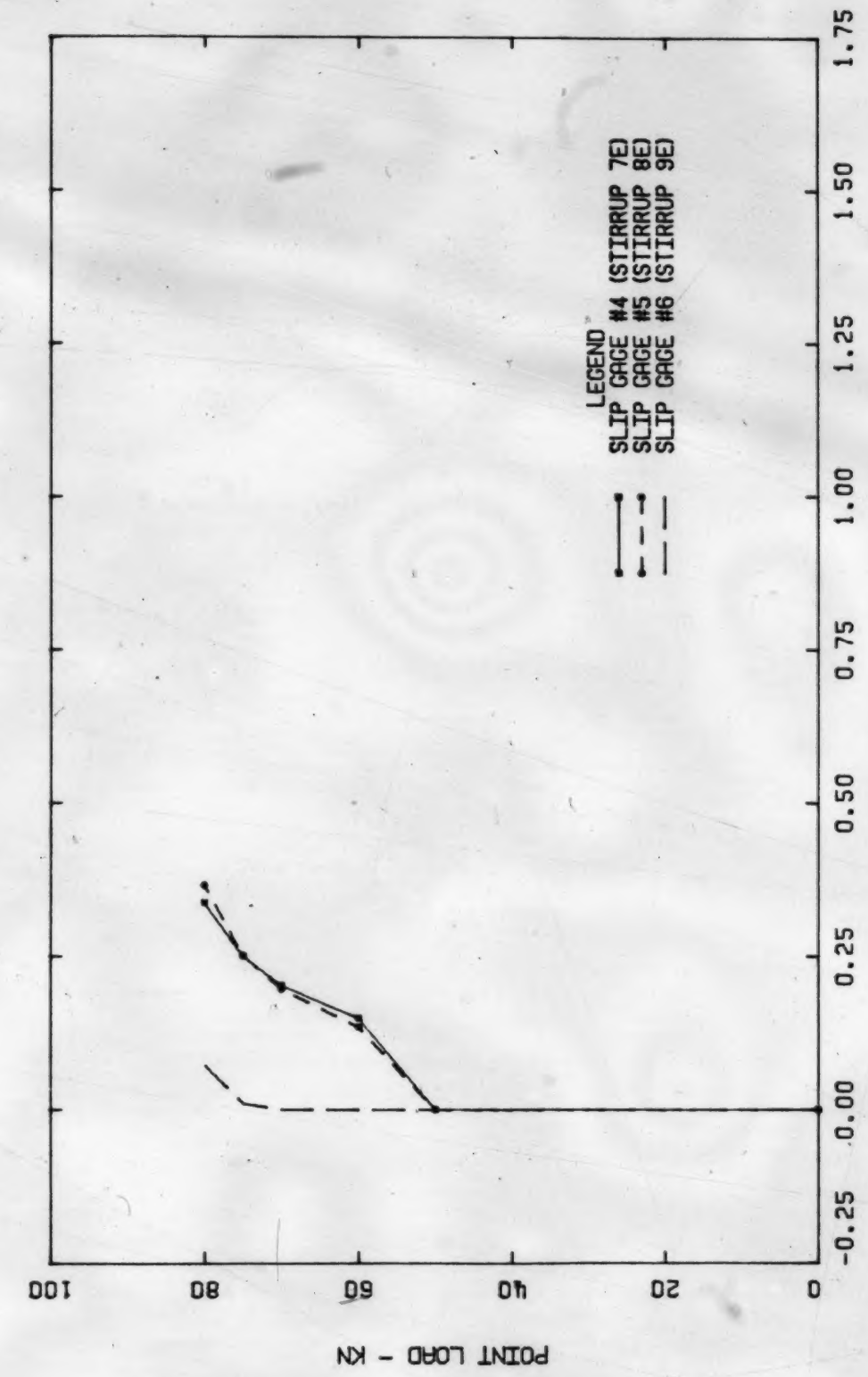

FIGURE 6.24 - Graph of Load Versus Stirrup Slip as Measured from the Top Gauges of TB 4 in the East Shear Span

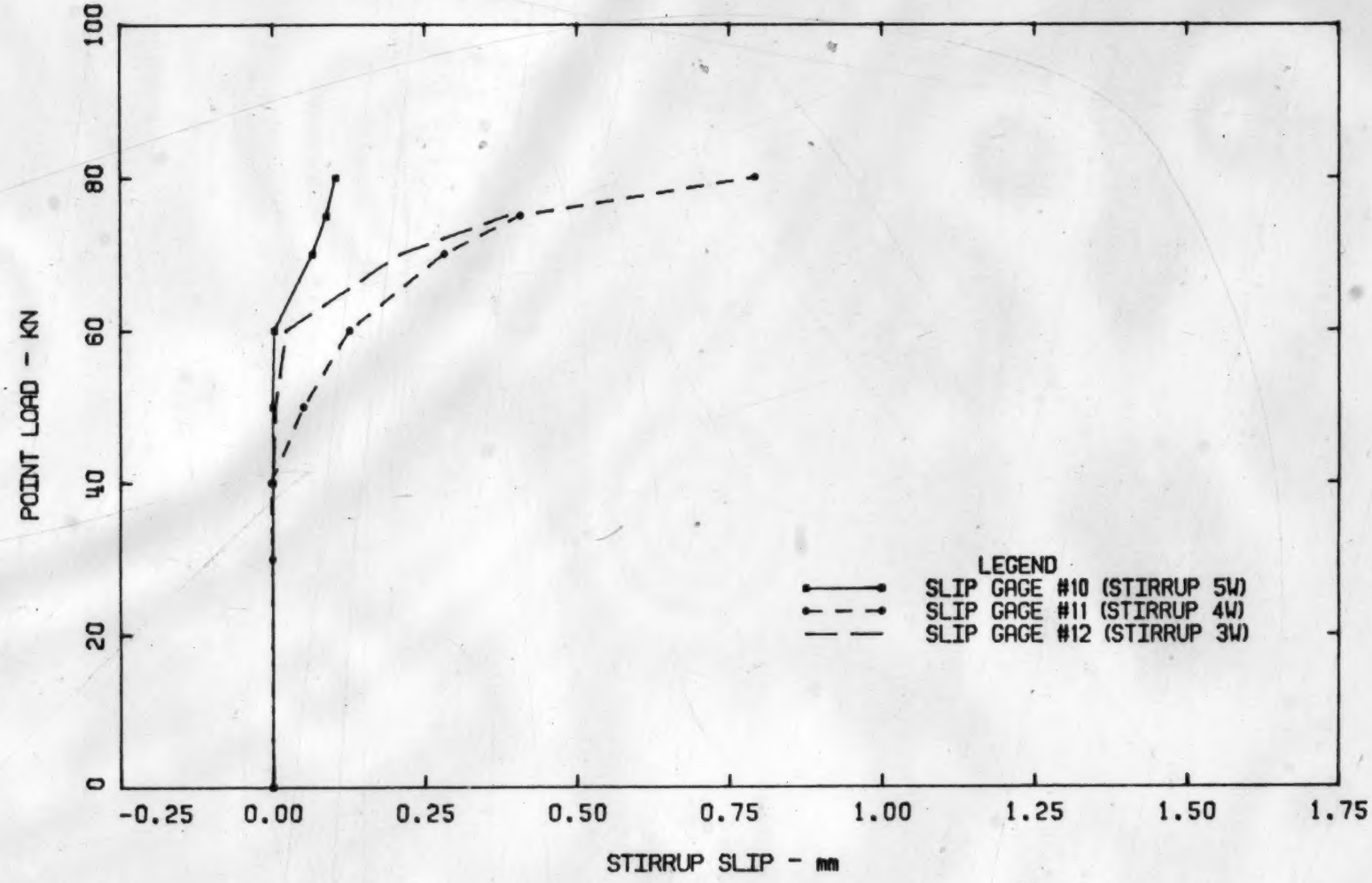

FIGURE 6.25 - Graph of Load Versus Stirrup Slip as Measured from the Bottom Gauges of TB 4 in the West Shear Span

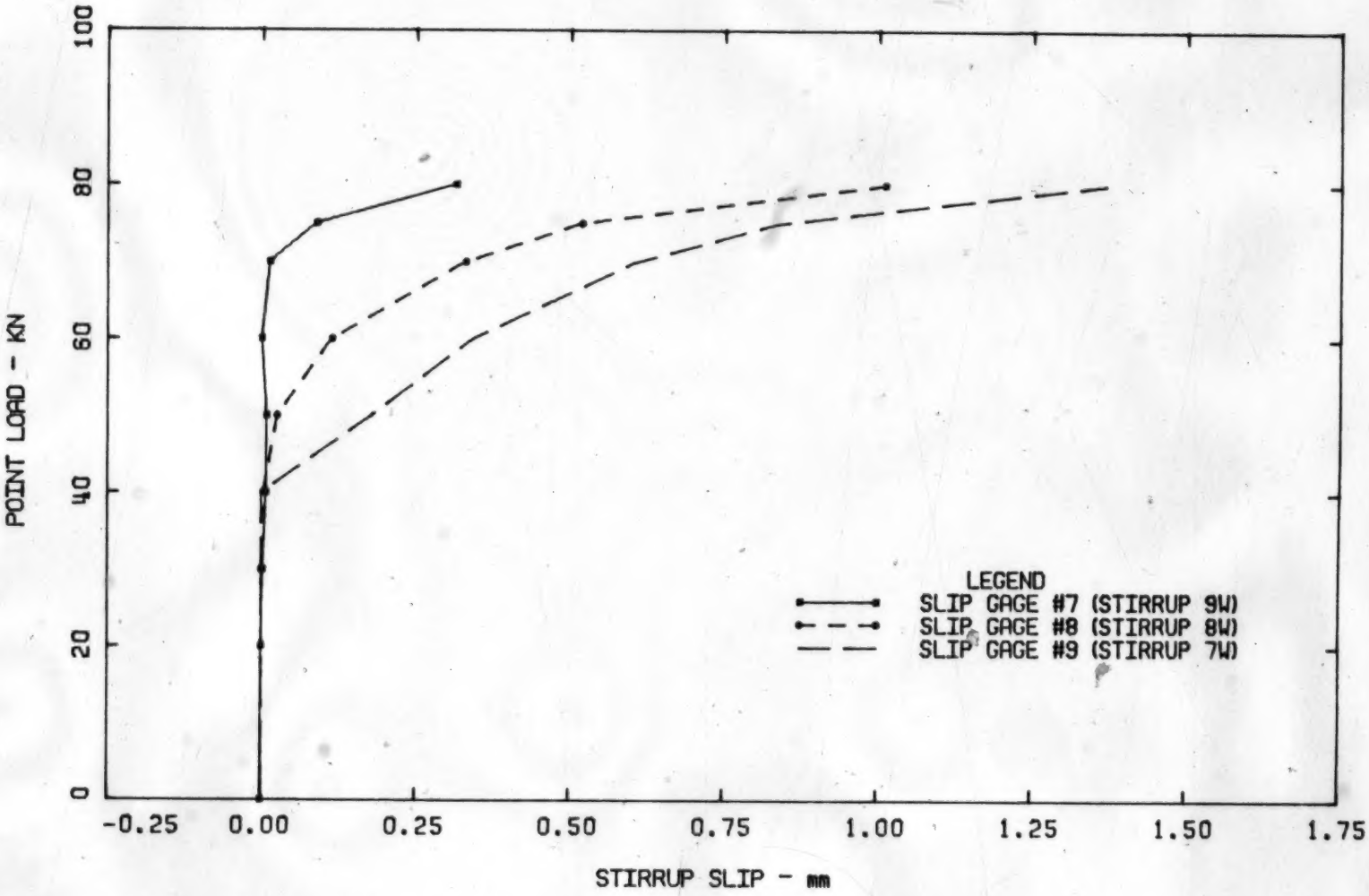

FIGURE 6.26 - Graph of Load Versus Stirrup Slip as Measured From the Top Gauges of TB 4 in the West Shear Span

other span. Damage to the anchorage was evident after the beam failed on the stirrups crossed by the failure crack in the region near the anchorage wires.

The largest slip measured before failure was 1.37 mm (0.0539 inches) at slip gauge 9 on stirrup 7W (see Figure 5.3). The failure crack crossed this stirrup near the interior cross-wire of the top anchorage. This cross-wire fractured at the weld to the stirrup as the failure crack widened and the segment of the beam furthest from the support dropped. The weld at the exterior anchorage also failed. The stirrup was no longer anchored above the failure crack so it simply pulled out of the flange. At the load step prior to failure, the dial gauge reading began to increase even though the load remained constant. This creep was a good indication that the ultimate load was close.

At stirrups 8W and 9W, the failure crack crossed above both anchorage wires at the top of the beam. The slips measured just prior to failure were 1.01 mm (0.0398 inches) and 0.32 mm (0.0124 inches), respectively. Because these stirrups were not anchored above the failure crack they pulled out of the flange when the beam failed.

Stirrup 4W was crossed by the failure crack near the level of the main reinforcement. The slip at this location was

0.79 mm (0.0312 inches) just before failure. At failure, the interior cross-wire at the bottom anchorage fractured at the weld to the stirrup as the segment of the beam furthest from the support dropped relative to the other segment. The exterior cross-wire also fractured at the weld and the weld at this location failed. This can be seen in the photograph in Figure 6.27.

Stirrup 5W fractured at the location where it was crossed by the failure crack approximately 100 mm (4 inches) above the interior cross-wire for the bottom anchorage. There was no damage to the anchorage above or below the failure crack and, as expected, the slip reading measured from the bottom of the beam was relatively small, 0.10 mm (0.0041 inches).

In the east shear span, the slip measured was largest at stirrups 7E and 8E; 0.34 mm (0.0133 inches) and 0.37 mm (0.0144 inches), respectively. These stirrups were crossed by inclined cracks near their top anchorage. Stirrup 9E was crossed by an inclined crack in the middle region of the beam and, as expected, it had a low slip measurement of 0.07 mm (0.0029 inches).

6.1.9 Deflection - TB 4

The load versus centerline deflection graph for TB 4 is shown in Figure 6.28. The graph can be broken into three

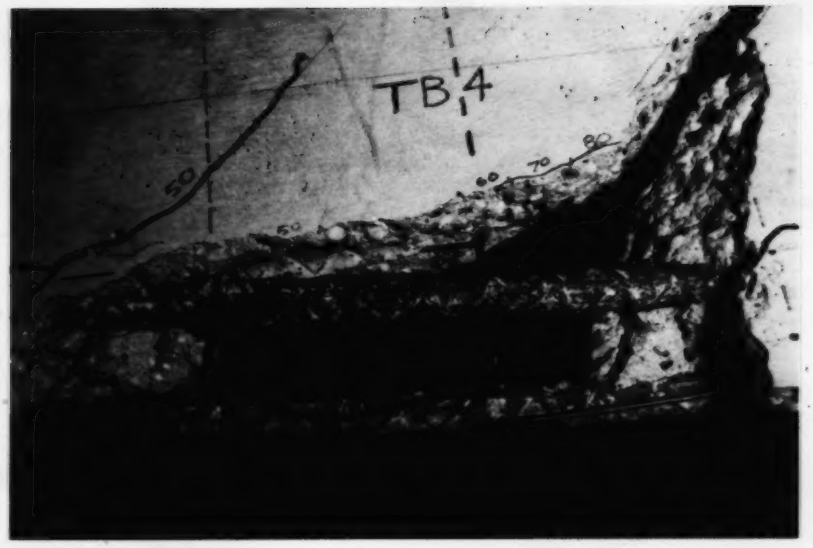

FIGURE 6.27 - Damage to anchorage at bottom of failure crack in TB 4

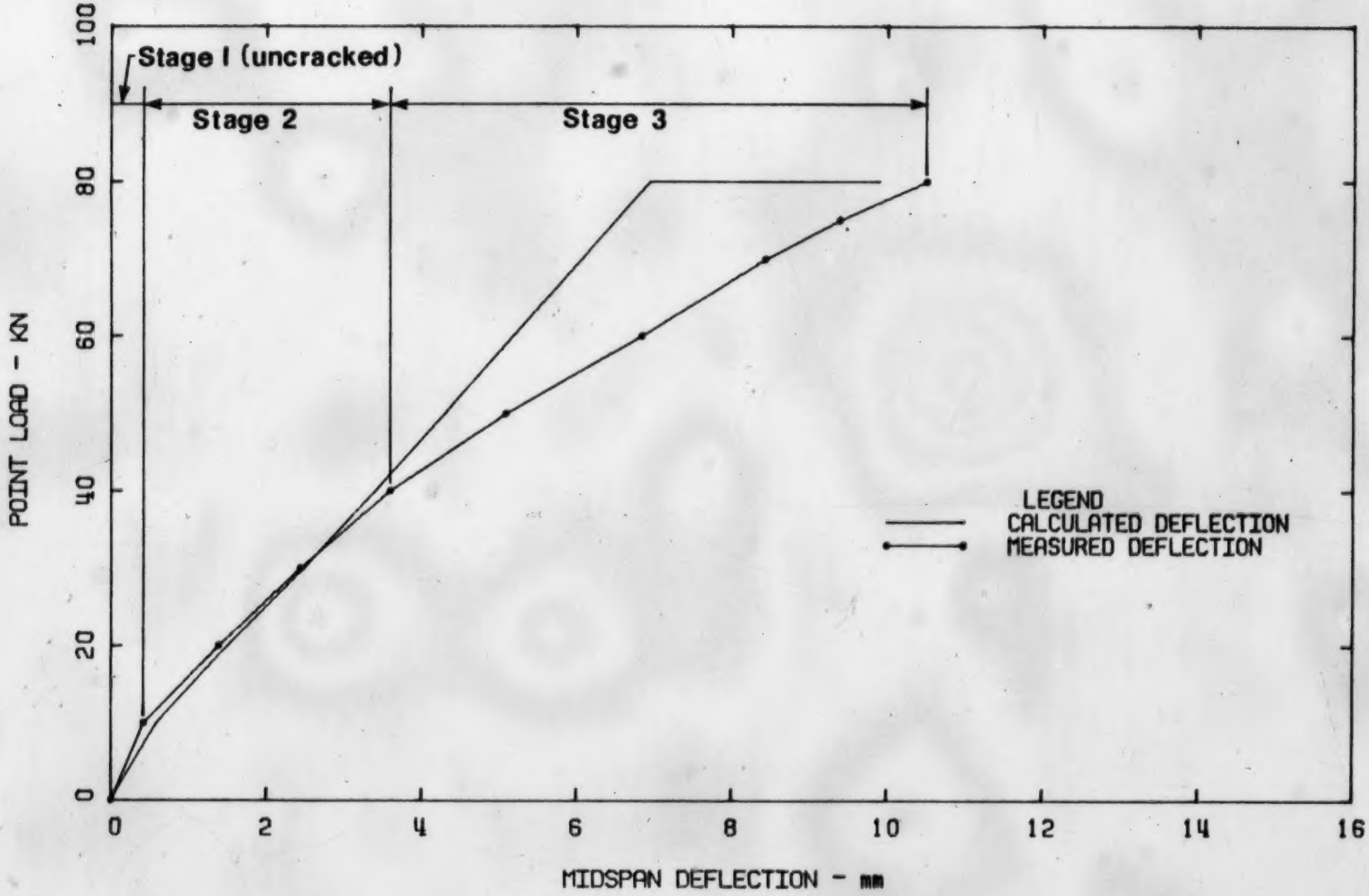

FIGURE 6.28 - Load Versus Midspan Deflection for TB 4

sections. The initial portion of the graph from 0 to 10 kN represents the uncracked region. The calculated cracking moment for this beam is approximately 19 kN/m (14 ft./kips) which corresponds to a load of 13.8 kN (3.1 kips). After the cracking load, the rate of deflection increases. The slope of the second portion of the graph between 10 and 40 kN is relatively constant. This corresponds to the load stage between the flexural cracking load the the inclined cracking load. In the final portion of the graphs from inclined cracking to failure, the rate of deflection increases again.

The estimated deflection calculated using the procedure given in the ACI and CSA Codes for immediate deflection is also shown in Figure 6.28. These values agree quite well with the experimental results up to approximately the inclined cracking load. After this, the experimental deflections increase at a much higher rate. Adding an estimate of shear deflection (shown by horizontal line in Figure 6.28), such as that given by Park and Paulay (1975), to the estimate obtained from the Code equations, results in a better prediction of actual results. It is obvious from this graph that the formation and widening of inclined cracks has a significant effect on the deflection of the beam.

6.2 Comparison of Beam Strength

Comparisons of the beam strengths obtained from the tests with those calculated using the various procedures outlined in Chapter 2 are given in Table 6.1. The beams have been categorized according to web reinforcement ratios, $r = \frac{A_v}{b_w s}$.

The value $V_{u,test}$ was the shear resulting from the point loads applied to the beam from the MTS machine. The beam self-weight was neglected. In calculating the strength of the beams, the yield strength of the wires in the WWF sheets was the stress measured at 0.0035 strain. No strength reduction factors, ϕ, were used for any of the calculations.

In the Haddadin et al approach, the value V_u was calculated using Equation 2.10. For the Placas and Regan approach, Equation 2.12 was used. The ACI Code estimate was calculated from Equations 2.2 and 2.3. For the fourth estimate, Equations 2.8 and 2.3 were used.

For the beams with the WWF web reinforcement, the best estimate of beam strength, using the four approaches described above, was calculated using the ACI (or CSA) Code approach. Each of the other procedures over-estimated the strength of the beams. The procedure outlined by Haddadin et al predicted strengths approximately 15 to 30 percent higher than those obtained. However, this procedure was developed from tests of beams with $b/b_w \leq 3.5$ whereas the

TABLE 6.1

RATIO OF TEST STRENGTH DIVIDED BY PREDICTED STRENGTH $\frac{V_{u,test}}{V_{u,calc}}$

Category	Beam No.	Type of Web Reinf.	Web Reinf Ratio[1] r	$V_{u,test}$ kN	Haddadin et al Method	Placas & Regan Method	ACI Code Method	ASCE-ACI Comm. 426 and ACI Code Method	Placas & Regan Method Adjusted	$\frac{M_n}{V_{u,test} \cdot a}$
1	1	W2.5	1.04×10^{-3}	65	0.73	0.78	0.98	0.89	0.99	1.64
	2	D2.5	"	70	0.81	0.90	1.03	0.91	1.10	1.56
	6	D2.5	"	69	0.79	0.89	1.00	0.87	1.09	1.57
2	3	W2.9	1.21×10^{-3}	78	0.85	0.91	1.15	1.04	1.16	1.38
	8	W2.9	"	80	0.81	0.89	1.07	0.94	1.11	1.36
	4	D2.9	"	80	0.82	0.90	1.08	0.95	1.12	1.36
	5	D2.9	"	85	0.88	0.96	1.15	1.02	1.13	1.28
	7	D2.9	"	70	0.73	0.79	0.95	0.84	1.00	1.56
3	9	6 mm	1.52×10^{-3}	90	0.89	0.96	1.17	1.04	1.20	1.21
	10	6 mm	"	96	0.73	1.02	1.23	1.09	1.29	1.13

1) Based on nominal area for wires and on measured area for 6 mm bars

beam tests done for this program had $b/b_w = 5.0$. The other two procedures over-estimated the beam strength by between 5 and 15 percent.

The strength of TB 7 was lower than the other beams in this category because the web reinforcement was not anchored as well as in the other beams. The WWF sheet in TB 7 had D2.9 vertical wires with only the interior cross-wires for anchorage.

For the beams with the conventional 6 mm diameter stirrups, the best estimate of beam strength using these four approaches was given by the Placas and Regan procedure. The procedure using V_c from the ACI-ASCE Committee 426 equation and V_s from the ACI and CSA Codes also gave a good estimate. The existing ACI and CSA Code approach under-estimated the beam strength while the Haddadin et al approach over-estimated it.

The only procedure to give conservative estimates of beam strength for each of the categories was the existing ACI and CSA Code approach. However, as the web reinforcement ratio decreased, the predicted strength became less conservative.

In the Haddadin et al approach, the web reinforcement is 1.75 times as effective as that given by the ACI and CSA

Codes. This was not evident from the tests conducted in this program. The ratio $\frac{v_{u,test} - v_{c,ACI}}{r\, f_{vy}}$ as obtained from Equation 2.10 is used as a measure of the effectiveness of the web reinforcement. For category 1 from Table 6.1, the average value of this ratio was 1.02. The corresponding values for category 2 and category 3 were 1.27 and 1.48, respectively. The best results for TB 7 were neglected.

The Placas and Regan approach assumed that the angle of the failure crack was about 26 degrees. The average value for the average inclination of the failure cracks for the beams tested here was approximately 37 degrees. If Equation 2.16 is adjusted accordingly, then the results are much better as shown on the second last column of Table 6.1.

The strength predicted using V_c from the ACI-ASCE Committee 426 proposal plus V_s from the existing ACI and CSA Codes, gave good results for categories 2 and 3 but not for Category 1.

In all cases, the procedures for estimating beam strength gave better results for the beams with the highest web reinforcement ratios. Care must be taken when using these procedures for beams with such small amounts of web reinforcement.

Also shown in Table 6.1 is the ratio of the calculated beam moment capacity divided by the maximum beam moment at failure. The lowest value, 1.13, occurred in the test of TB 10. The beams were designed to fail in shear before flexure and were loaded well below their moment capacity when they failed in shear.

6.3 Comparisons of Beam Behaviour

6.3.1 Introduction

This section compares the results from the various tests to point out differences and similarities between the behaviour of the beams with the various types of web reinforcement and anchorages. Photographs of the beams after failure are given in the Appendix.

6.3.2 Crack Formation

The formation of cracks as described in Section 6.1.2 for TB 4 was generally the same for all the beams tested. The type of web reinforcement did not affect the type of crack formation.

In the shear spans, the first cracks to form were short vertical flexural cracks which generally did not extend past the top of the main reinforcement. This was followed by the formation of inclined flexure-shear cracks at loads above

the 20 to 30 kN (4.5 to 6.7 kip) range. As the load increased, these cracks propagated up towards the loading point to the web-to-flange transition and in some cases up to the bottom of the flange. At the same time, secondary cracks along the main reinforcement at the lower ends of the inclined cracks began to form. Flatter inclined cracks formed on the support side of the original inclined cracks as the load approached ultimate. If the initial crack made an angle of approximately 60 degrees or greater with the horizontal in the region between the reference line and the neutral axis, then generally a flatter crack would form next to it, or join with the upper portion of it.

At ultimate load, one of the wider cracks entered the flange near the load point and in the beams with the WWF web reinforcement it simultaneously propagated along the main reinforcement before going down to the bottom of the beam near the support. In the beams with the conventional stirrups, the failure crack did not propagate along the main reinforcement before going to the bottom of the beam. The opening up of the secondary cracks along the main reinforcement in these beams was not as significant because the stirrups were hooked around the main reinforcement which apparently confined this horizontal cracking.

In every beam, except TB 10, the failure crack propagated up through the flange at the load point. This resulted in a transverse crack across the top of the flange at this location. These beams also had another transverse crack across the top of the flange above the location where the failure crack entered the web-to-flange transition. The beam flange was kinked downwards at this location after failure. In these beams, there was a longitudinal crack along the center of the top of the flange which formed between the two transverse cracks. In TB 10 the only transverse crack across the top of the flange occurred above the location where the failure crack entered the web-to-flange transition.

There was no pattern regarding where the inclined cracks formed, but there was at least one inclined crack that crossed the reference line in each half of each shear span. The location where the failure cracks crossed the reference line varied considerably. In four of the beams, the failure crack was in the inner half of the shear span and in the remaining six beams, it was in the outer half. The failure cracks are superimposed in Figures 6.29 and 6.30. In TB 8 and TB 10, there were two major inclined cracks in the failure span and both are shown in these figures. TB 3 and TB 6 also had two major cracks but only the failure cracks are shown for these beams.

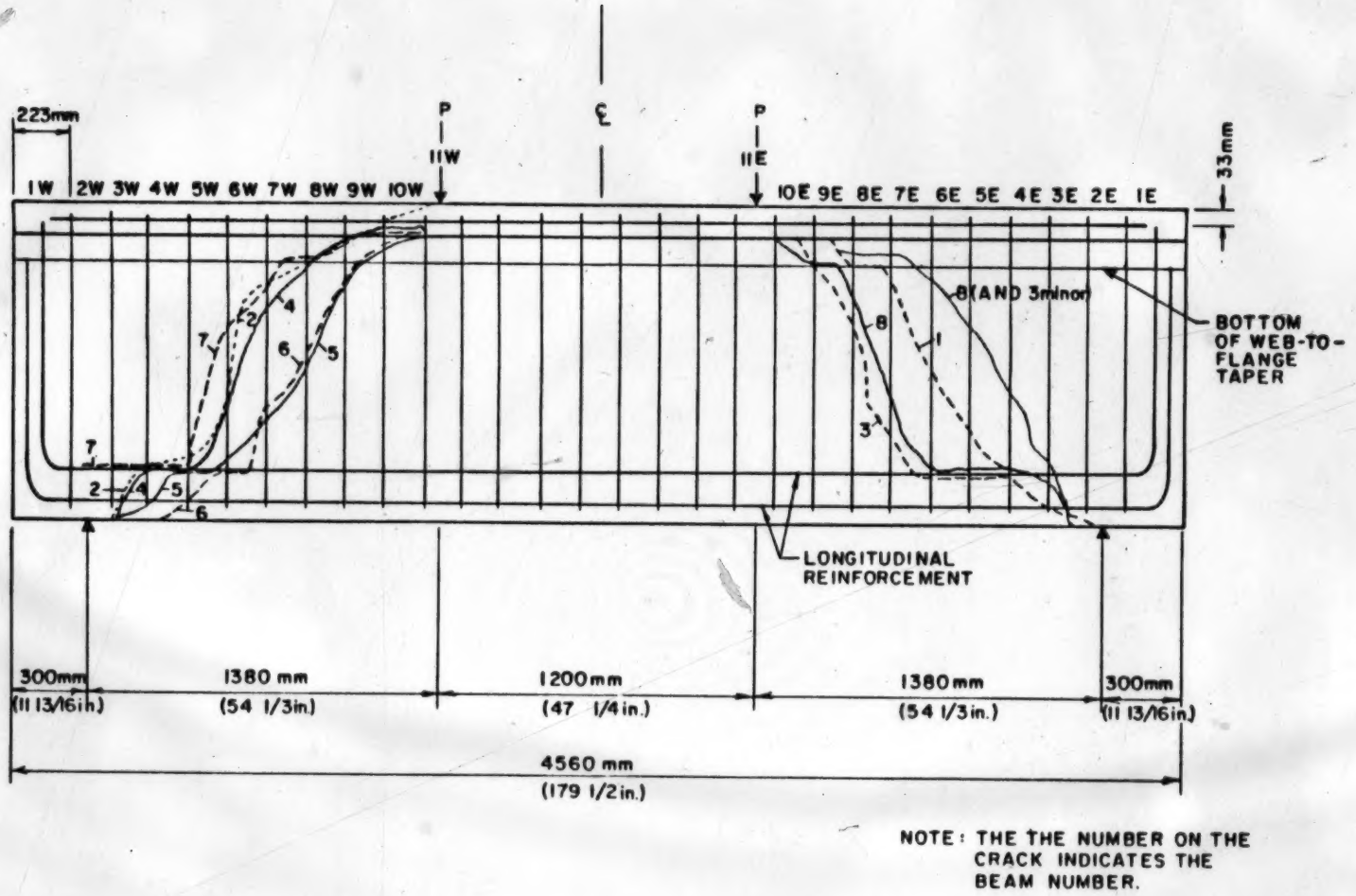

FIGURE 6.29 - Locations of Failure Cracks in TB 1 to TB 8 (Not to Scale)

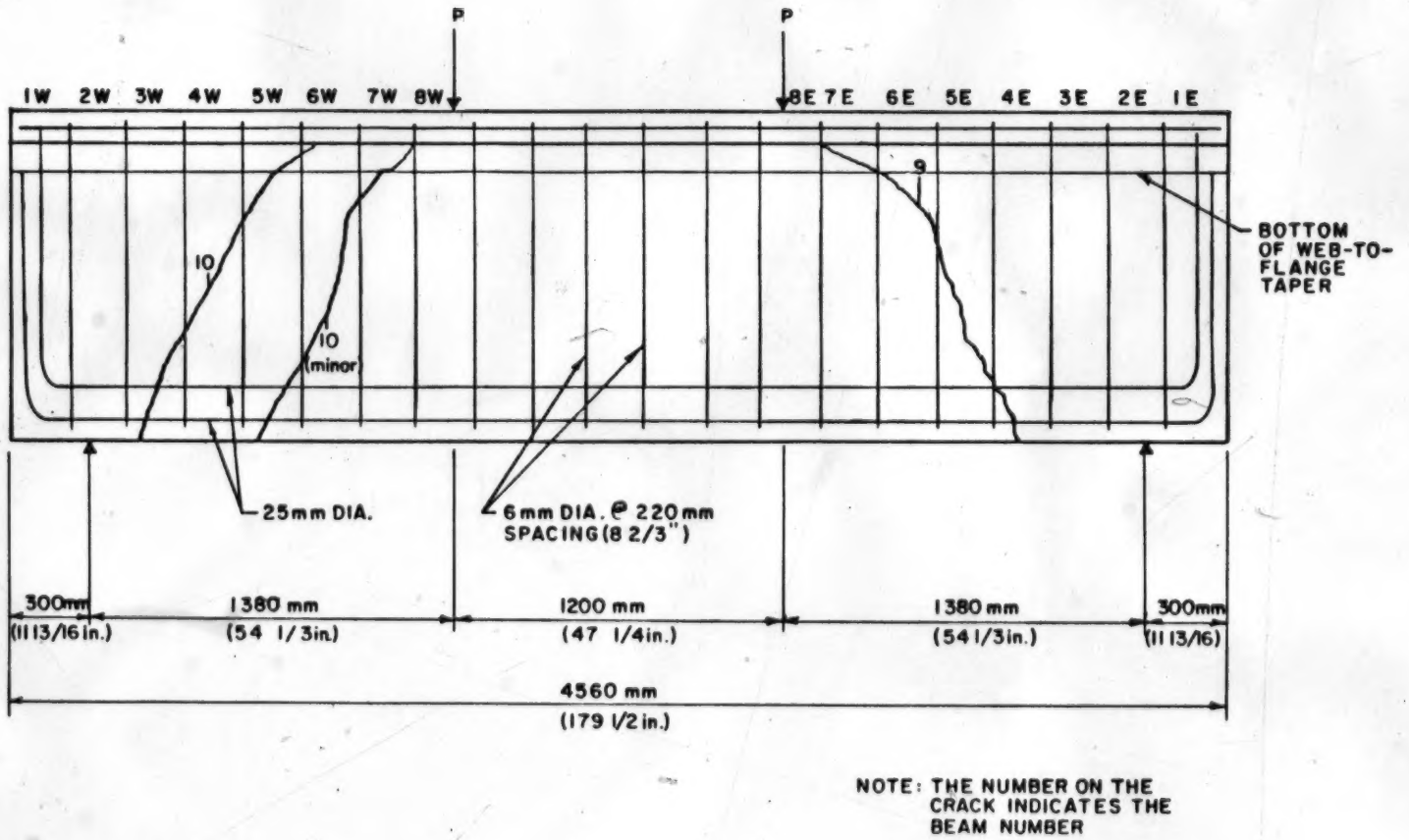
P
P
1W 2W 3W 4W 5W 6W 7W 8W
8E 7E 6E 5E 4E 3E 2E 1E
9
10
10
(minor)
BOTTOM OF WEB-TO-FLANGE TAPER
25mm DIA.
6mm DIA. @ 220mm SPACING (8 2/3")
300mm (11 13/16 in.)
1380 mm (54 1/3 in.)
1200 mm (47 1/4 in.)
1380 mm (54 1/3 in.)
300mm (11 13/16)
4560 mm (179 1/2 in.)
NOTE: THE NUMBER ON THE CRACK INDICATES THE BEAM NUMBER

FIGURE 6.30 - Locations of Failure Cracks in TB 9 and TB 10 (Not to Scale)

In the constant moment region of each beam, the cracks were virtually all vertical flexural cracks. The longest of these generally extended up to the centroidal axis of the uncracked section, although in some cases they extended slightly beyond. The type or spacing of the web reinforcement did not affect the formation of cracks in this region.

It should be noted that most of the beams had some vertical shrinkage cracks at the bottom prior to testing. As the beam was tested, further flexural cracking usually formed as extensions to these. There was also some horizontal shrinkage cracking at the bottom of the web-to-flange transition in most beams. This did not appear to affect the cracking during testing. A photograph of this second type of cracking is given in Figure 6.31.

The number of cracks that formed in the shear spans was not significantly affected by the type of web reinforcement although the beams with the higher web reinforcement ratios had slightly more cracking.

There were from four to six cracks crossing the reference line in the shear spans of the beams with W2.5 and D2.5 stirrups. The corresponding numbers for the beams with W2.9 and D2.9 stirrups were five to seven. For the two beams

FIGURE 6.31 - Typical shrinkage cracks at bottom of web-to-flange taper

with the 6 mm diameter stirrups, there were from five to eight cracks of this type.

There were either two or three inclined cracks crossing the centroidal axis in each shear span in the beams with W2.5 and D2.5 wire stirrups, whereas in the beams with W2.9 or D2.9 wire stirrups, there were from two to four such cracks. There were three to five of these cracks in each shear span in the beams with the conventional stirrup reinforcement.

The average inclination of the inclined cracks which crossed the centroidal axis ranged from 28 to 64 degrees with the steeper cracks generally closer to the load point. The average inclination of the widest of these cracks ranged from 28 to 46 degrees. The average value for the failure cracks was 37 degrees.

The type of web reinforcement had no effect on the load range in which inclined cracking took place. The estimated load ranges for the inclined cracking load for each span of each beam are shown in Table 6.2 along with the ACI (or CSA) Code values for V_c. The methods used to determine these estimates were explained in Section 6.1.3.

The load range estimated using visual Method 1 was generally lower than the value of V_c predicted using the code

TABLE 6.2

INCLINED CRACKING LOAD

Inclined Cracking Load Range from Tests - kN

Beam No.	East Shear Span			West Shear Span			$V_{c,ACI}$ kN
	Visual Method 1	Visual Method 2	Strain Gauge Method	Visual Method 1	Visual Method 2	Strain Gauge Method	
1	20 - 30	40 - 50	40 - 50	30 - 40	30 - 40	20 - 30	36.6
2	20 - 30	30 - 40	20 - 30	20 - 30	40 - 50	20 - 30	44.4
3	-	-	-	-	-	-	37.1
4	30 - 40	40 - 50	50 - 60	30 - 40	30 - 40	40 - 50	44.4
5	30 - 40	40 - 50	-	30 - 40	40 - 50	30 - 40	43.7
6	40 - 45	40 - 45	45	35 - 40	35 - 40	35 - 40	45.3
7	35 - 40	40 - 45	40 - 45	40 - 45	55 - 60	30 - 35	43.8
8	40 - 45	40 - 45	35 - 40	30 - 35	45 - 50	30 - 35	44.2
9	20 - 30	40 - 50	20 - 30	20 - 30	30 - 40	20 - 30	43.8
10	35 - 40	45 - 50	20 - 25	40 - 45	45 - 50	35 - 50	45.0

equations. The estimates obtained using visual Method 2 agreed quite well with the code predictions. The method of estimating the inclined cracking load range as the range in which the stirrup strain began to significantly increase, also gave values lower than the code values.

6.3.3 Crack Widths

As the load increased, the width of the inclined cracks also increased but no well defined relationship was exhibited. Some general trends were evident from comparisons of the average and maximum crack widths. The average crack width was calculated using the widths of all the cracks in both shear spans that crossed the reference line drawn at 200 mm (7.9 inches) above the bottom of the beam. The crack widths were measured perpendicular to the direction of the crack at the height of the reference line.

In order to make better comparisons of crack width for beams with different web reinforcement and concrete strength, graphs of $\frac{P}{P_{ult}}$ versus crack width were plotted using both maximum and average crack widths. These graphs appear in Figures 6.32 to 6.37.

The crack widths for values of $\frac{P}{P_{ult}}$ equal to 0.50 and 0.61 and also the crack widths prior to failure are summarized in

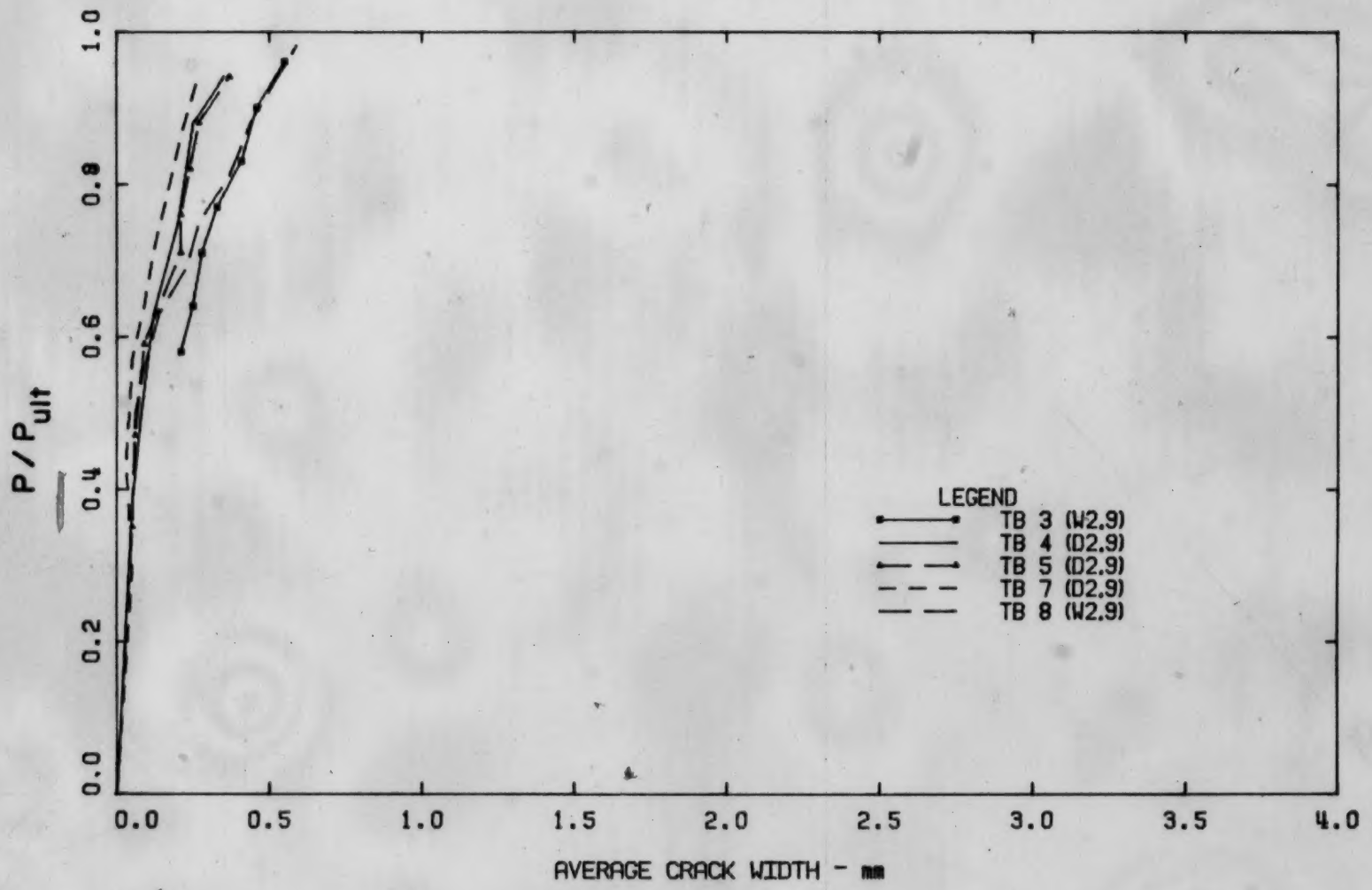

FIGURE 6.32 - Graphs of $\frac{P}{P_{ult}}$ Versus Average Crack Width for TB 3, TB 4, TB 5, TB 7 and TB 8

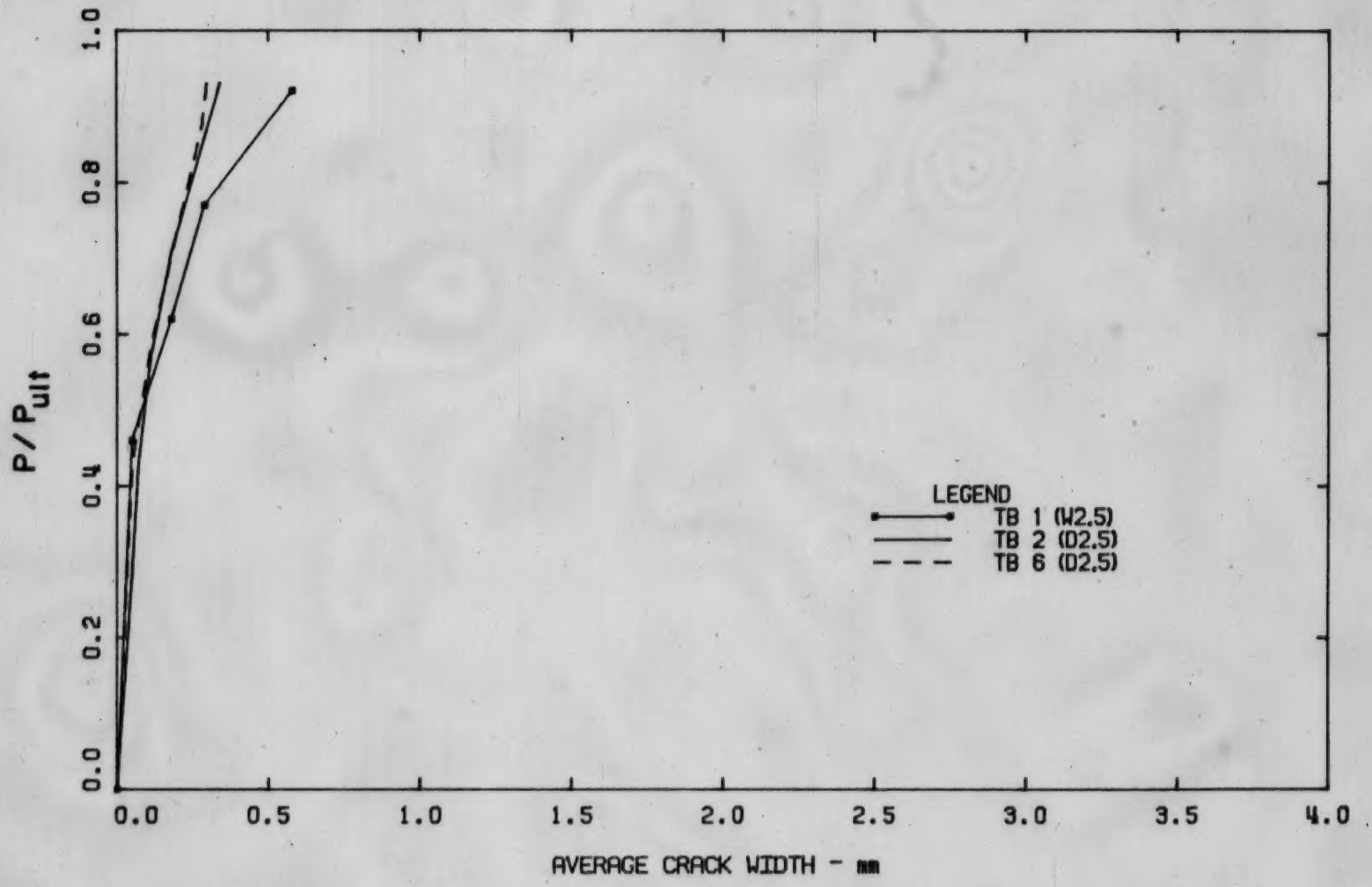

FIGURE 6.33 - Graphs of $\frac{P}{P_{ult}}$ Versus Average Crack Width for TB 1, TB 2 and TB 6

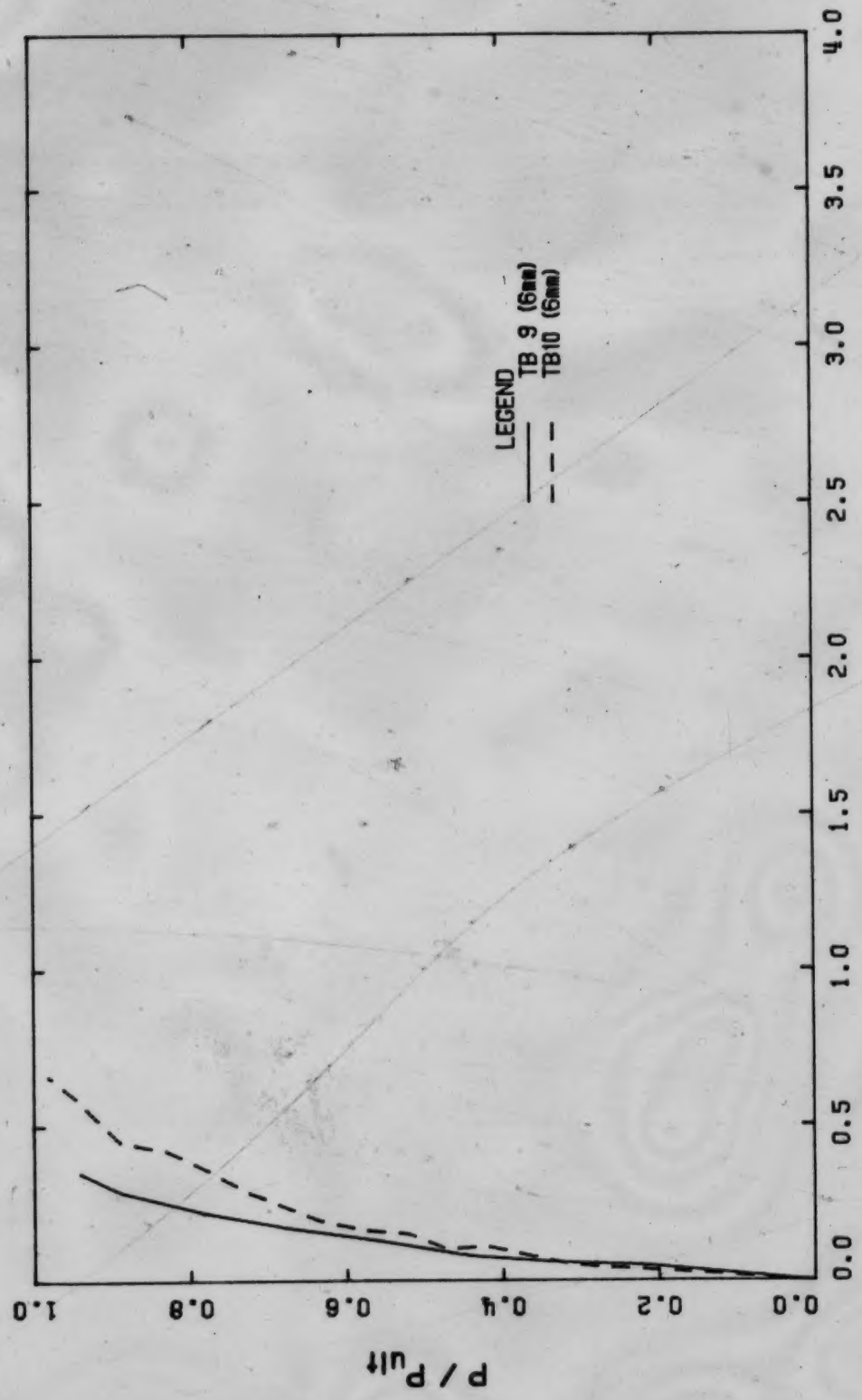

FIGURE 6.34 - Graphs of $\frac{P}{P_{ult}}$ Versus Average Crack Width for TB 9 and TB 10

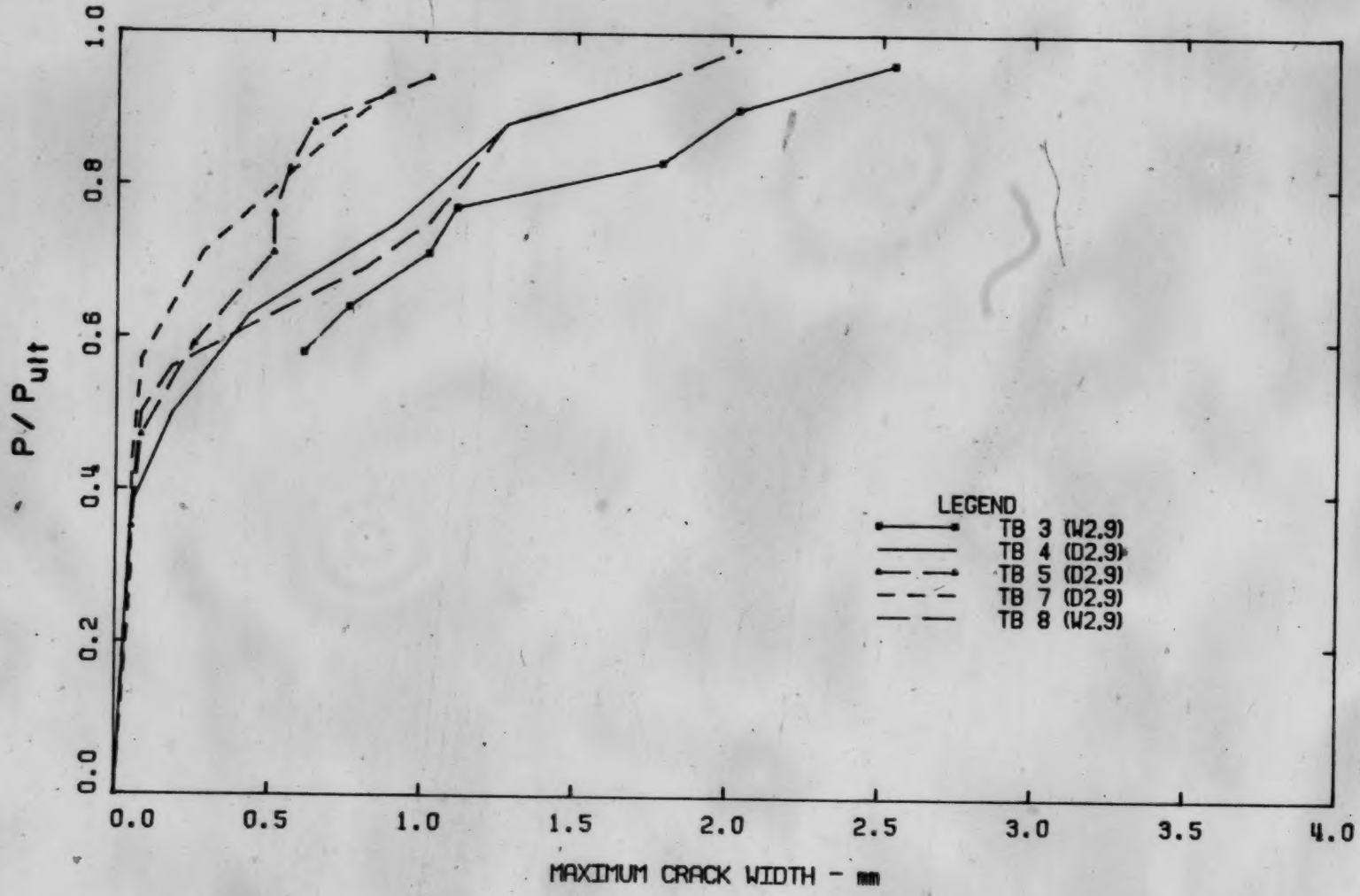

FIGURE 6.35 - Graphs of $\frac{P}{P_{ult}}$ Versus Maximum Crack Width for TB 3, TB 4, TB 5, TB 7 and TB 8

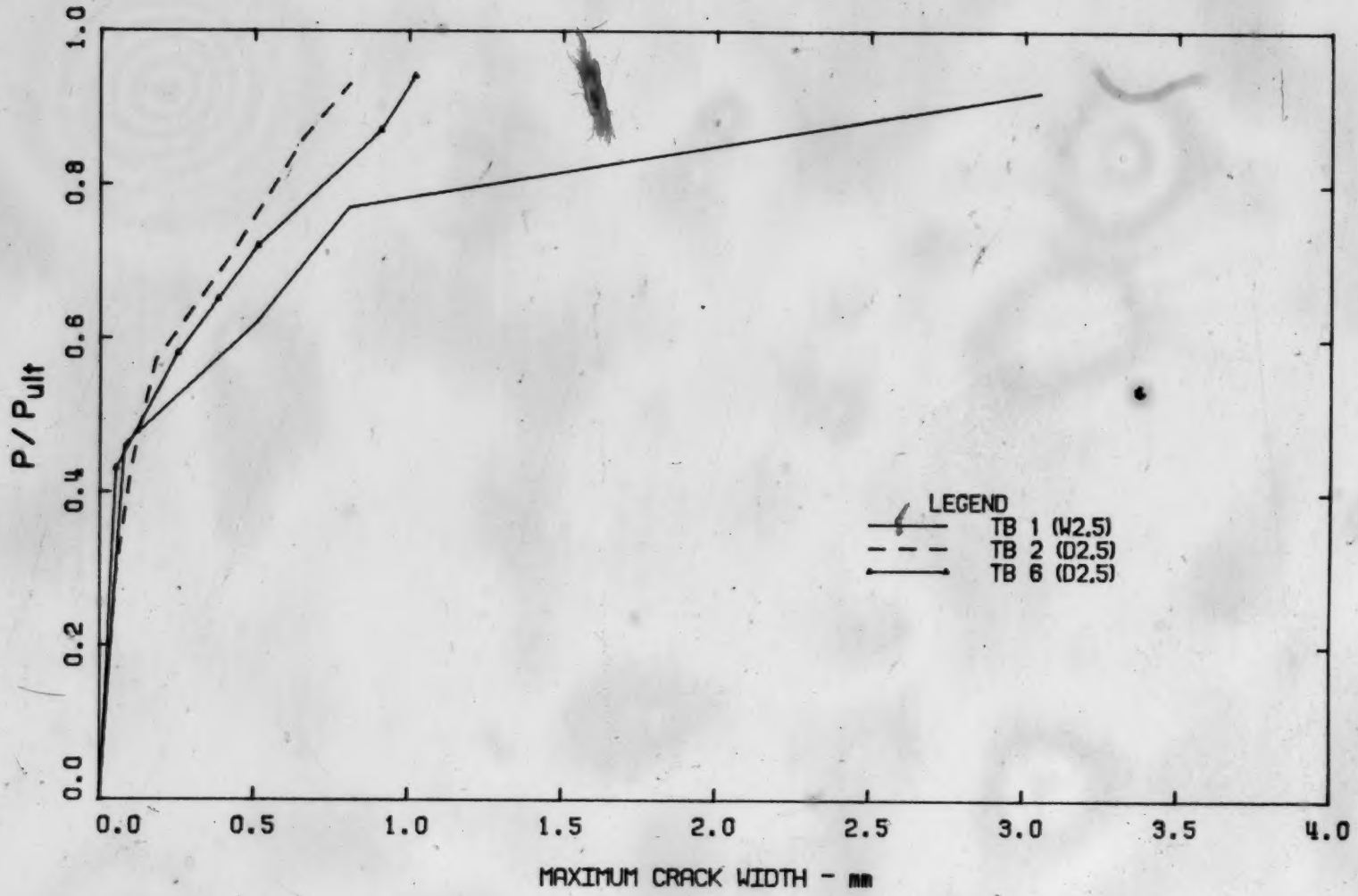

FIGURE 6.36 - Graphs of $\frac{P}{P_{ult}}$ Versus Maximum Crack Width for TB 1, TB 2 and TB 6

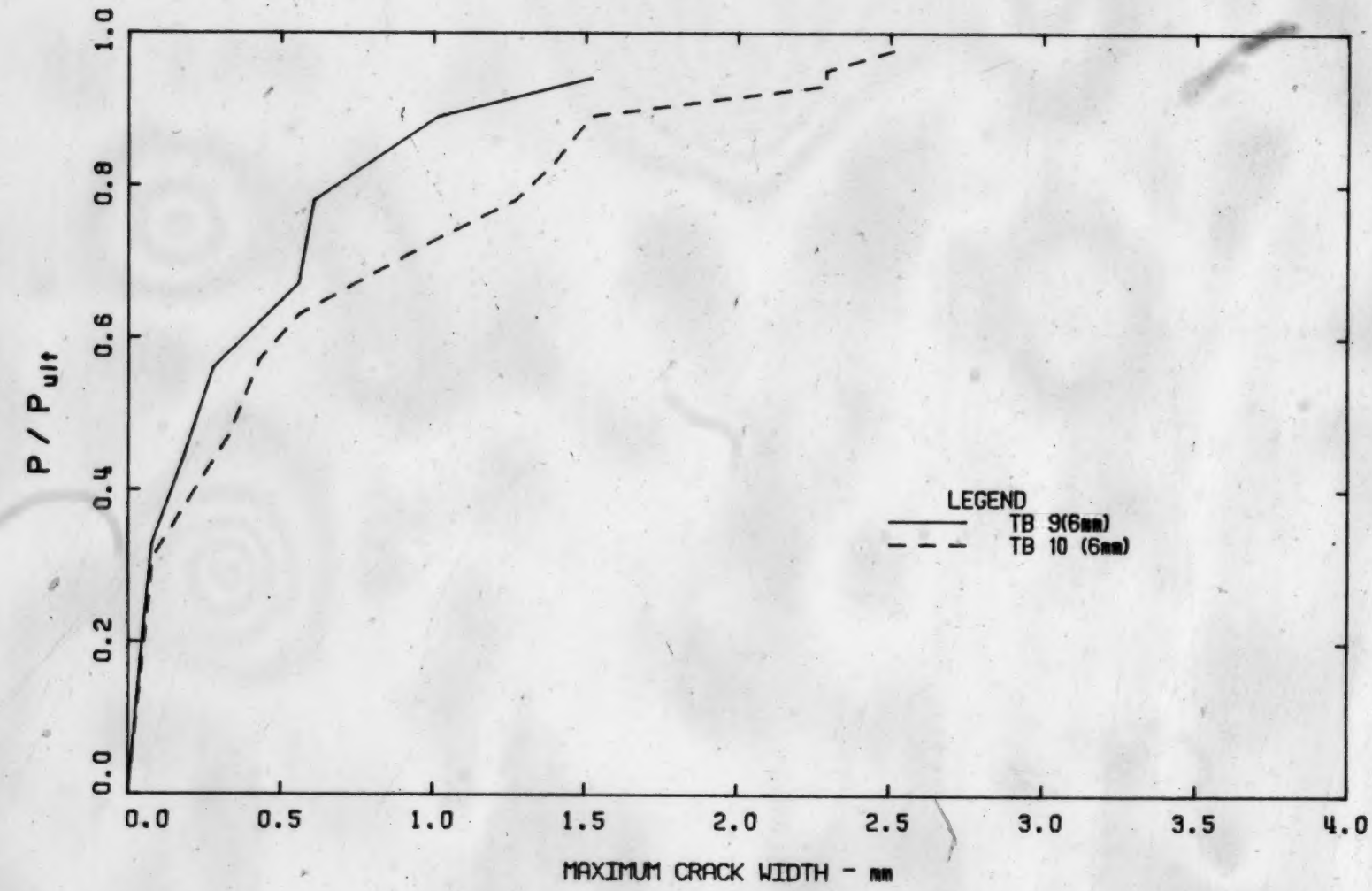

FIGURE 6.37 - Graphs of $\frac{P}{P_{ult}}$ Versus Maximum Crack Width for TB 9 and TB 10

Table 6.3. These values of $\frac{P}{P_{ult}}$ correspond to the service load range for the beams and were calculated as follows:

$$\frac{P}{P_{ult}} = \frac{\phi}{LF}$$

where:

ϕ = strength reduction factor = 0.85

LF = load factor

The load factors used to obtain the above values were 1.7 and 1.4, which are the live load and dead load factors given in the ACI and CSA Codes.

A comparison of the average crack width curve for TB 4, which had D2.9 wire stirrups, and those for TB 3 and TB 8, which had W2.9 wire stirrups, suggested that the average crack widths were similar up to service loads with the crack widths in the beam with the smooth wire stirrups increasing more rapidly for higher loads. In all of these beams, two longitudinal cross-wires, top and bottom, were used to anchor the WWF sheets. A similar observation was made when the average crack widths in TB 1 and TB 2 were compared. TB 1 had W2.5 wire stirrups and TB 2 had D2.5 wire stirrups.

A comparison of the maximum crack widths for these beams showed similar trends to the comparison of average crack width. In the lower load range, the maximum crack widths

TABLE 6.3

CRACK WIDTH DATA

Type of Web Reinf.	Beam No.	Approx f'c (MPa)	Average Crack Width (mm)			Maximum Crack Widths (mm)		
			at $\frac{P}{P_{ult}} = 0.5$	at $\frac{P}{P_{ult}} = 0.61$	Prior to Failure	at $\frac{P}{P_{ult}} = 0.5$	at $\frac{P}{P_{ult}} = 0.61$	Prior to Failure
W2.5	1	20	0.08	0.18	0.58	0.19	0.51	3.05
W2.9	3	20	-	0.23	0.55	-	0.68	2.54
	8	30	0.06	0.13	0.59	0.08	0.43	2.03
D2.5	2	30	0.09	0.13	0.34	0.14	0.25	0.81
	6	30	0.08	0.13	0.32	0.14	0.30	1.14
D2.9	4	30	0.08	0.11	0.35	0.18	0.40	1.78
	5	30	0.07	0.11	0.37	0.12	0.30	1.02
	7	30	0.04	0.07	0.26	0.06	0.13	0.91
6 mm	9	30	0.10	0.15	0.35	0.23	0.39	1.52
	10	30	0 13	0.18	0.66	0.36	0.52	2.54

were approximately the same for both deformed and smooth wire stirrups but in the higher load range, the maximum crack widths were larger in the beams with smooth wire stirrups.

These observations suggest that the crack widths were essentially independent of the type of wire (i.e. deformed or smooth) up to the service load but were wider in beams with smooth wire stirrups at high loads. Presumably this resulted from the poorer bond between the stirrups and the concrete in the case of the smooth wire.

A comparison of both the average and maximum crack widths between the beams with D2.5 wire stirrups (TB 2 and TB 6) and the beams with D2.9 wire stirrups (TB 4 and TB 5) indicated that there was relatively little difference. However, the crack widths for these beams were lower than for the beams with the conventional 6 mm diameter stirrups. This was in agreement with the results of Haddadin et al (1972) which stated that the service load crack widths increase as the value of rf_{vy} increases for rf_{vy} less than 2.76 MPa (400 psi).

The suggested maximum crack width given by ACI Committee 224 (1972) are summarized in Table 6.4. The maximum crack

TABLE 6.4

SUGGESTED MAXIMUM CRACK WIDTHS

ACI COMMITTEE 224 (1972)

Exposure Condition	Maximum Allowable Crack Width - mm
Dry air or protective membrane	0.41
Humidity, moist air, soil	0.30
De-icing chemicals	0.18
Seawater and seawater spray, wetting and drying	0.15
Water retaining structures	0.10

widths at $\frac{P}{P_{ult}} = 0.50$ for the beams tested here were generally within these limits. However, at $\frac{P}{P_{ult}} = 0.61$ some of the maximum crack widths exceeded these limits. This occurred in the beams with the smooth wire stirrups and in one of the beams with the 6 mm diameter conventional stirrups.

In almost every beam, the widest crack crossed the reference line in the outer half of the shear span. The widest crack was not the failure crack in all of the beams. In TB 3, TB 6 and TB 8, the widest crack prior to failure was in the outer half of the shear span but the crack that eventually caused the beam to fail was in the inner half.

6.3.4 Mode of Failure

All of the beams tested in this program had diagonal tension type failures similar to that described in Section 6.1.5 for TB 4. Failure was initiated when one of the inclined cracks simultaneously propagated up towards the loading point into the top flange and down to the bottom of the beam near the support. As this happened, the crack widened and separated the beam into two segments. The segment farthest from the support dropped relative to the segment closer to the support. The applied load dropped off significantly at

failure. No concrete crushing was evident in any of the beams.

At failure, the anchorages for the stirrups in the WWF sheets were damaged at the location where they were crossed by the failure cracks. Also, many of the wire stirrups crossed by the inclined portion of the failure crack fractured at failure. In the case of the beams with the conventional stirrups, the 9.5 mm (No. 3) bar around which the stirrups were hooked was slightly bent at failure in the region where it was crossed by the upper portion of the failure crack. There was no damage to the lower anchorage and none of those stirrups fractured at failure.

The failure cracks were much wider after failure in the beams with WWF web reinforcement than in the beams with the 6 mm diameter stirrups. This was a result of the anchorage behaviour and the fracturing of the stirrups. At the lower end of the failure crack at the beam failure load, dowel splitting occurred along the main reinforcement in the beams with WWF web reinforcement. The anchorage of this reinforcement apparently did not support the main reinforcement to help prevent this. The inclined portion of the failure crack then became wider and as a result most of the stirrups that were crossed by it fractured. This enabled the crack to widen further. Also, the stirrups that had

damaged anchorages and the stirrups that had the upper portion of the crack cross above their top anchorage were not effective in preventing the crack from widening. In the beams with the conventional stirrups, dowel splitting did not occur. Because these stirrups did not fracture and because dowel splitting did not take place, the failure cracks in these beams did not widen as much.

6.3.5 Stirrup Strain

The measured strain was negligible until the load range at or near which an inclined crack crossed the stirrup. After this, the strain increased with loading. The amount of this increase was dependent on the location of the gauge with respect to the crack, the type of crack and the anchorage of the stirrup.

The largest strains were recorded in the stirrups which were crossed by the wider inclined cracks in the region between the top of the main reinforcement and the web-to-flange transition. These stirrups were able to develop larger strains because they tended to be well anchored above and below the crack.

The stirrups with the lower strain readings were either crossed by the wider inclined cracks in the anchorage zones near the top or bottom of the beam or they were crossed by

relatively minor cracks that did not widen significantly during testing.

Strain gauge readings indicated unbonding between the concrete and smooth wire stirrups in several locations. At these locations, a crack crossed either above or below both gauges on the stirrup but not in between them and the readings from the two gauges were almost identical. An example of this is shown in Figure 6.38 for strain gauges 5 and 6 on stirrup 7E in TB 8 (see also Figure A.11). In this beam, a crack crossed below both gauges between 35 to 40 kN (7.9 to 9.0 kips). No other crack crossed the stirrup until between 60 to 65 kN (13.5 to 14.6 kips). This second crack crossed above both gauges. The readings from the two gauges were so close during testing that the stirrup was obviously not bonded to the concrete.

Some partial loss of bond was evident in the case of the deformed wire stirrups as discussed in Section 6.1.7. This was not observed in the case of the conventional stirrups. For the conventional stirrups, the strain gauge located closest to the crack generally had the highest reading. This indicated that there was some bond between the concrete and these stirrups.

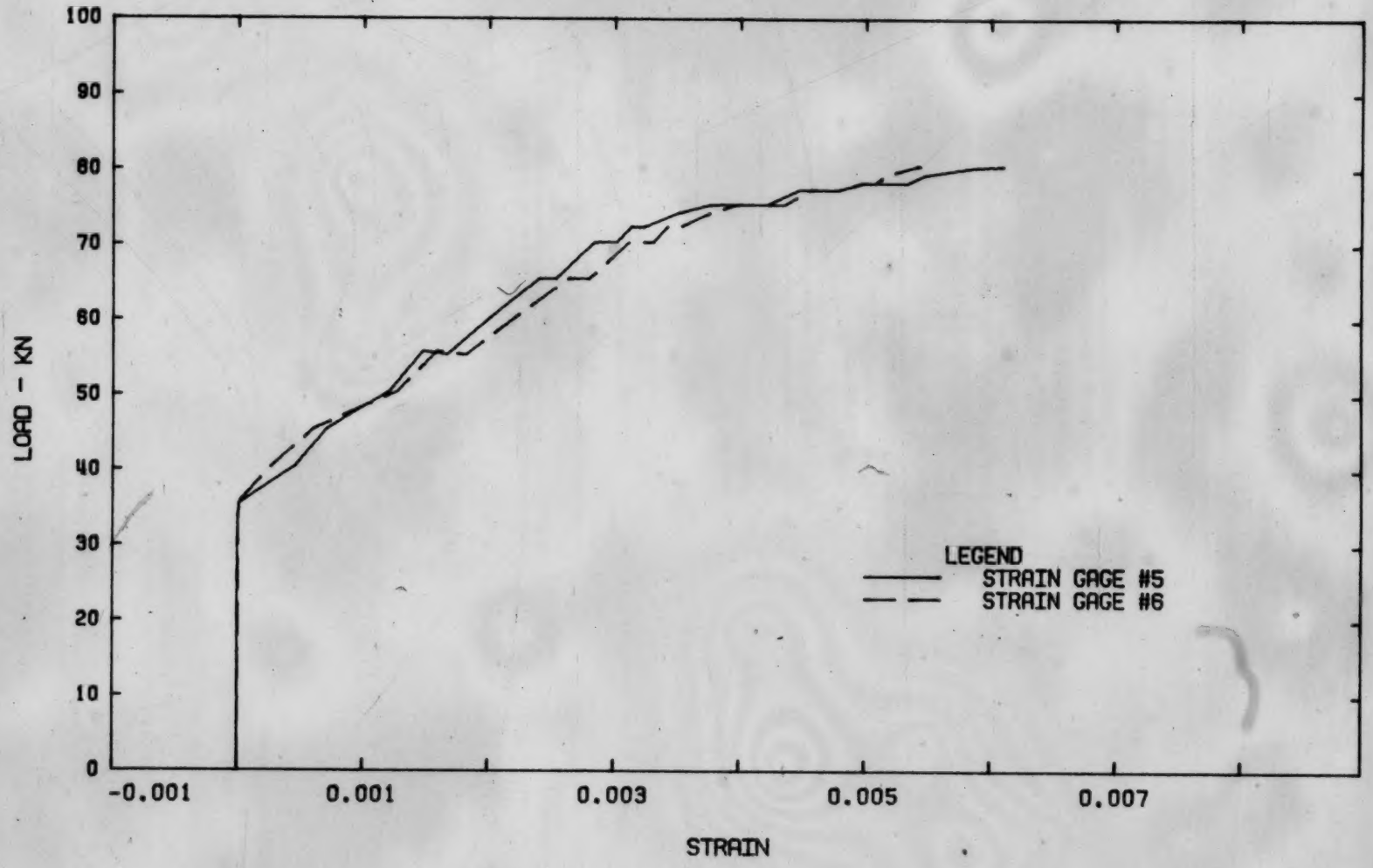

FIGURE 6.38 - Graph of Load Versus Strain for Strain Gauges 5 and 6 from TB 8 Showing Unbonding Between Concrete and Stirrup Wire

Relatively few strain gauges gave readings indicating that the stirrups had yielded prior to failure but in the cases where yielding was recorded, the failure crack crossed near the middle of stirrup and the strain gauge was located close to the crack. It is possible that more of the stirrups crossed by the failure crack yielded before failure because not all of the stirrups crossed by this crack were instrumented. It is also possible that the stirrups yielded at the failure crack but not at the location of the strain gauge. The difference would be due to the bond between the concrete and the stirrup.

In the beams with the WWF web reinforcement, most of the stirrups crossed by the failure crack fractured when the ultimate load was reached. It was obvious that these stirrups yielded and fractured in tension but it could not be determined at what load the yielding began. The fractured wires exhibited necking down at the location of the fracture similar to that obtained in the tension tests. The stirrups that fractured were well anchored both above and below the failure cracks. The stirrups which fractured in each of these beams are listed in Table 6.5.

None of the conventional stirrups fractured at the beam ultimate load. The strain readings in the stirrups crossed by the major inclined cracks were close to yield in most

TABLE 6.5

WIRE STIRRUPS FRACTURED AT FAILURE

Beam No.	Reinf. Size	Type of Anchorage	Stirrups which Fractured
1	W2.5		5E, 6E
2	D2.5		4W, 5W, 6W, 7W
3	W2.9		8E
4	D2.9		5W, 6W
5	D2.9		5W, 6W, 7W, 8W
6	D2.9		6W, 7W, 8W
7	D2.9		5W, 6W
8	W2.9		None

cases but only two gauges gave readings greater than yield before the beam failure load. Neither of these gauges was on a stirrup that was crossed by a failure crack.

6.3.6 Stirrup Slip and Anchorage Behaviour

The stirrup slip was measured as close as possible up to the failure load of the beam. Many of the gauges mounted on the bottom of the beam fell off either during testing or at failure. Readings from the gauges on the top of the beams were taken up to the failure load but no readings could be taken after failure either because the slip was too great or because the gauge became unseated from the stirrup.

There was a large variation in the amount of slip that was measured. The range in slip measurements taken just prior to failure are shown in Tables 6.6 and 6.7. The results have been categorized for each shear span according to type of reinforcement, concrete strength, location of inclined crack at the stirrup, and anchorage damage. Because of the numerous factors affecting the slip and the large variation in the results, it was not possible to determine any differences in behaviour for the different wire sizes used in the WWF sheets. However, some general observations were made and the results were compared to those from the beams with conventional stirrups.

TABLE 6.6

FINAL SLIP MEASUREMENTS IN FAILURE SPAN - mm

Category	WWF Web Reinforcement $f'_c = 20$	WWF Web Reinforcement $f'_c = 30$	6 mm Dia. Stirrups $f'_c = 30$
1. Stirrup with damage to anchorage and crossed by failure crack	0.26 to 2.96	0.15 to 1.37	0.61 to 2.90
2. Stirrup fractured at failure and crossed by failure crack	0.007 & 1.48	0.10 to 1.22	-
3. Slip measured at bottom of beam on stirrup crossed by failure crack propagating along main reinforcement (no damage to anchorage)	0.02 & 0.10	0.07 to 0.52	0.04 to 0.24
4. Stirrup crossed by failure crack either above top anchorage or below bottom anchorage	0.83	0.07 to 1.01	0.08

TABLE 6.7

FINAL SLIP MEASUREMENTS IN NON-FAILURE SPAN - mm

Category	WWF Web Reinforcement $f'_c = 20$	WWF Web Reinforcement $f'_c = 30$	6 mm Dia. Stirrups $f'_c = 30$
1. Stirrup crossed by inclined crack near top anchorage zone	0.73	0.19 to 0.43	0.32
2. Stirrup crossed by inclined crack at location other than near top anchorage	0.09 to 0.52	0.04 to 0.34	0.16 to 0.33

The maximum slip in almost every beam occurred at a stirrup that was crossed by the failure crack either in the region of the top anchorage in the web-to-flange transition or in the region of the bottom anchorage at the level of the main reinforcement. In the beams with WWF web reinforcement and concrete strengths of approximately 30 MPa (4350 psi), this slip was between 0.52 mm and 1.37 mm (0.0203 to 0.0539 inches). In the beams with WWF web reinforcement and with concrete strengths of approximately 20 MPa (2900 psi) the maximum values were 1.92 mm (0.0759 inches) and 2.96 mm (0.1164 inches). The maximum slip measured in the beams with the conventional 6 mm diameter stirrups were 0.61 mm (0.0241 inches) and 2.90 mm (0.1142) inches.

In several of the beams, the slip readings began to creep near the failure load. An increase in the slip readings when the load was constant was a good indication that failure was close.

At the stirrup with the maximum slip in the beams with the WWF web reinforcement (excluding TB 7), there was some type of damage to the exterior cross-wire anchorage in almost every case. Because of this damage, the effectiveness of these anchorages was reduced and the stirrups were not able to develop their full loads. In two of the beams, the stirrup with the maximum slip did not have any damage to the

exterior anchorage so the stirrups were able to develop fully and they fractured when the beam ultimate load was reached.

After entering the upper flange in the beams with the conventional stirrups, the failure crack propagated along the top of the 9.5 mm (No. 3) bar that ran through the top stirrup hooks. This effectively destroyed the upper anchorage of the stirrups in this region. This bar was bent as the stirrups were pulled down at failure. The maximum slip occurred at the stirrups where this took place. The cracking above the 9.5 mm (No. 3) bar is shown in Figure 6.39.

The damage to the anchorages of the wire stirrups resulted either when the weld between the stirrup and the anchorage wire failed, the anchorage wire fractured at the weld, or both of these occurred together. A typical failure case is illustrated in Figure 6.40. The exterior anchorage at the top of the beam was usually damaged when the failure crack crossed the stirrups below this anchorage in the web-to-flange transition. The stirrup remained well anchored below the failure crack so as the crack widened and the segment of the beam below the crack dropped, either the exterior weld or cross-wire or both failed and the stirrup was pulled out of the flange. The exterior anchorage at the bottom of the beam failed in a similar manner. Damage to the anchorage

FIGURE 6.39 - Crack forming above 9.5 mm bar at top of failure crack in TB 10

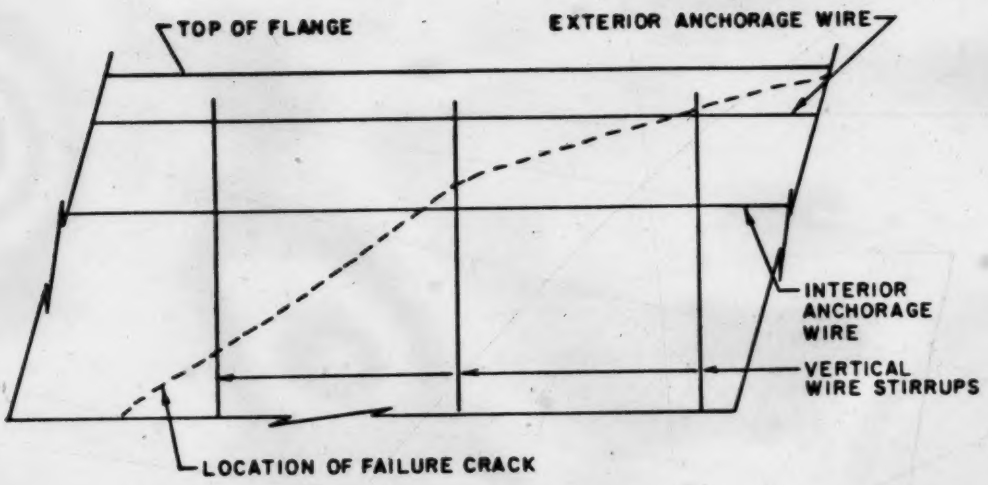

BEFORE BEAM FAILURE LOAD

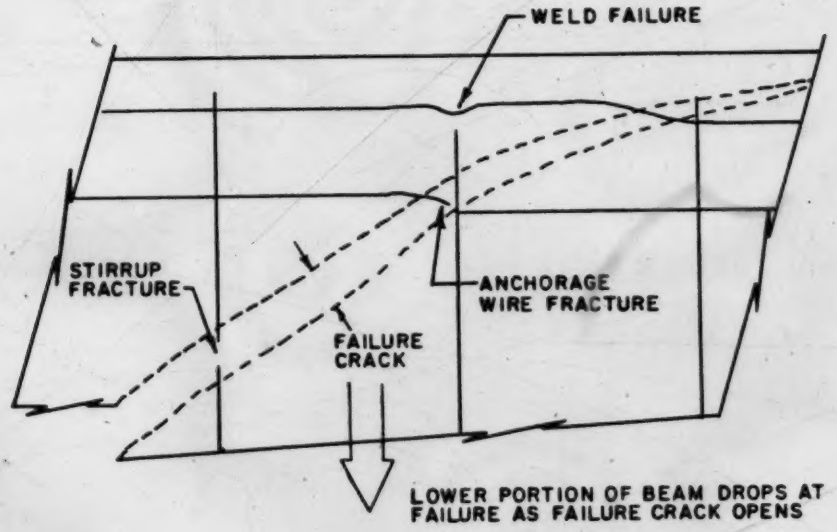
WELD FAILURE
STIRRUP FRACTURE
ANCHORAGE WIRE FRACTURE
FAILURE CRACK
LOWER PORTION OF BEAM DROPS AT FAILURE AS FAILURE CRACK OPENS

AFTER BEAM FAILURE LOAD

FIGURE 6.40 - Illustration Showing How the Anchorage Wires at the Top of the Beams were Damaged at the Beam Failure Load

wires at the bottom of some beams is shown in Figures 6.41 and 6.42. The interior anchorages both at the top and at bottom of the beams usually failed when the cross-wire was sheared off at the weld as the segment of the beam below the crack dropped with respect to the segment of the beam above the failure crack.

The failure cracks were much wider after failure in the beams with the WWF web reinforcement than in the beams with the 6 mm diameter stirrups. This was partially due to the behaviour of the anchorage of the web reinforcement. In the beams with the WWF web reinforcement, the bottom anchorage did not give any support to the main reinforcement to prevent dowel splitting and the damage to the stirrup anchorages crossed by the failure cracks in these beams reduced the effectiveness of these stirrups. The failure crack was, therefore, able to open up and the portion of the beam below this crack dropped relative to the portion above. The conventional stirrups seemingly prevented the failure crack from widening significantly after the beam failed because they were hooked around the main reinforcement at the bottom of the beam and around the 9.5 mm diameter (No. 3) bar in the flange so that the effectiveness of the anchorage was not as severely damaged. Also, the support given to the main reinforcement by these stirrups apparently prevented dowel splitting.

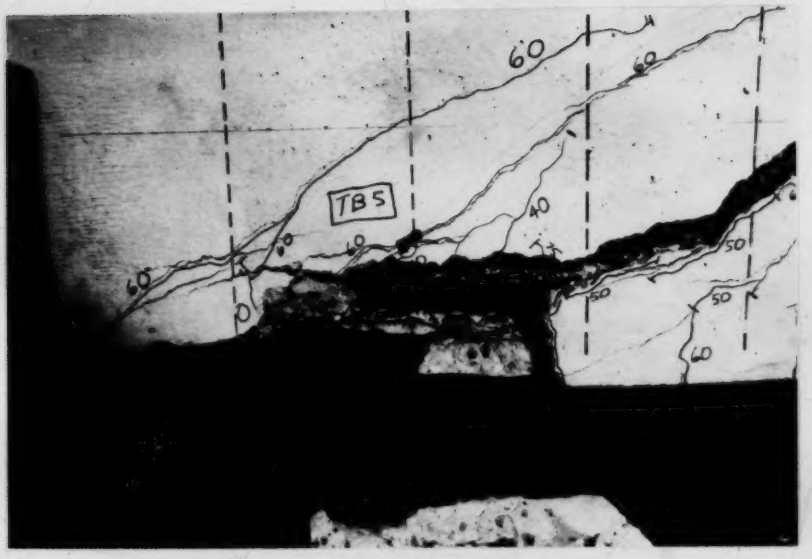

FIGURE 6.41 - Damage to anchorage at bottom of failure crack in TB 5

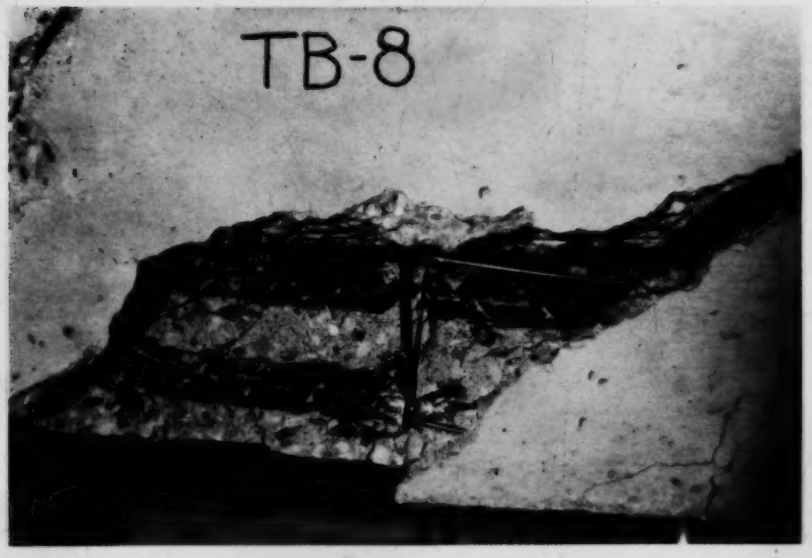

FIGURE 6.42 - Damage to anchorage at bottom of failure crack in TB 8

In TB 7, only the interior cross-wire anchorages were provided on the WWF sheet. This was not a satisfactory method of anchorage. The portion of the stirrups that was effectively anchored was reduced appreciably. The stirrups crossed by the inclined cracks outside of the zone between the anchorage wires were ineffective. This beam failed well below the load reached by beams with similar stirrups but with exterior anchorage wires.

The behaviour of the beams with only the exterior anchorage wires on the WWF sheets was comparable to that of the beams with both the interior and exterior anchorage wires.

In the beams with two anchorage wires top and bottom on the WWF sheets, the stirrups that fractured did so in the region between the top and bottom anchorages in every case except one.

6.3.7 Deflections

The load versus deflection graphs for all of the beams were similar to that described in Section 6.1.9 for TB 4. There was considerable difference between the measured and the calculated midspan deflections. The calculated deflections were made using the average value of Young's Modulus obtained from the cylinder tests for the beams and the

effective moment of inertia, I_e, given in the ACI and CSA Codes. No estimate of deflection due to shear was included. These values are shown in Table 6.8. The difference between the measured and the calculated deflections is due to effect of the inclined cracks in the shear spans.

The deflections from the load versus deflection graphs made with the MTS plotter were very close to the deflections measured with the LVDT.

TABLE 6.8

BEAM DEFLECTION PRIOR TO FAILURE

Beam No.	Type of Web Reinf.	Failure Load (kN)	Load at Reading Prior to Failure (kN)	Midspan Deflection Prior to Failure (1) (mm)	Calculated Midspan Deflection (mm)	Difference Between Measured & Calculated Deflection (mm)
TB 1	W2.5	65	60	9.47	5.52	3.95
TB 2	D2.5	70	70	10.43	6.07	4.36
TB 3	W2.9	78	75	11.24	6.91	4.33
TB 4	D2.9	80	80	10.51	6.95	3.56
TB 5	D2.9	85	80	10.18	6.95	3.23
TB 6	D2.5	69	69	9.96	6.07	3.89
TB 7	D2.9	70	65	8.79	5.63	3.16
TB 8	W2.9	80	80	14.50	6.95	7.55
TB 9	6 mm	90	85	12.53	7.38	5.15
TB 10	6 mm	96	96	16.01	8.26	7.75

1) Measured with LVDT

CHAPTER 7

SUMMARY AND CONCLUSIONS

1. The existing ACI and CSA Code procedures for calculating beam shear strength gave conservative estimates for the beams with adequately anchored web reinforcement tested in this program. However, the amount by which the estimates were conservative decreased considerably as the web reinforcement ratio, r, decreased. The ratio of test strength divided by predicted strength based on the Code procedures for the different web reinforcements ranged from approximately 1.0 for the W2.5 and D2.5 wires ($r = 1.04 \times 10^{-3}$), to approximately 1.1 for the W2.9 and D2.9 wires ($r = 1.21 \times 10^{-3}$), to approximately 1.2 for the 6 mm diameter conventional stirrup ($r = 1.52 \times 10^{-3}$). Thus, for smaller amounts of web reinforcement, the Code equations were less conservative.

2. The ductility of the beams tested increased as the web reinforcement ratio, r.

3. All the beams tested had diagonal tension type failures with the failure crack entering the flange near the load point and propagating down to the bottom of the beam near the support when the failure load was reached. There was no evidence of concrete crushing.

The average value of the average inclination of the failure cracks was 37 degrees.

4. Secondary cracks (splitting cracks) formed along the main reinforcement as the failure load was approached. When the ultimate load was reached for the beams with the WWF web reinforcement, these cracks opened up and formed part of the failure crack near the bottom of the beam. This did not occur in the beams with the conventional stirrups which were hooked around the longitudinal reinforcement. Therefore, the anchorage of the WWF sheets was not effective in supporting the main reinforcement to prevent this dowel splitting.

5. In most cases, the vertical wires in the WWF sheets which were crossed by the failure crack in the middle region of the beam fractured when the beam failure load was reached. This was due to the relatively low values of ultimate strain, ε_u, for these wires. These fractures, along with the lack of confinement of the dowel splitting, caused the failure crack to open considerably at the ultimate load of the beam. None of the conventional 6 mm diameter stirrups fractured when the beam failed and the failure crack did not open up as wide as in the beams with the WWF web reinforcement. The fracturing of the WWF stirrups eliminated the

strength component V_s and the opening up of the failure crack eliminated the aggregate interlock. The loss of these shear transfer mechanisms together with the reduction of the "dowel shear" due to the splitting along the main reinforcement resulted in shear failure of these beams. This would not be desirable in situations where load redistribution would be required.

6. The anchorage of the WWF sheets using two horizontal cross-wires top and bottom proved to be satisfactory. In the case of the welded deformed wire fabric, the use of only the exterior cross-wire anchorages top and bottom was also satisfactory. The use of only the interior cross-wire anchorage top and bottom did not give acceptable anchorages. The 1983 ACI Code proposal for anchorage of single leg WWF shear reinforcement would be acceptable for these beams. It should be noted that the exterior cross-wires in the compression zone (i.e. in the flange) should be as close as possible to the outer face because once the inclined crack crosses above the anchorage, the stirrup is no longer effective.

7. Total loss of bond between the concrete and the vertical wires in the welded smooth wire fabric was evident. Also, partial loss of bond was evident between the

concrete and the vertical wires in the welded deformed wire fabric.

8. The maximum crack widths in the beams with the WWF web reinforcement were essentially the same for the smooth and deformed wires up to service load levels ($\frac{P}{P_{ult}} = 0.5$). At higher loads, the maximum crack width was larger in the beams with the welded smooth wire fabric. At the upper end of the service load range ($\frac{P}{P_{ult}} = 0.61$) the maximum crack width in the beams with the smooth vertical wires were larger than the suggested maximums given by ACI Committee 224 (1972).

9. Placing the WWF sheet slightly offset from the center-line of the web (TB 8) did not appear to have any effect on the beam behaviour.

CHAPTER 8

RECOMMENDATIONS FOR FURTHER STUDY

1. The beams tested in this program were designed to fail in shear before flexure. The behaviour of this type of web reinforcement should be investigated in the case of beams designed for a balanced failure.

2. Because of the large number of factors affecting the behaviour of beams under shear loading, further investigation should be carried out to determine effects of varying such parameters as a/d, b/b_w, and ρ_w.

3. Additional specimens with the conventional reinforcement stirrups detailed so that the failure crack cannot pass above the upper anchorage should be tested to compare their behaviour to that of the beams with the WWF web reinforcement.

4. The behaviour of WWF web reinforcement should be investigated under dynamic loading conditions.

LIST OF REFERENCES

ACI Committee 224, "Control of Cracking in Concrete Structures", ACI Journal, Proceedings, Vol. 69, No. 12, Dec. 1972, pp 717-752.

ACI Committee 326, "Shear And Diagonal Tension", ACI Journal, Proceedings, Vol. 59, Jan., Feb., and March 1962, pp 1-30, 277-334, and 353-396.

ACI-ASCE Commiteee 426, "Suggested Revisions to Shear Provisions for Building Codes", ACI Journal, Proceedings, Vol. 74, No. 9, Sept. 1977, pp 458-469.

ACI-ASCE Committee 426, "The Shear Strength of Reinforced Concrete Members", Journal of the Structural Division, ASCE, Vol. 99, No. ST6, June 1973, pp 1091-1187.

American Concrete Institute, Building Code Requirements for Reinforced Concrete (ACI 318-77), Detroit, Mich., 1977.

American Concrete Institute, Commentary on Building Code Requirements for Reinforced Concrete (ACI 318-77), Detroit, Mich., 1977.

Attiogbe, E.K., Palaskas, M.N., and Darwin, D., "Shear Cracking and Stirrup Effectiveness of Lightly Reinforced Concrete Beams", Structural Engineering and Engineering Materials, SM Report No. 1, University of Kansas Center for Research, Inc., Lawrence, Kansas, July 1980.

Batchelor, B. deV., Kwun, M., "Shear in Reinforced Concrete Beams without Web Reinforcement", Journal of the Structural Division, ASCE, Vol. 107, No. ST5, May 1981.

Bresler, B., and MacGregor, J.G., "Review of Concrete Beams Failing in Shear", Journal of the Structural Division, ASCE, Vol. 93, No. ST1, Proc. Paper 5106, Feb. 1967, pp 343-372.

Canadian Standards Association (CSA), Code for the Design of Concrete Structures for Buildings (CAN 3-A23.3-M77), Rexdale, Ontario, 1977.

Dove, A.B., Some Observations on the Physical Properties of Wire for Plain and Deformed Welded Wire Fabric, Burlington, Ontario, Jan. 1982, Commentary on the article "Strength and Ductility of Concrete Slabs

Reinforced with Welded Wire Fabric" by Mirza, S.A., and MacGregor, J.G., which appeared in the ACI Journal, Vol. 78, Sept.-Oct. 1981, pp 374-381.

Haddadin, M.J., Hong, S., and Mattock, A.H., "Stirrup Effectiveness in Reinforced Concrete Beams with Axial Forces", Journal of the Structural Division, ASCE, Vol. 97, No. ST9, Proc. Paper 8394, Sept. 1971, pp 2277-2298.

Kani, M.W., Huggins, M.W., Wittkopp, R.R., Kani on Shear in Reinforced Concrete, Dept. of Civil Engineering, University of Toronto, 1979.

Leonhardt, F. and Walther, R., "Welded Wire Mesh as Stirrup Reinforcement, Shear Tests of T-Beams and Anchorage Tests", (German) Bautechnik, Vol. 42, Oct. 1965, English Translation by W. Dilger.

MacGregor, J.G., and Gergely, P., "Suggested Revisions to ACI Building Code Clauses Dealing with Shear in Beams", ACI Journal, Proceedings, Vol. 74, No. 10, Oct. 1977, pp 493-500.

Mirza, S.A., and MacGregor, J.G., "Strength and Ductility of Concrete Slabs Reinforced with Welded Wire Fabric", ACI Journal, Proceedings, Vol. 78, No. 5, Sept-Oct. 1981, pp 374-381.

Park, R., and Paulay, T., Reinforced Concrete Structures, Toronto, John Wiley and Sons, 1975, pp 270-319.

Placas, A., and Regan, P.E., "Shear Failures of Reinforced Concrete Beams", ACI Journal, Proceedings, Vol. 68, No. 10, Oct. 1971, pp 763-773.

Prestressed Concrete Institute Technical Activities Committee's Joint PCI/WRI Ad Hoc Committee on Welded Wire Fabric for Shear Reinforcement, "Welded Wire Fabric for Shear Reinforcement", PCI Journal, Vol. 25, No. 4, July-Aug. 1980, pp 32-36.

Rajagopalan, K.S., Ferguson, P.M., "Exploratory Shear Tests Emphasizing Percentage of Longitudinal Steel", ACI Journal, Proceedings, Vol. 65, No. 8, Aug. 1968, pp 634-638.

Swamy, R.N., Bandyopadhyay, A.K., and Erikitola, M.K., "Influence of Flange Width on the Shear Behaviour of Reinforced Concrete T-Beams", Institution of Civil Engineers, London, Proceedings, Vol. 55, March 1973, pp 167-190.

Taylor, H.P.J., "The Fundamental Behaviour of Reinforced Concrete Beams in Bending and Shear", Shear in Reinforced Concrete, ACI Publication SP-42, Detroit, Mich., 1974, pp 43-77.

Taylor, M.A., El-Hammasi, S., "Web Cracking Behaviour of Beams using Welded Wire Fabric as Shear Reinforcement", ACI Journal, Proceedings, Vol. 77, No. 1, Jan.-Feb. 1980, pp 12-17.

Wire Reinforcement Institute, Manual of Standard Practice - Welded Wire Fabric, McLean, Virginia, 1979.

Zsutty, T.C., "Beam Shear Strength Prediction by Analysis of Existing Data", ACI Journal, Proceedings, Vol. 65, No. 11, Nov. 1968, p 943.

APPENDIX

TABLE A.1

TENSION TEST RESULTS FOR W2.5 WIRES

Test No.	Stress at 0.0035 Strain $f_{y,ACI}$ MPa	Stress at 0.005 Strain $f_{y,ASTM}$ MPa	Ultimate Stress f_u MPa	Ultimate Strain ε_u %	Young's Modulus From Test E Test MPa	Cross-wire Between Gauge Marks	Type of Failure
I	632	676	701	-	207.9×10^3	No	Failed at cross-wire outside gauge marks
II	626	-	682	-	202.1×10^3	No	Failed at cross-wire outside gauge marks
III	620	-	670	-	201.8×10^3	No	Failed in grips
IV	-	-	707	-	-	No	Failed in grips
V	601	651	701	2.0	193.8×10^3	Yes	Failed at cross-wire between gauge marks
VI	626	682	701	1.2	194.5×10^3	Yes	Failed at cross-wire between gauge marks
VII	614	-	651	1.0	202.0×10^3	Yes	Failed at cross-wire between gauge marks
VIII	645	-	707	-	213.5×10^3	No	Failed outside of gauge marks
IX	639	682	719	3.1	205.3×10^3	No	Failed between gauge marks (30 mm from mark)
AVG	625	673	693	a) 1.4 b) 3.1	202.6×10^3	-	a) Failure at cross-wire b) Failure away from cross-wire

TABLE A.2

TENSION TEST RESULTS FOR W2.9 WIRES

Test No.	Stress at 0.0035 Strain $f_{y,ACI}$ MPa	Stress at 0.005 Strain $f_{y,ASTM}$ MPa	Ultimate Stress f_u MPa	Ultimate Strain ε_u %	Young's Modulus From Test E Test MPa	Cross-wire Between Gauge Marks	Type of Failure
I	540	583	639	-	199.9×10^3	No	Failed outside of gauge marks
II	561	599	631	2.8	199.3×10^3	No	Failed between gauge marks
III	-	-	652	2.9	196.0×10^3	No	Failed between gauge marks
IV	551	588	636	-	193.5×10^3	No	Failed outside gauge marks
V	588	609	641	-	228.2×10^3	Yes	Failed outside gauge marks in grips
VI	577	604	641	-	211.4×10^3	Yes	Failed at lowest gauge mark
AVG	563	597	640	2.8	204.7×10^3	-	-

TABLE A.3

TENSION TEST RESULTS FOR D2.5 WIRES

Test No.	Stress at 0.0035 Strain $f_{y,ACI}$ MPa	Stress at 0.005 Strain $f_{y,ASTM}$ MPa	Ultimate Stress f_u MPa	Ultimate Strain ε_u %	Young's Modulus From Test E Test MPa	Cross-wire Between Gauge Marks	Type of Failure
I	-	-	533	1.2	175.8×10^3	No	Failed between gauge marks
II	496	515	539	1.1	187.5×10^3	No	Failed between gauge marks
III	496	527	533	-	177.9×10^3	No	Failed at cross-wire outside of gauge marks
IV	477	533	564	-	164.7×10^3	No	Failed in grips
V	496	527	533	1.2	191.7×10^3	Yes	Failed at cross-wire between gauge marks
VI	490	533	552	-	179.9×10^3	No	Failed in grips
VII	471	502	533	-	180.4×10^3	Yes	Failed in grips
VIII	508	-	521	1.0	176.6×10^3	Yes	Failed at cross-wire between gauge marks
IX	515	515	515	1.0	185.8×10^3	Yes	Failed at cross-wire between gauge marks
AVG	494	522	536	1.1	180.0×10^3	-	

TABLE A.4

TENSION TEST RESULTS FOR D2.9 WIRES

Test No.	Stress at 0.0035 Strain $f_{y,ACI}$ MPa	Stress at 0.005 Strain $f_{y,ASTM}$ MPa	Ultimate Stress f_u MPa	Ultimate Strain ε_u %	Young's Modulus From Test E Test MPa	Cross-wire Between Gauge Marks	Type of Failure
I	-	-	577	1.4	188.1×10^3	Yes	Failed at cross-wire between gauge marks
II	-	-	609	-	-	No	Failed outside gauge marks
III	529	567	593	1.25	200×10^3	No	Failed between gauge marks
IV	561	609	657	1.8	196.6×10^3	Yes	Failed at cross-wire between gauge marks
V	551	583	596	1.5	185.1×10^3	No	Failed between gauge marks (10 mm from mark)
VI	-	-	631	1.75	-	Yes	Failed at cross-wire between gauge marks
VII	534	556	575	1.9	225.9×10^3	Yes	Failed between gauge marks but not at cross-wire (8 mm from mark)
AVG	545	577	604	1.6	199.1×10^3	-	-

TABLE A.5

TENSION TEST RESULTS SUPPLIED BY WIRE MANUFACTURER

Specimen No.	Area of Specimen sq. in.	sq. mm	Ultimate Stress f_u MPa	Ultimate Strain ε_u %	Size of Wire Made with this Specimen
1	0.034	21.9	671	2.3	W2.9 or D2.9
2	0.034	21.9	608	-	
3	0.034	21.9	614	2.3	
4	0.029	18.7	637	2.3	
5	0.024	15.5	698	1.6	W2.5 or D2.5
6	0.024	15.5	664	2.3	
7	0.025	16.1	582	3.1	

NOTE: These tests were performed using plain, smooth wires

TABLE A.6

AS-BUILT BEAM DIMENSIONS

Beam Number	Effective Depth, d mm	Flange Width, b mm	Beam Depth, h mm	Shear Span at Failure End, a mm	Shear Span to Depth Ratio, a/d, at Failure End
TB 1	443	-	-	1380	3.12
TB 2	450	509	512	1377	3.06
TB 3	447	-	-	1375*	3.08
TB 4	447	-	-	1375*	3.08
TB 5	445	-	-	1375*	3.09
TB 6	448	-	510	1385	3.09
TB 7	441	517	509	1378	3.12
TB 8	445*	512	508	1382	3.11
TB 9	445*	510	510	1381	3.10
TB 10	445*	510	508	1381	3.10
Design	445	508	508	1380	3.10

*Estimated Value

NOTE: In the cases where no value is shown, there were no measurements taken

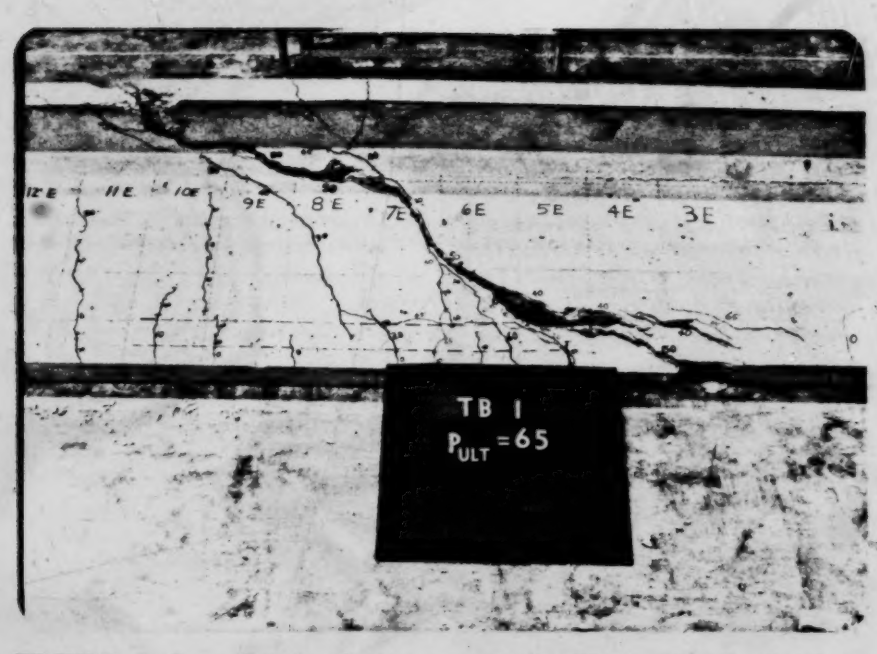

FIGURE A.1 - East shear span of TB 1 after failure

FIGURE A.2 - West shear span of TB 1 after failure

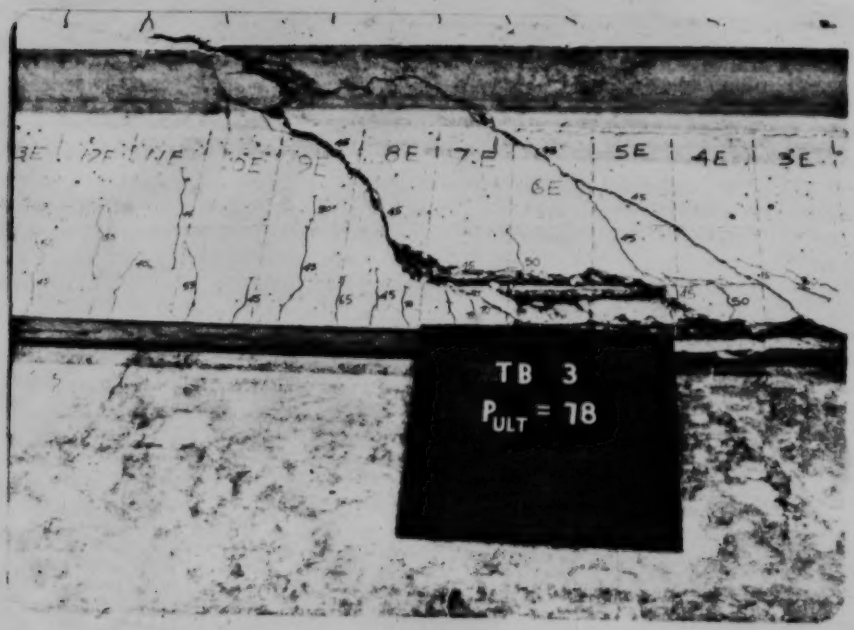

FIGURE A.3 - East shear span of TB 3 after failure

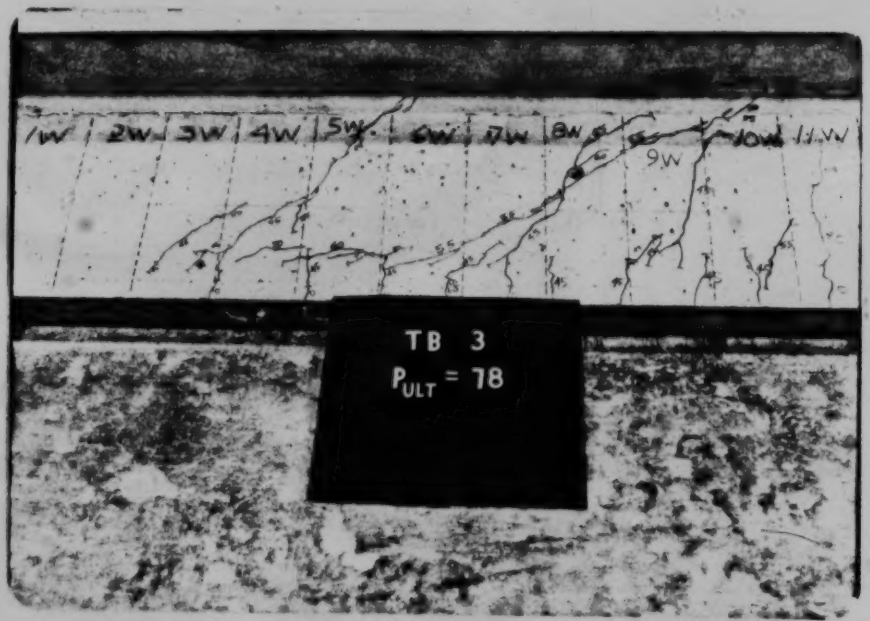

FIGURE A.4 - West shear span of TB 3 after failure

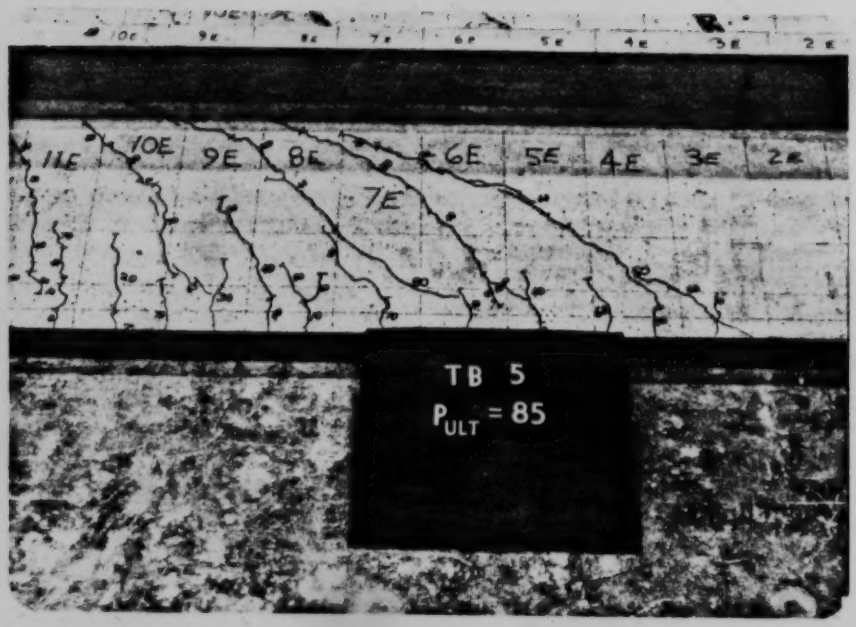

FIGURE A.5 - East shear span of TB 5 after failure

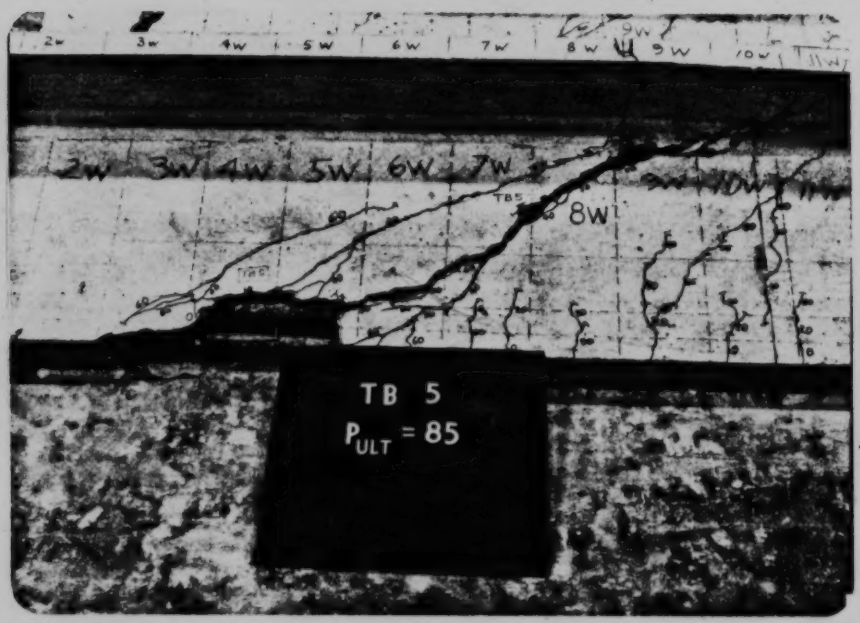

FIGURE A.6 - West shear span of TB 5 after failure

FIGURE A.7 - East shear span of TB 6 after failure

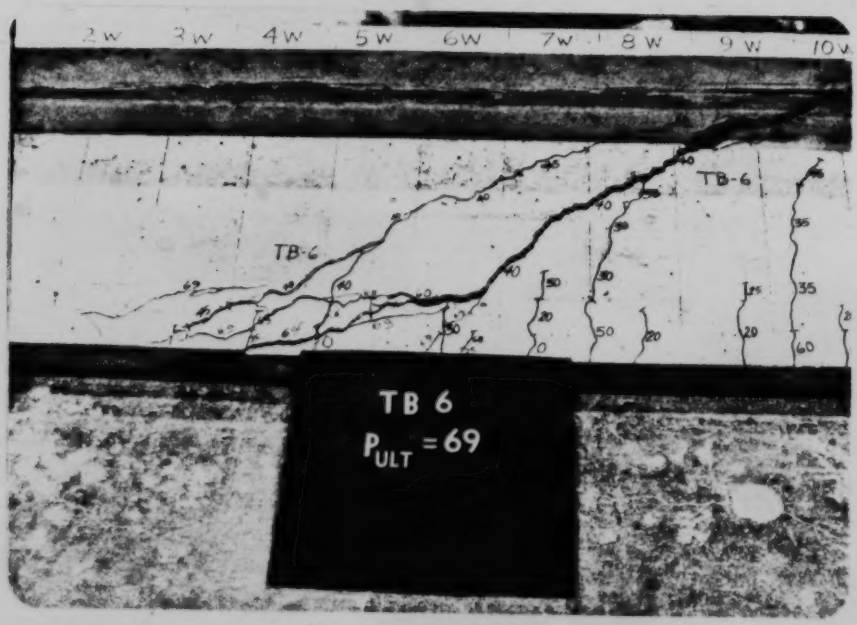

FIGURE A.8 - West shear span of TB 6 after failure

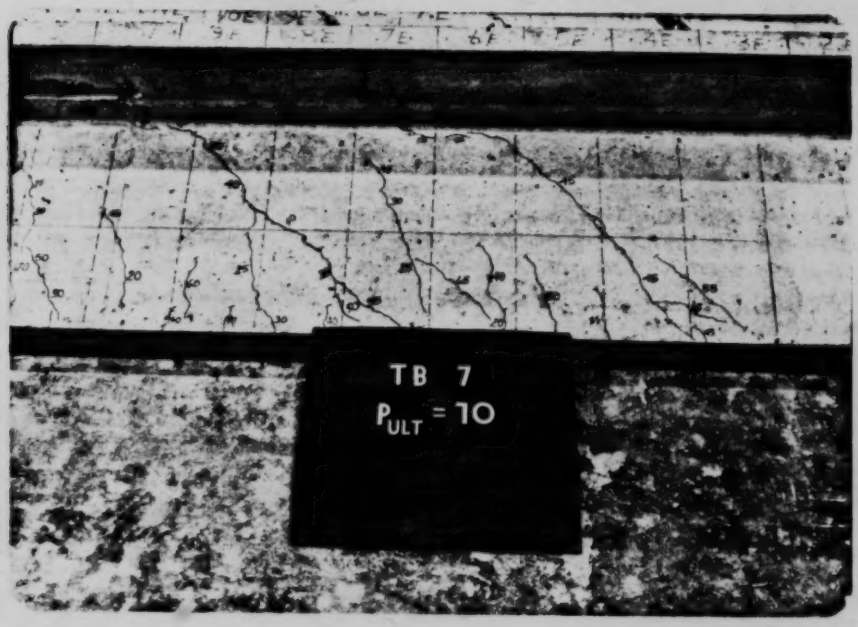

FIGURE A.9 - East shear span of TB 7 after failure

FIGURE A.10 - West shear span of TB 7 after failure

FIGURE A.11 - East shear span of TB 8 after failure

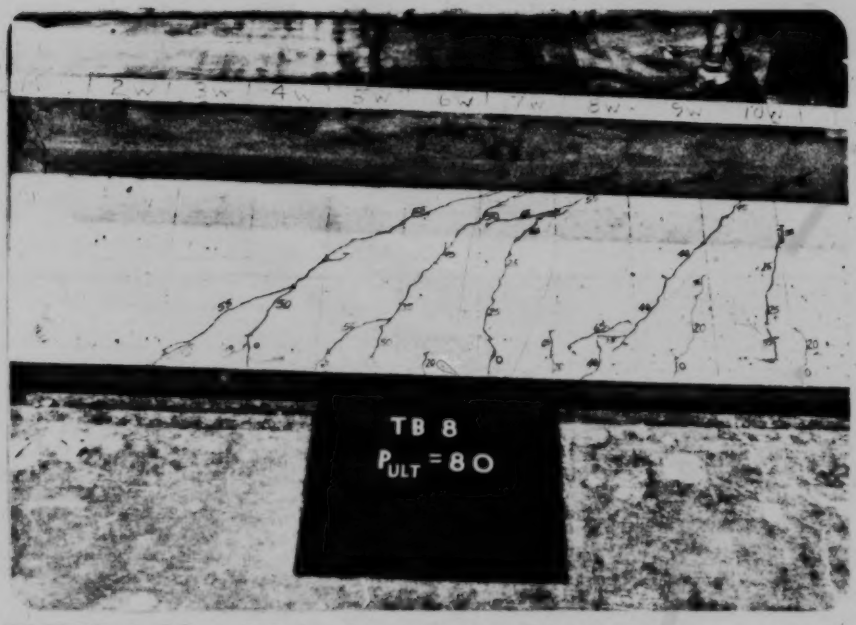

FIGURE A.12 - West shear span of TB 8 after failure

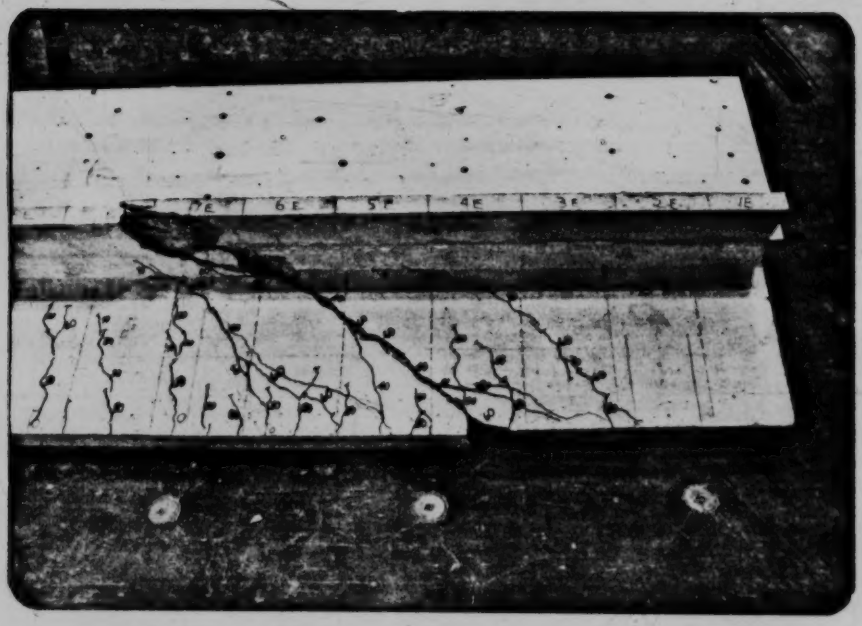

FIGURE A.13 - East shear span of TB 9 after failure

FIGURE A.14 - West shear span of TB 9 after failure

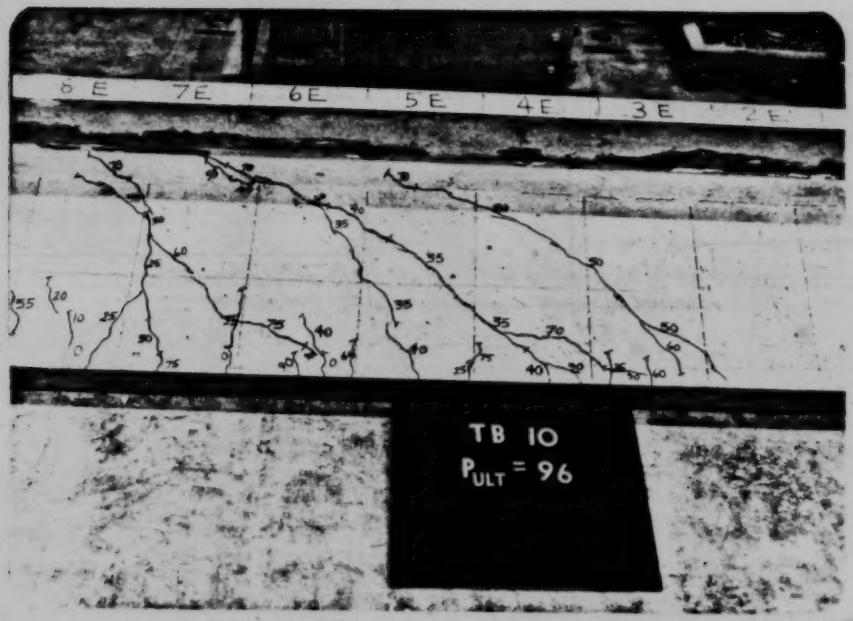

FIGURE A.15 - East shear span of TB 10 after failure

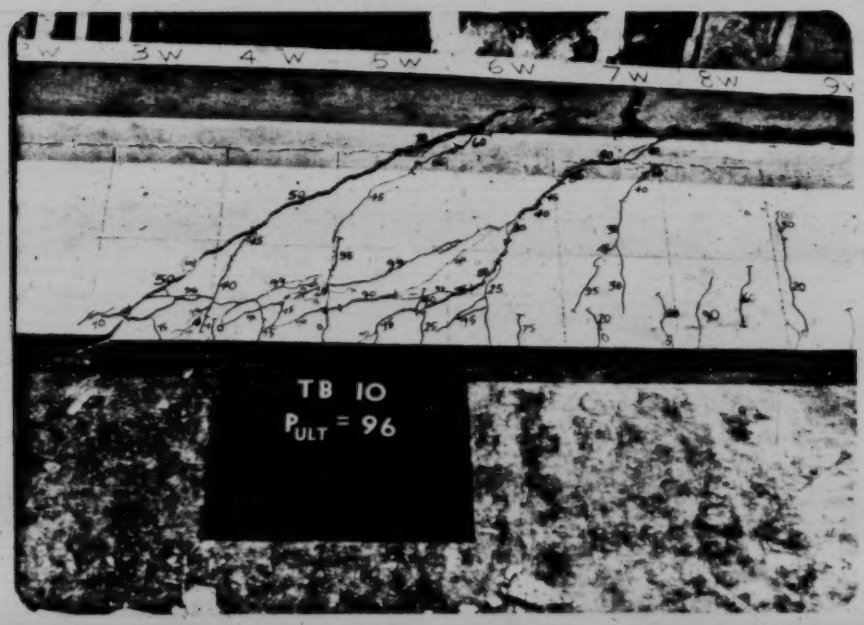

FIGURE A.16 - West shear span of TB 10 after failure

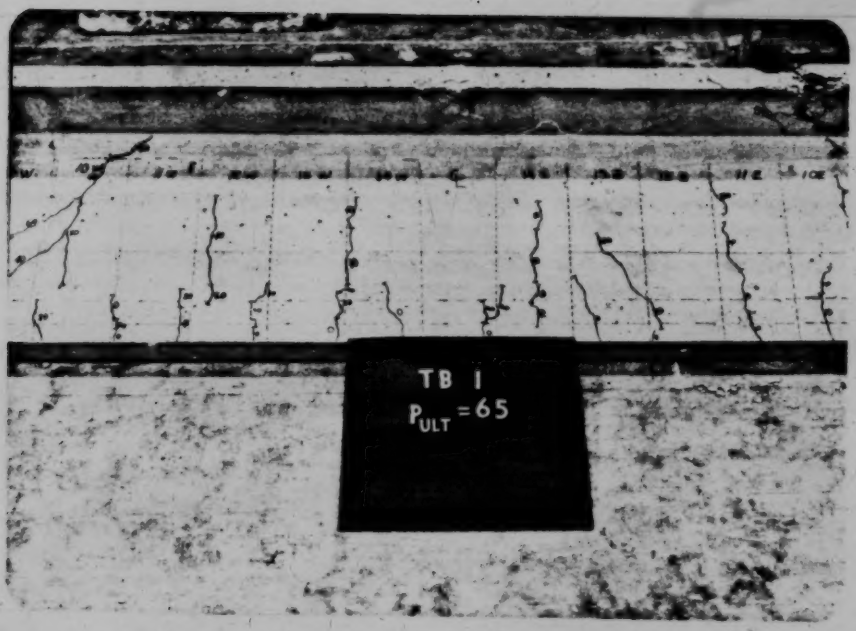

FIGURE A.17 - Pure moment region of TB 1 after failure

FIGURE A.18 - Pure moment region of TB 3 after failure

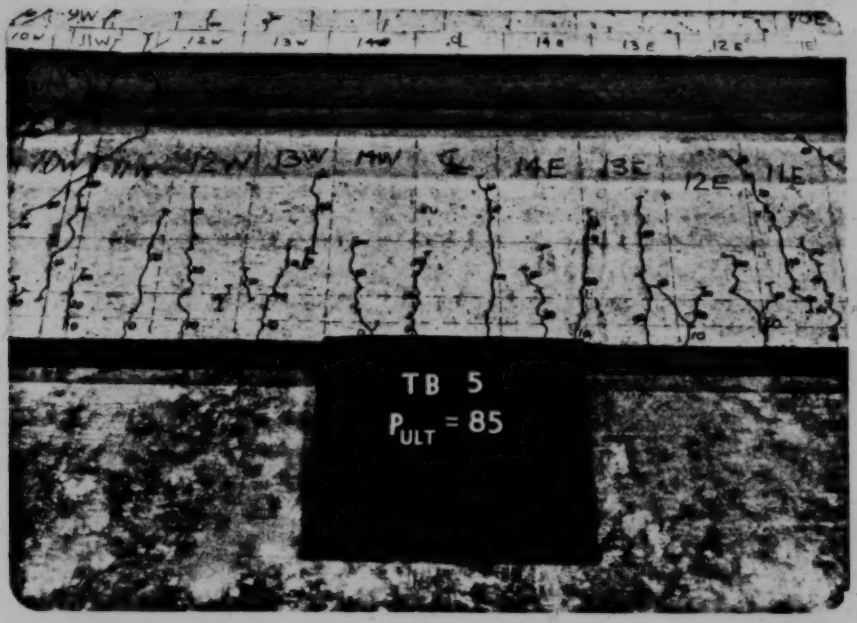

FIGURE A.19 - Pure moment region of TB 5 after failure

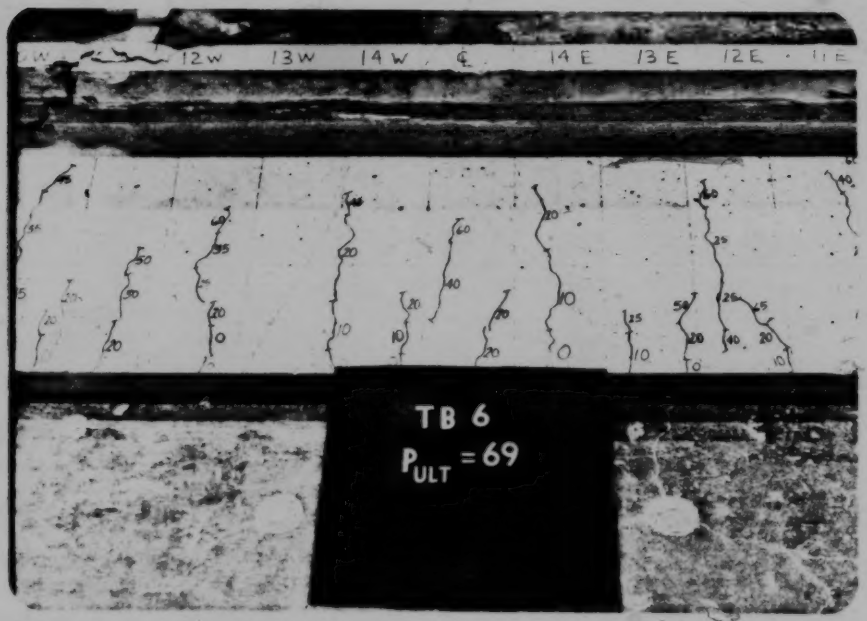

FIGURE A.20 - Pure moment region of TB 6 after failure

FIGURE A.21 - Pure moment region of TB 7 after failure

FIGURE A.22 - Pure moment region of TB 8 after failure

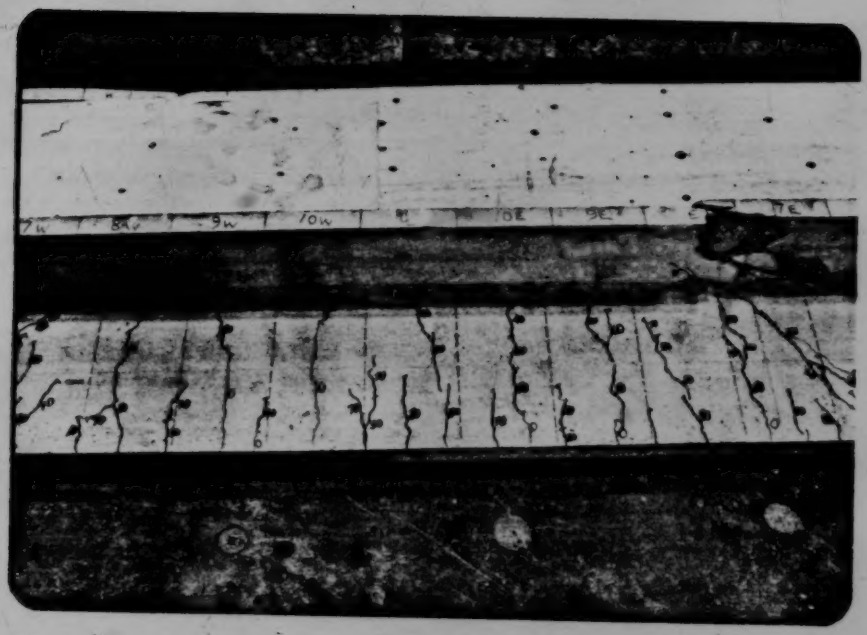

FIGURE A.23 - Pure moment region of TB 9 after failure

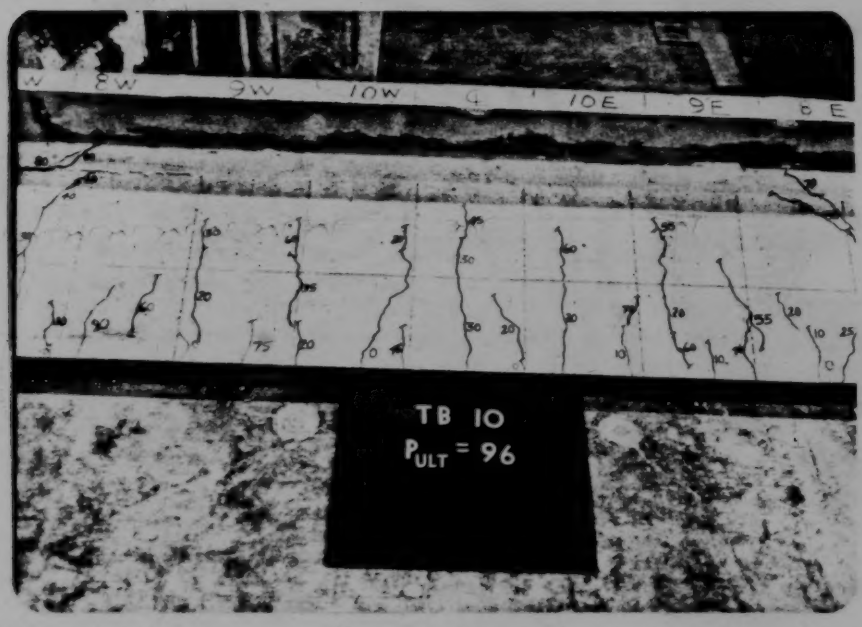

FIGURE A.24 - Pure moment region of TB 10 after failure